Overview:

1. Introduction and overview
2. Antimatter at high energies (SppS, LEP, Fermilab)
3. Meson spectroscopy (antimatter as QCD probe)

4. Astroparticle physics and cosmology
5. CP and CPT violation tests
6. Precision tests with Antihydrogen: spectroscopy

7. Precision tests with Antihydrogen: gravity
8. Applications of antimatter

Overview:

1. Introduction and overview
2. Antimatter at high energies (SppS, LEP, Fermilab)
3. Meson spectroscopy (antimatter as QCD probe)

4. Astroparticle physics and cosmology
5. CP and CPT violation tests
6. Precision tests with Antihydrogen: spectroscopy

7. Precision tests with Antihydrogen: gravity
8. Applications of antimatter


MATTER
ANTI-MATTER
S. Harris

Overview:

1. Search for primordial antimatter
2. Search for local antimatter
3. cosmic rays and antimatter
4. balloon measurements (CAPRICE)
5. space measurements (PAMELA, AMS)

1. Search for primordial antimatter

CMB

late annihilation:

- annihilation e^+/e^- → Compton scattering → CMB structures at domain boundaries
- annihilation photons → contribute to cosmic diffuse gamma-rays

A. G. Cohen *et al* 1998 *ApJ* **495** 539

"Thus, we have ruled out a B=0 universe with domains smaller than a size comparable to that of the visible universe. It follows that the detection of Z>1 antinuclei among cosmic rays would shatter our current understanding of cosmology or reveal something unforeseen in the realm of astrophysical objects."

BBN

- *early annihilation*: tiny domains: annihilation before nucleosynthesis
- *late annnihilation* (during or after nucleosynthesis)
  - $\bar{p}p$, $\bar{p}^4He \rightarrow {}^3He$; don't escape from annihilation zone
  - hadrodestruction: $\bar{p}X \rightarrow X'n$; $n + {}^4He \rightarrow {}^3He, D$
  - annihilation photons (pi^0's) are rescattered to below the pair-production threshold → photodisintegration of D, ^3He, ^3H at successively lower temperatures, and finally photodisintegration of ^4He (always into lighter isotopes) → large ^3He, D / ^4He ratio

http://prl.aps.org/pdf/PRL/v84/i17/p3756_1
(Phys. Rev. Lett. 84, 3756–3759 (2000))

2. Search for local antimatter

Inflation separates nearby matter-antimatter domains to beyond the scale of the observable Universe.

Very close matter-antimatter domains might only be separated to smaller scales, such as that of superclusters.

Search for annihilation (gamma-rays in addition to the normally produced X-rays) at supercluster boundaries.

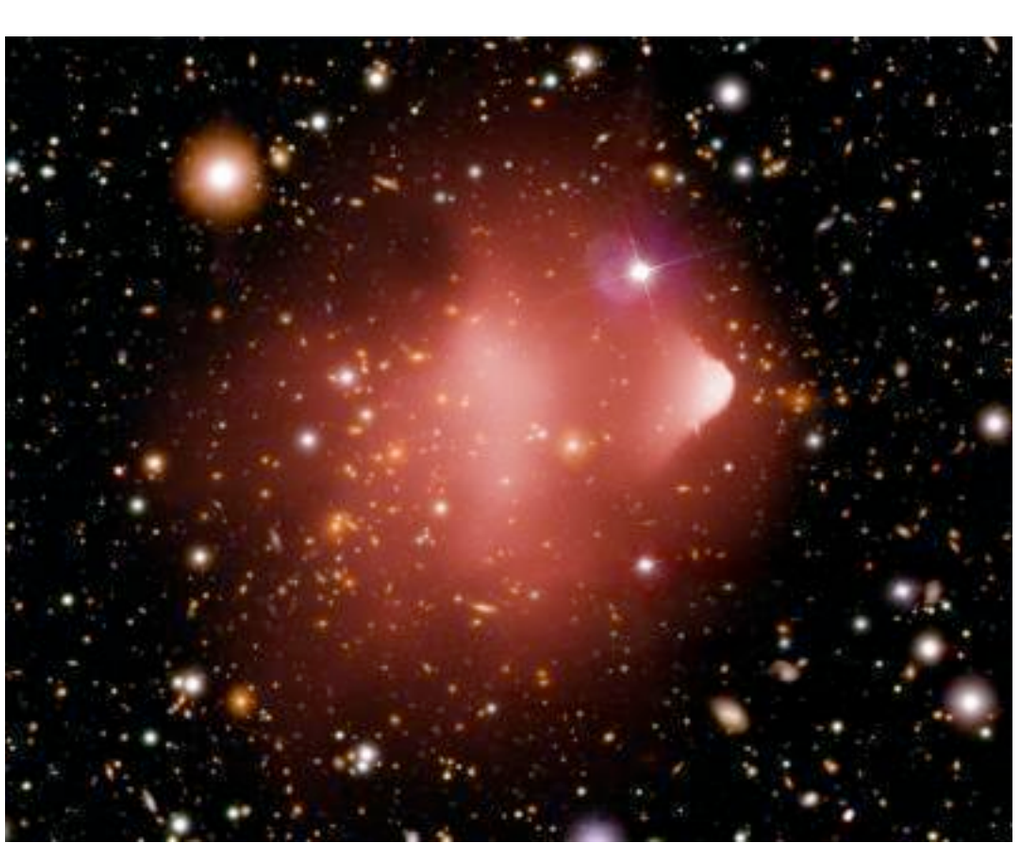

Bullet Cluster in combination of X-rays from Chandra (red) and optical data from the Hubble and Magellan telescopes (yellow).

Absence of gamma-rays → antimatter is less than 3 ppm in this system. http://arxiv.org/abs/0808.1122

X-ray: NASA/CXC/CfA/M.Markevitch et al. Optical: NASA/STScI; Magellan/U.Arizona/D.Clowe et al.)

(dark matter distribution in same cluster through gravitational lensing)

Searches in our own backyard

Observation by OSSE/Compton Gamma Ray Observatory in 1997 (known since 1970): strong & continuous production of positrons at the center of the galaxy

http://iopscience.iop.org/1538-4357/481/1/L43?ejredirect=migration

reconstructed maps of galactic center 511 keV line radiation distribution

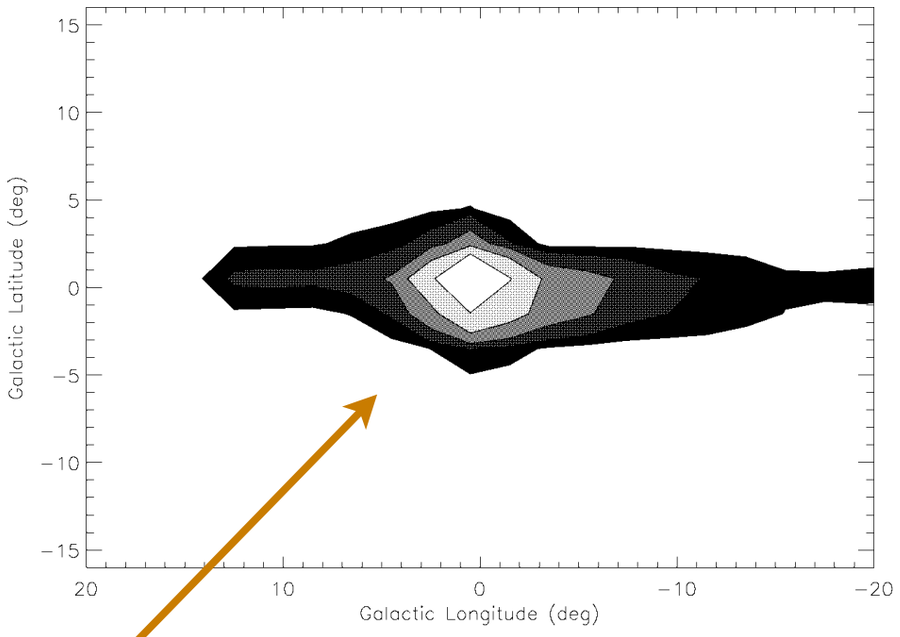

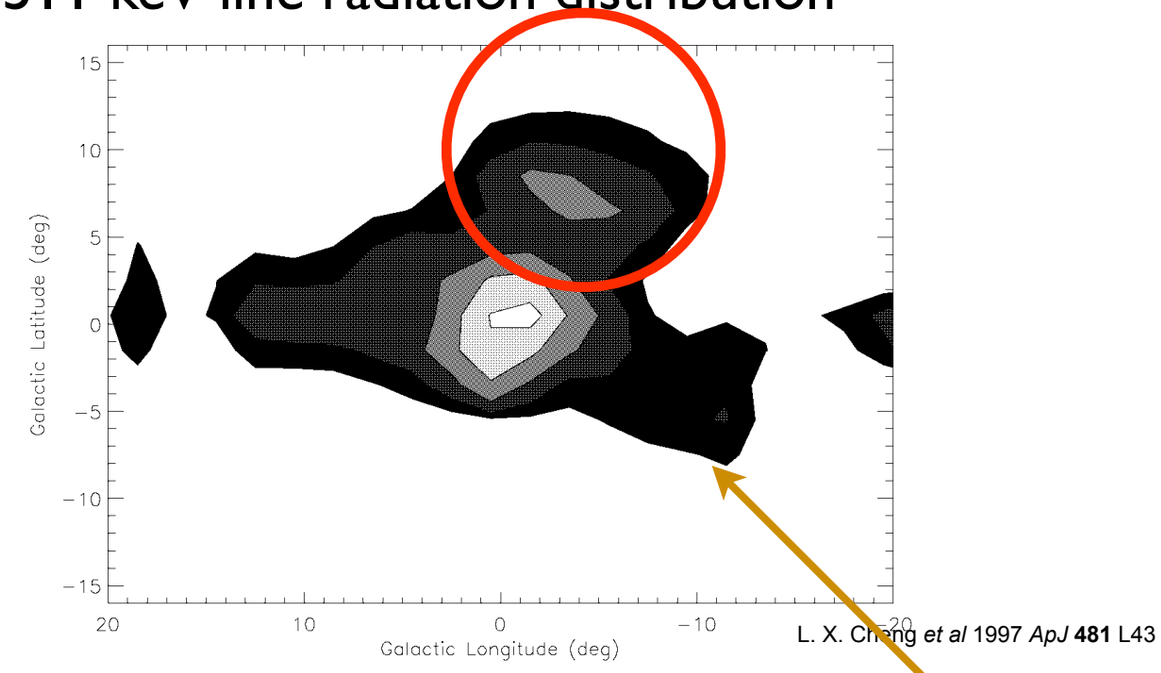

L. X. Cheng *et al* 1997 *ApJ* **481** L43

simulation

observation

extended, diffuse 511 keV emission cloud of annihilation radiation, probably about 4000 light years across, extending nearly 3500 light years above galactic plane : Causes?

10^{43} annihilations/s ~ 3 solar masses in 1 Gyr

INTEGRAL space telescope

ESA/ Integral/ MPE (G. Weidenspointner et al.)
http://www.esa.int/esaSC/SEMKTX2MDAF_index_0.html

INTEGRAL space telescope

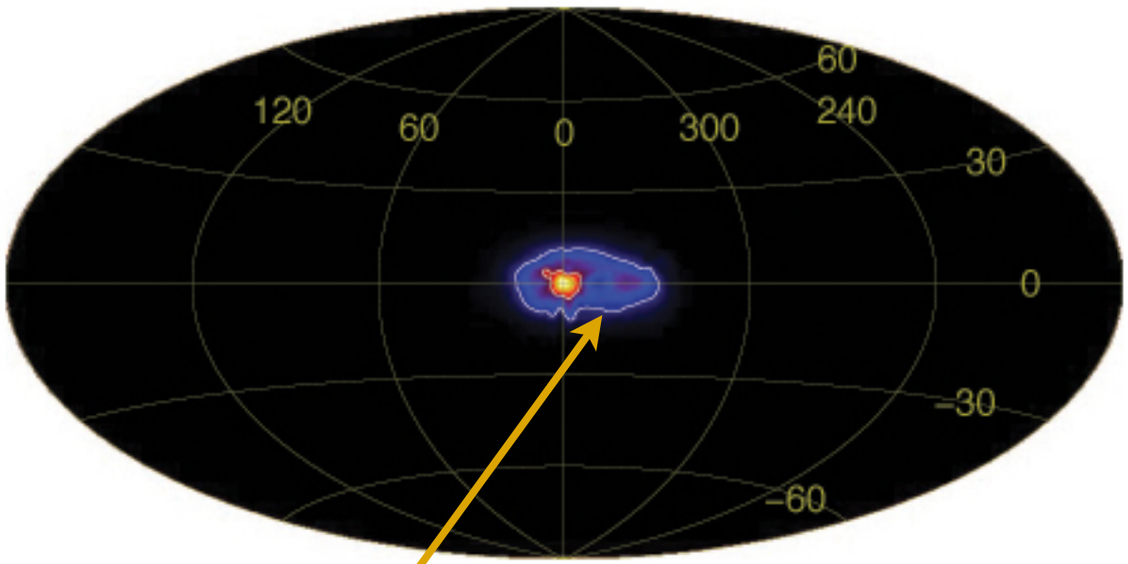

Asymmetry confirmed! but...

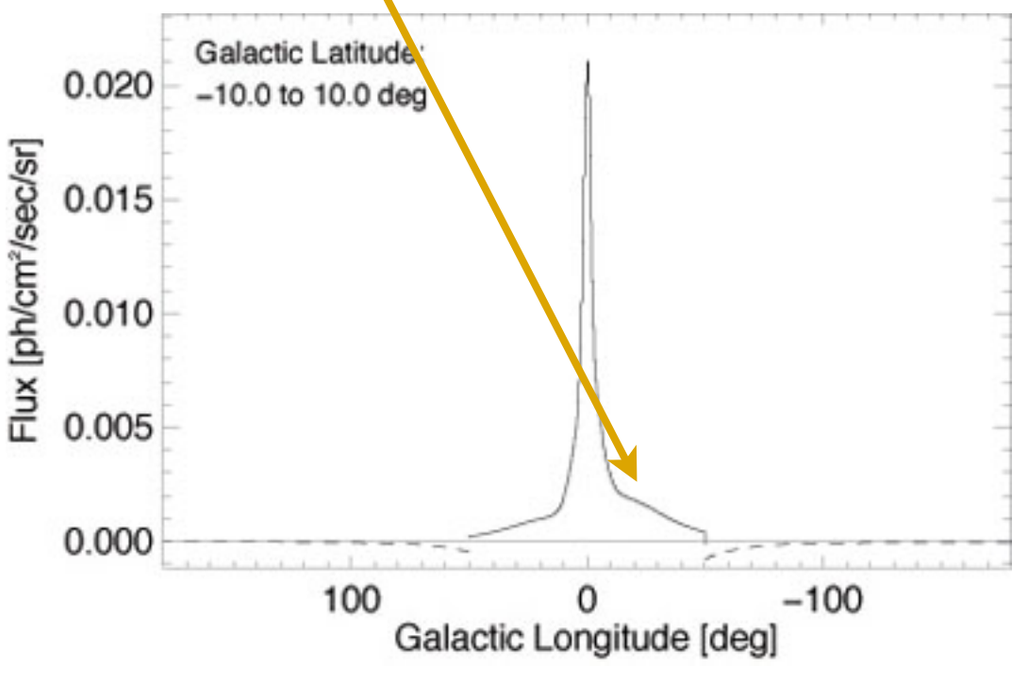

ESA/ Integral/ MPE (G. Weidenspointner et al.)
http://www.esa.int/esaSC/SEMKTX2MDAF_index_0.html

INTEGRAL space telescope

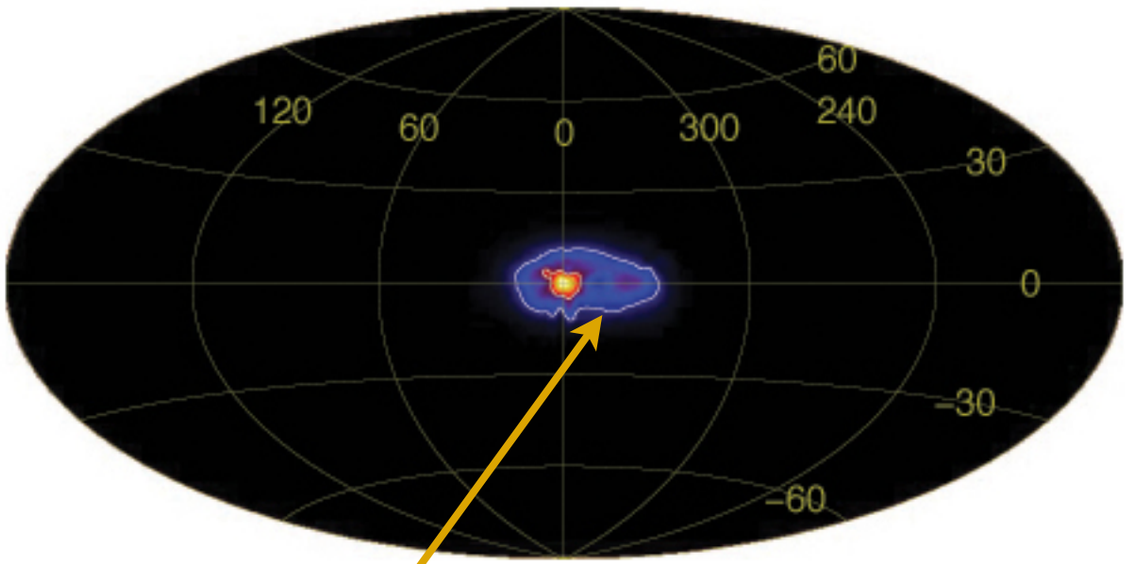

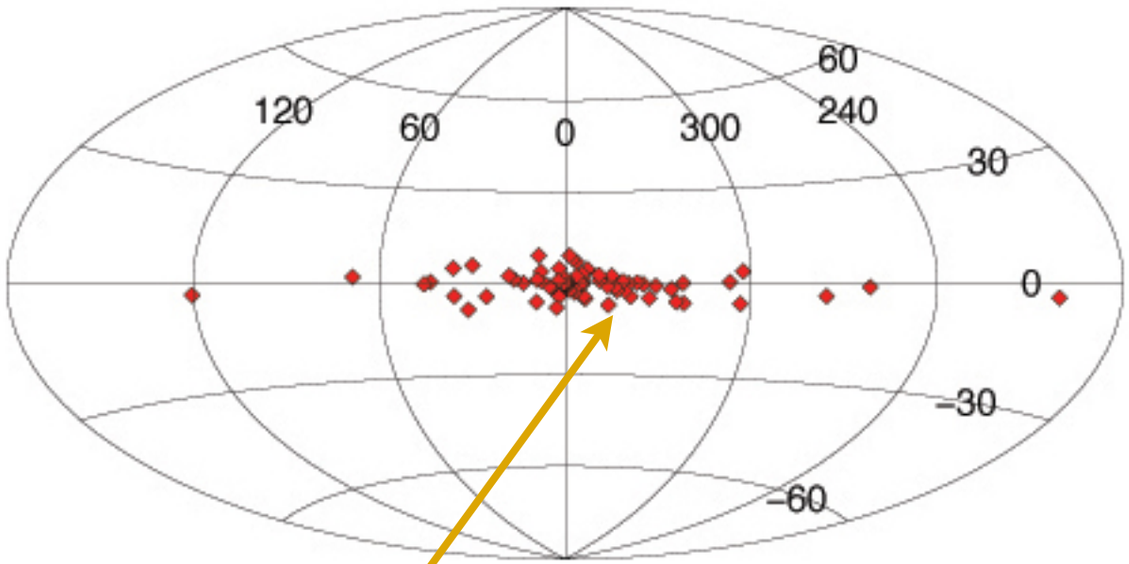

Asymmetry confirmed! but...

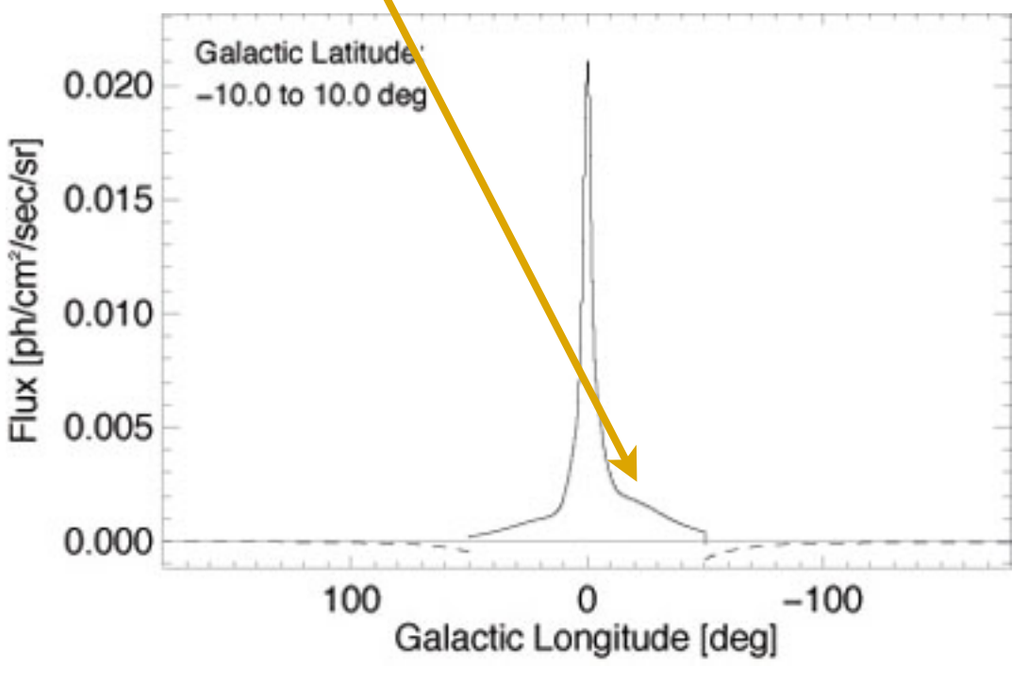

Asymmetry matches distribution of hard low-mass X-ray binary stars

gas in GC generally symmetrical, *except* for these stars

signal not caused by dark matter ;(

ESA/ Integral/ MPE (G. Weidenspointner et al.)
http://www.esa.int/esaSC/SEMKTX2MDAF_index_0.html

3. Cosmic rays and antimatter

A large part of positrons and antiprotons impinging on Earth are produced in high-energy interactions between cosmic rays nuclei with the interstellar medium. Their spectra can provide an insight on the origin, production and propagation of cosmic rays in our galaxy. Any observed flux larger than that predicted by the Leaky Box Model (LBM), the "standard" model of cosmic ray propagation, could indicate exotic sources of antimatter. The predictions of the propagation models are different above 10 GeV where more refined measurements are needed.

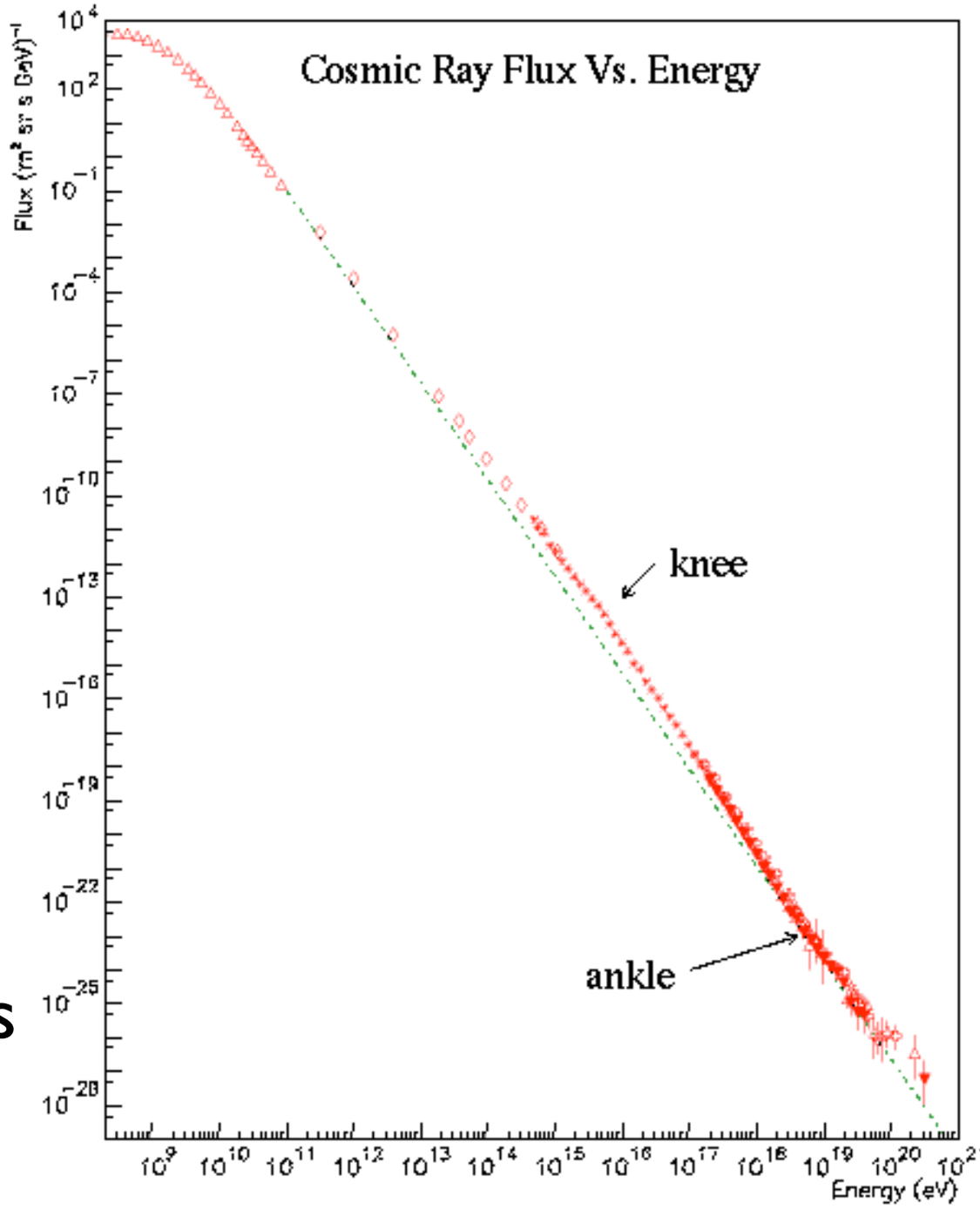

Nuclear Physics B - Proceedings Supplements
Volume 78, Issues 1-3, August 1999, Pages 32-37

Specific interests:

- Formation models for cosmic rays
- Propagation models for cosmic rays
- WIMPS/dark matter
- search for primordial antimatter (!)

... antimatter in cosmic rays ...

positrons and antiprotons in cosmic rays:
- produced in inelastic collisions in interstellar medium
- flux determined by propagation, energy distribution of primaries

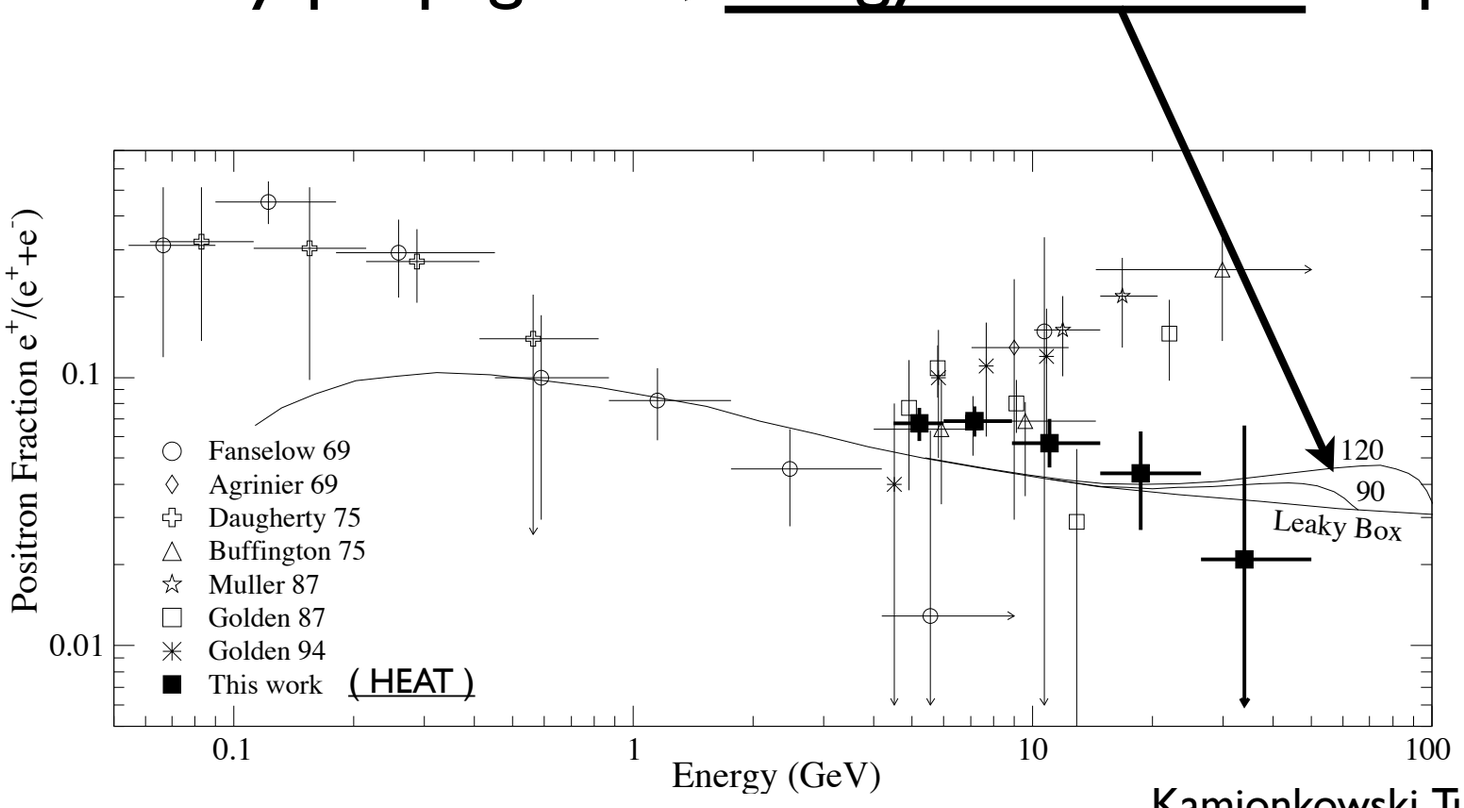

Kamionkowski, Turner, PRD 43 (1991) 1774

positrons are difficult to measure/interpret:
- radiative losses close to sources
- possibility of primary positron cosmic rays

Searching for antimatter in the cosmic rays reaching the Earth

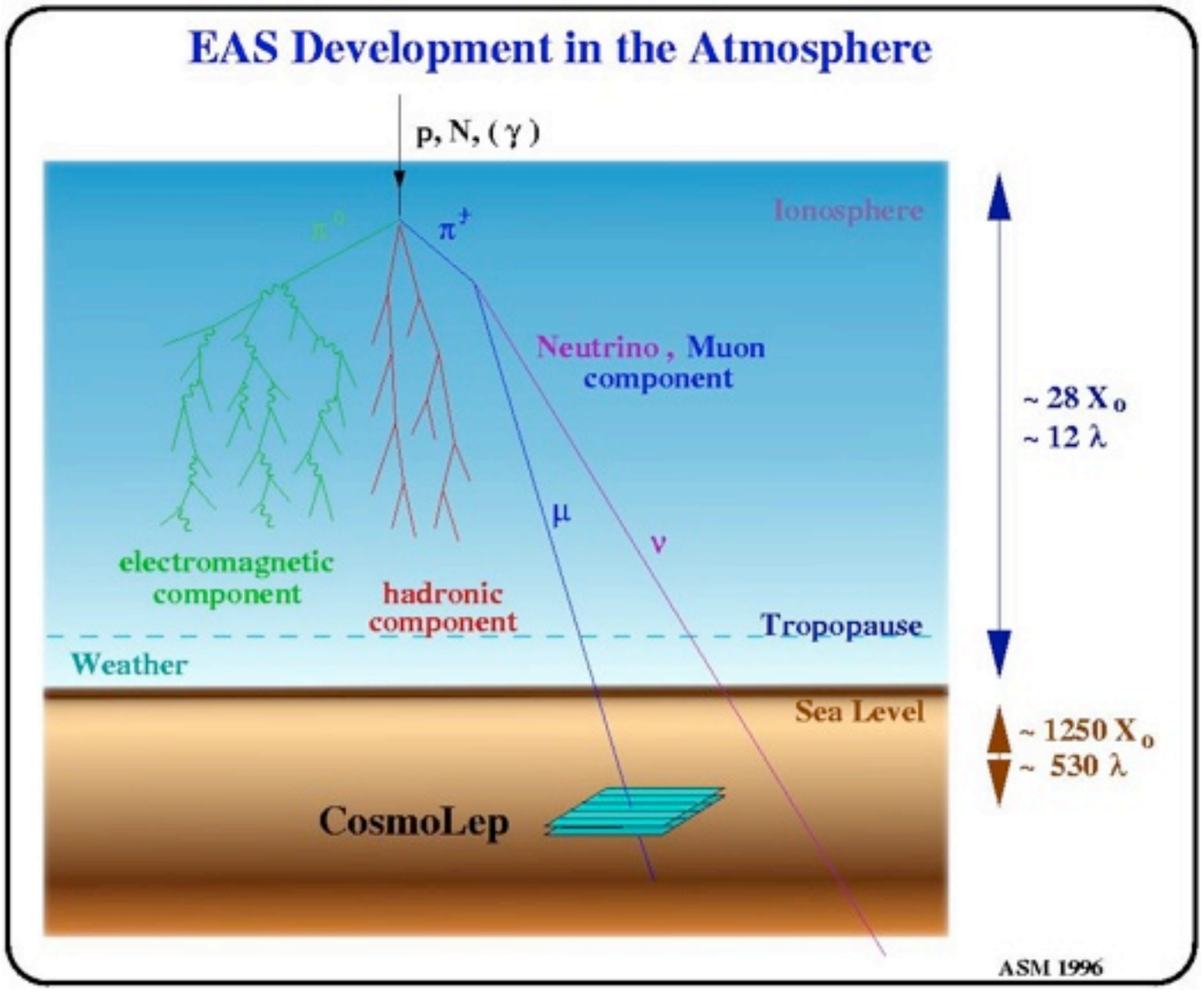

Searching for antimatter in the cosmic rays reaching the Earth

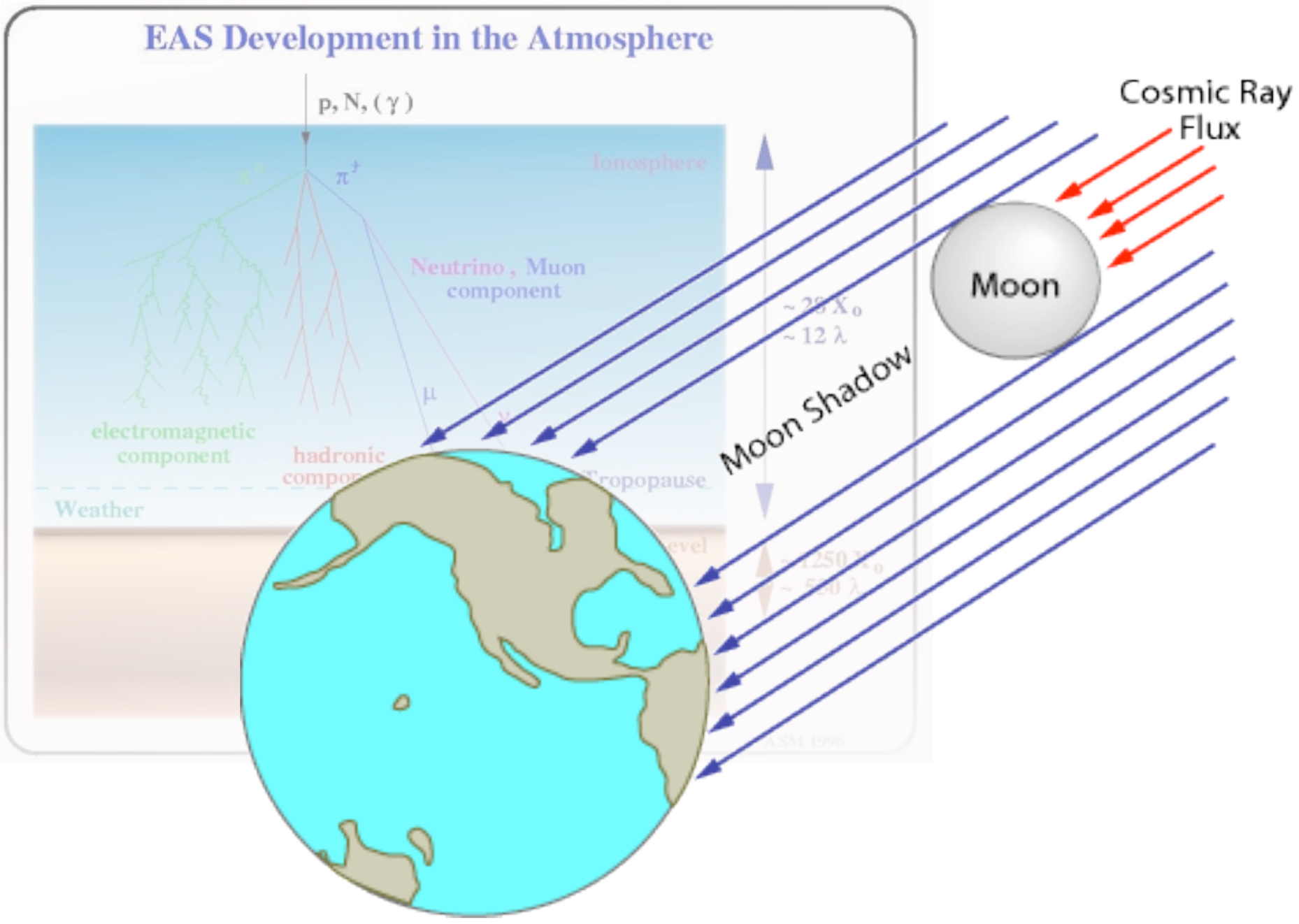

Searching for antimatter in the cosmic rays reaching the Earth

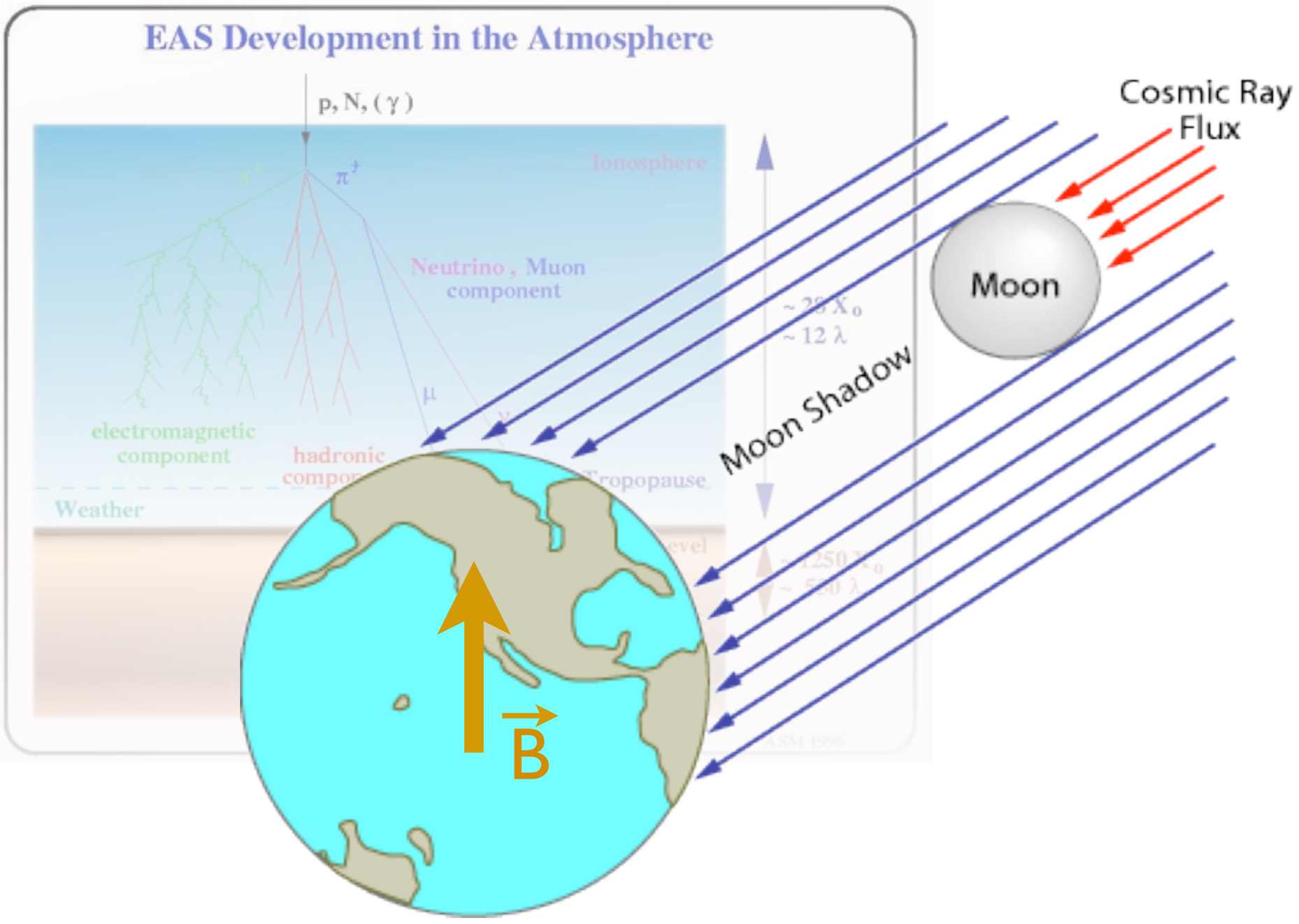

Shadow of the Moon as observed by Milagro

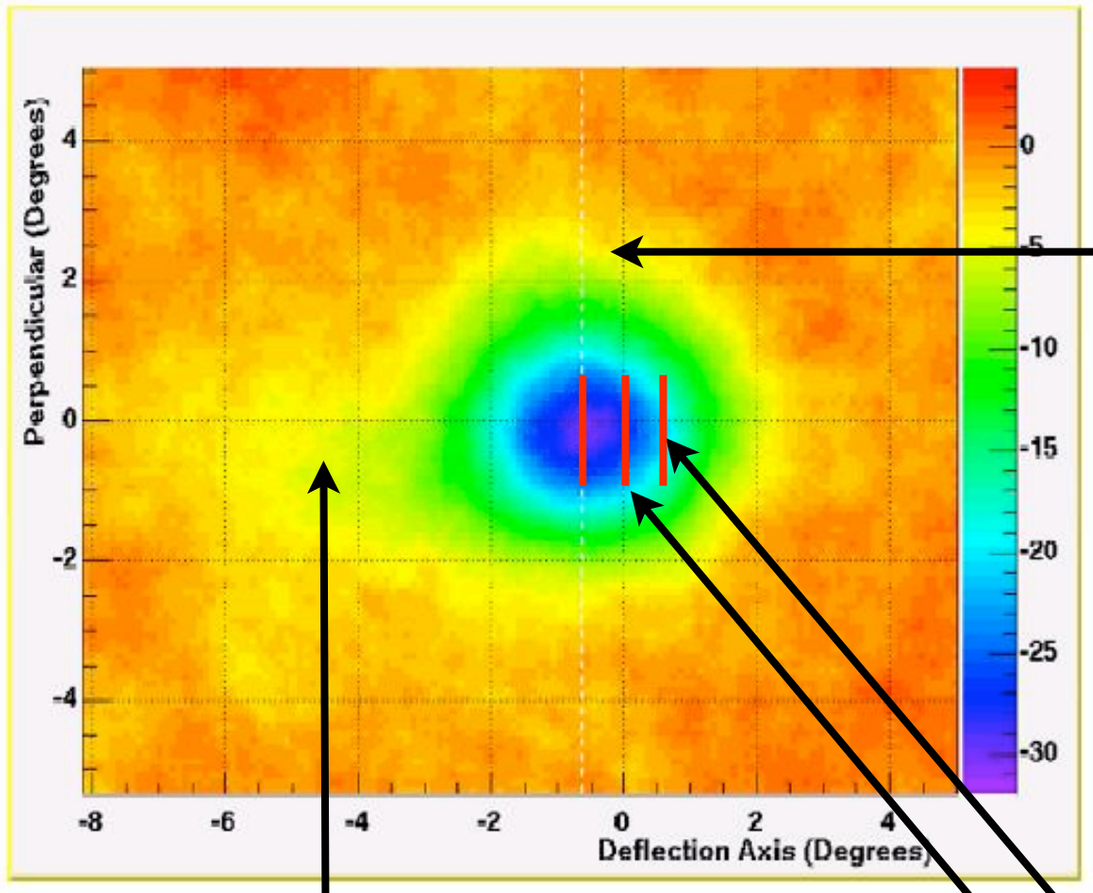

angular resolution of Milagro

low energy events

Moon shadow is affected by Earth's magnetic field

No double shadow = cosmic rays only have one charge

No neutral cosmic rays

Shadow of the Moon as observed by Milagro

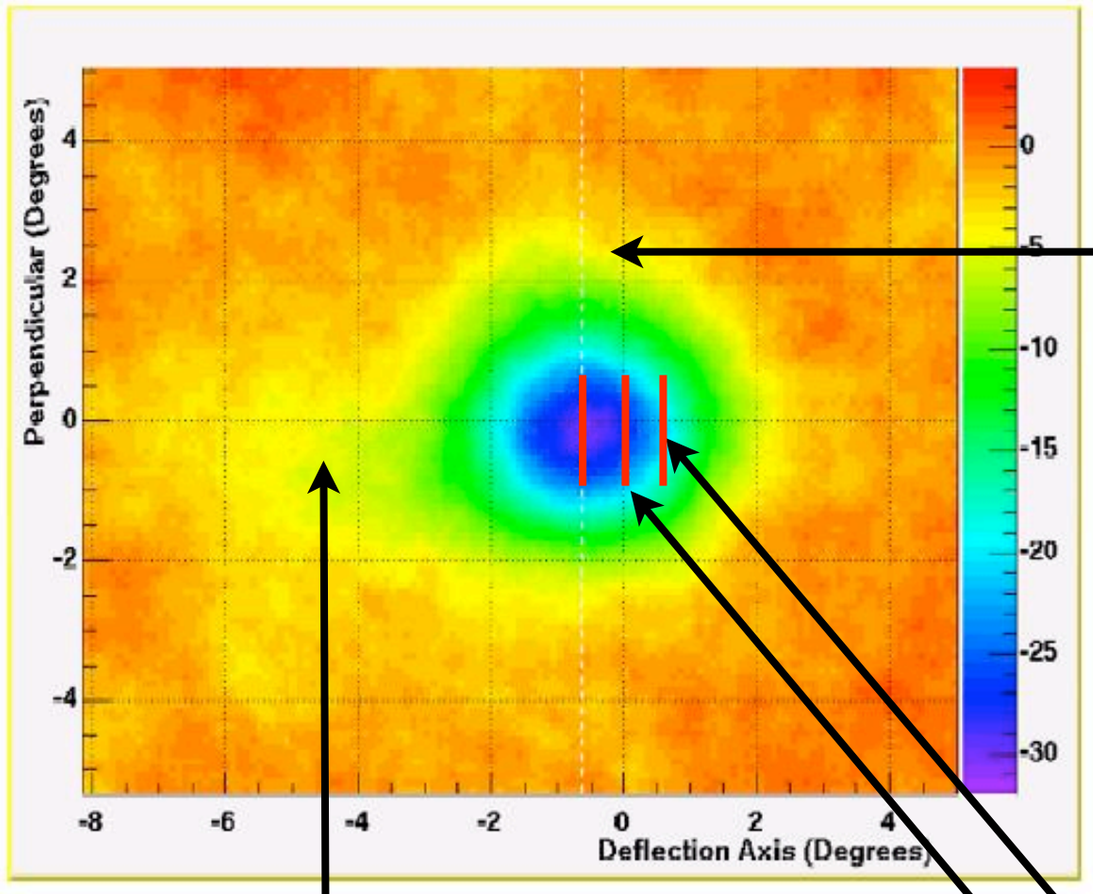

angular resolution of Milagro

low energy events

Moon shadow is affected by Earth's magnetic field

No double shadow = cosmic rays only have one charge

No neutral cosmic rays

can do better....

Cosmic Antiproton Ring-Imaging Cerenkov Experiment

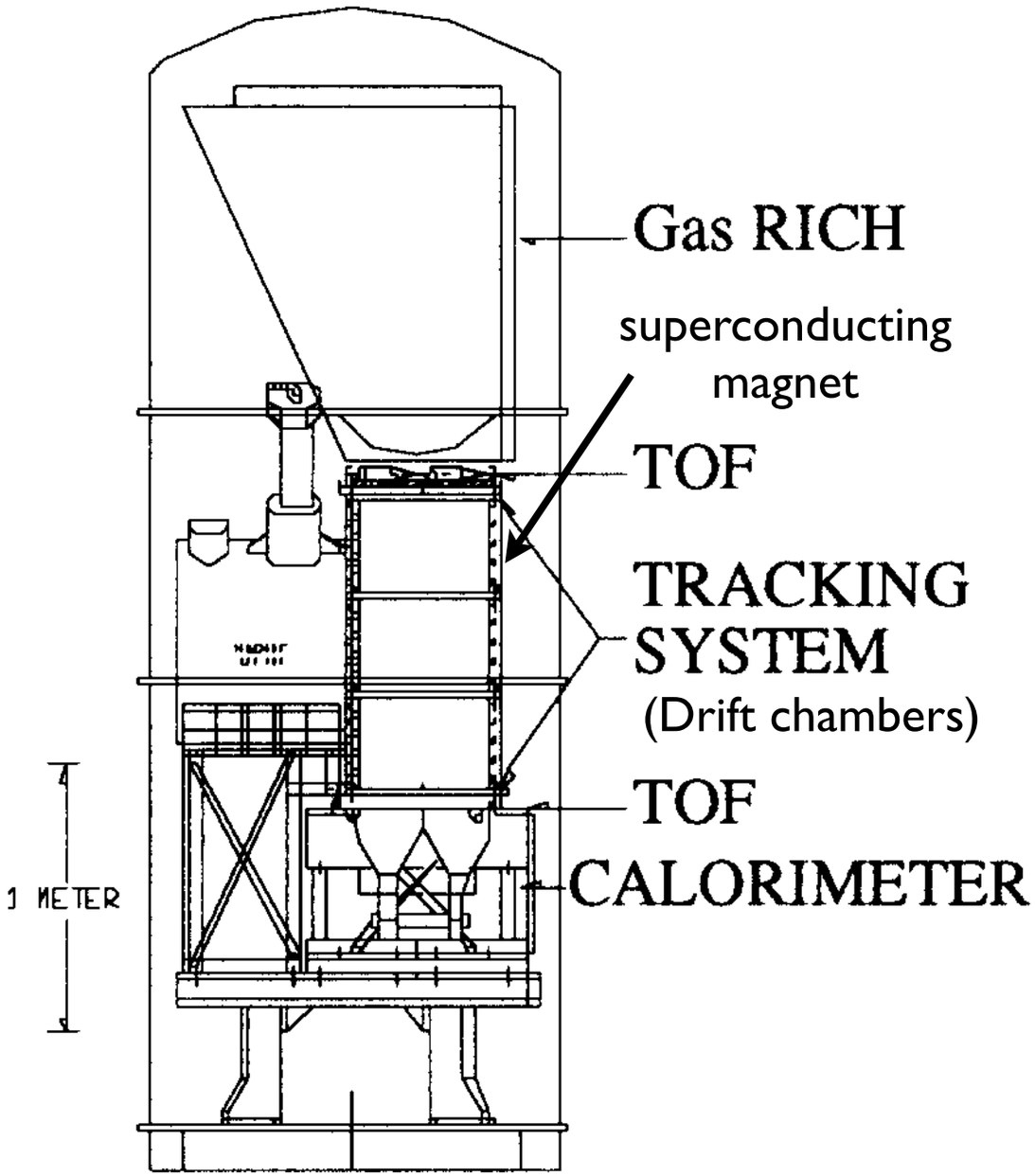

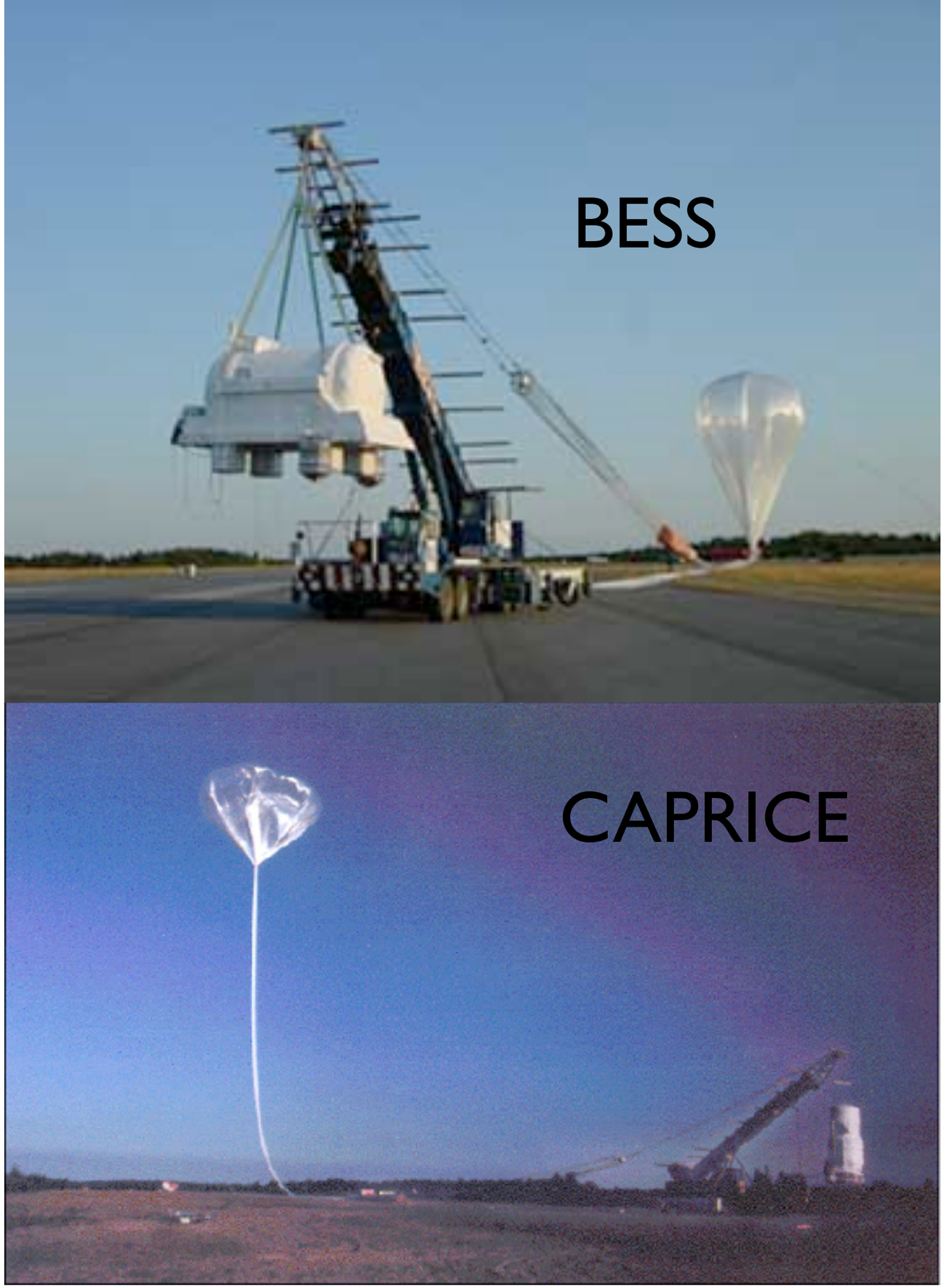

Results from CAPRICE/BESS

height of flight = 38 km = top of atmosphere

PRL 84 (2000) 1078 http://prl.aps.org/pdf/PRL/v84/i6/p1078_1

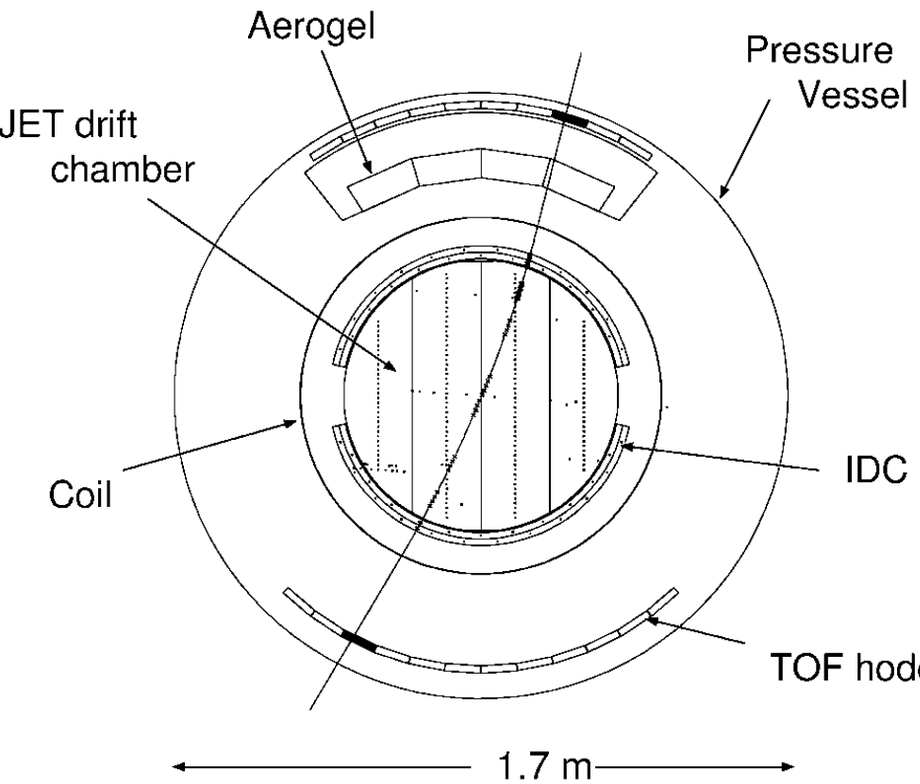

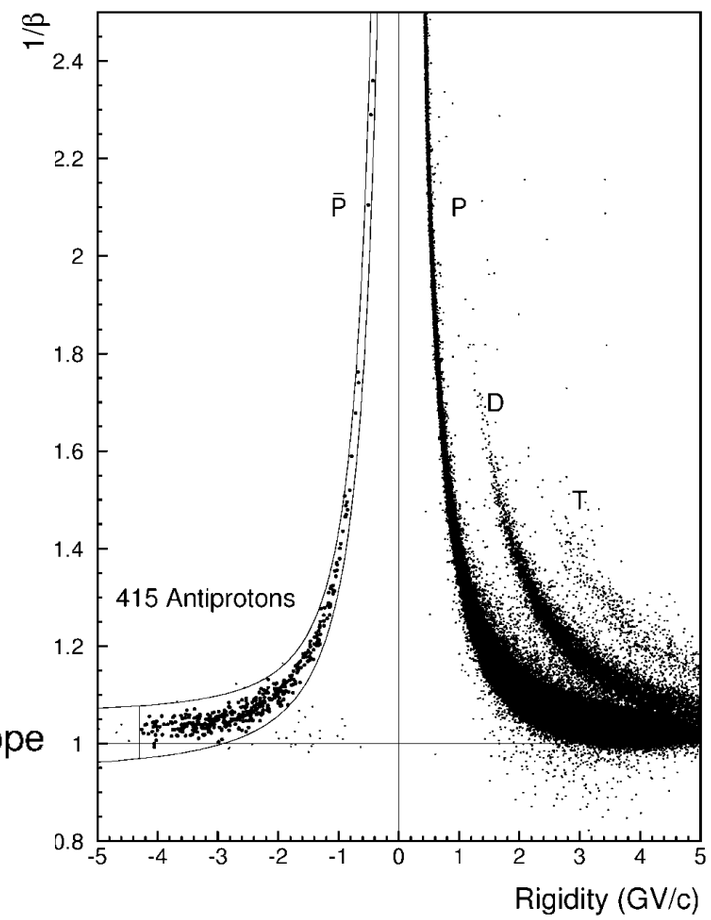

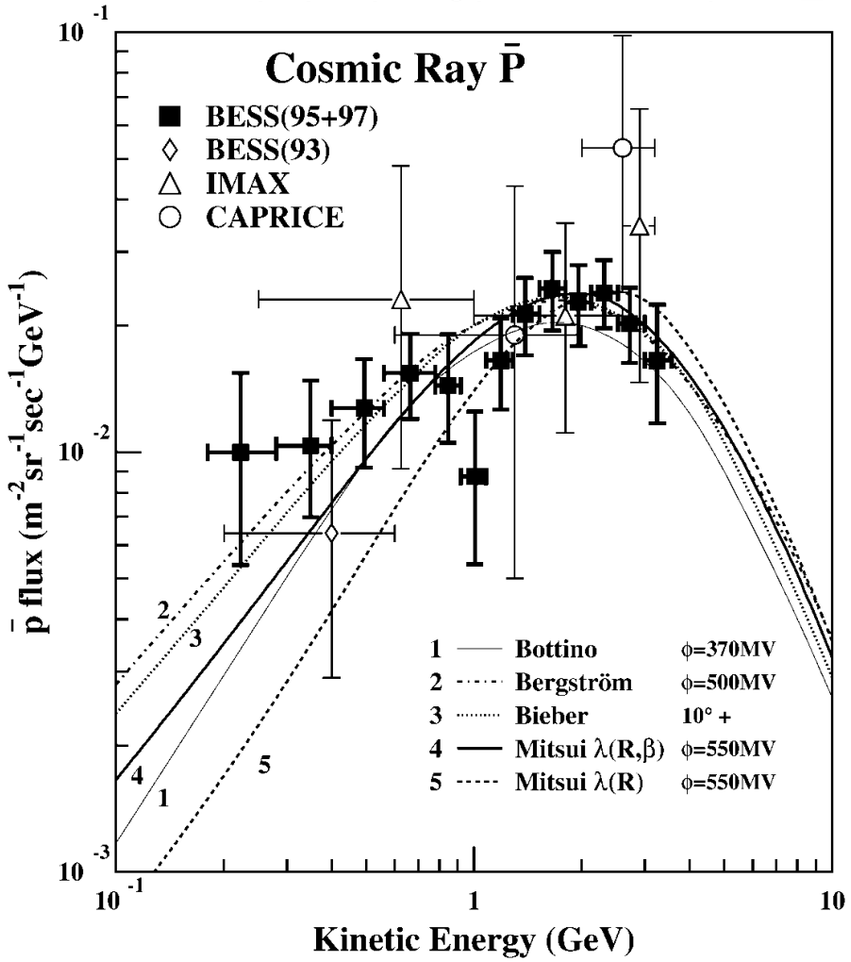

subsidiary result (data+propagation model) = tau($\bar{p}$) > 1.7 Myr

http://arxiv.org/abs/astro-ph/9809101

Space-based detectors

benefits:

- above atmosphere (primary, rather than secondary spectrum)
- WYSIWYG

disadvantages:

- above atmosphere (= satellite = cost! & reliability!)
- much more limited solid angle / detector size
- technology is fixed (and usually not cutting edge)

PAMELA

was launched in June 2006
part of the Resurs-DK1 satellite

AMS

installed on ISS (2011)

Results from PAMELA:

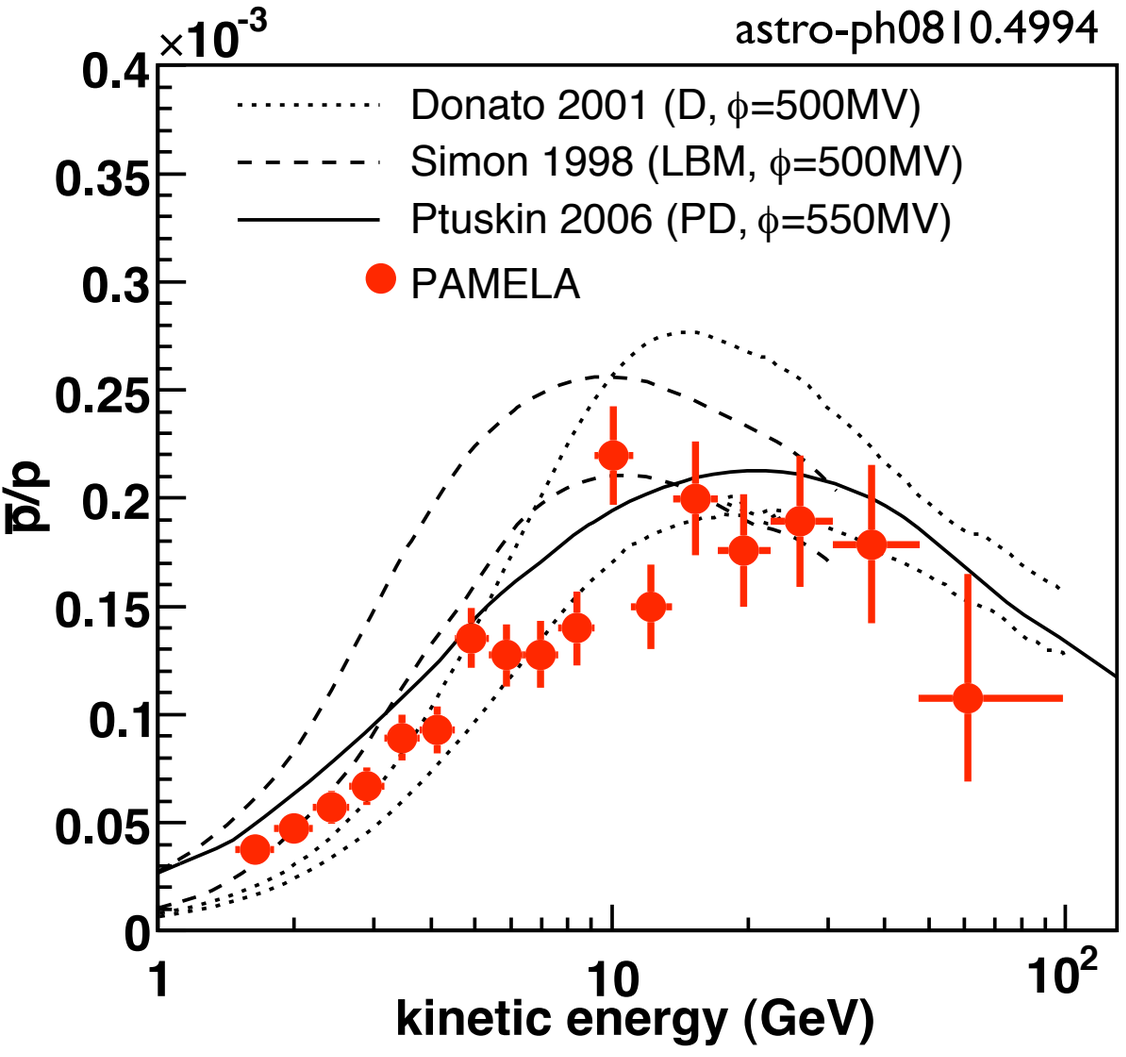

$\bar{p}$ produced in evaporation of primordial BH, annihilation of SUSY particles?

No: pure secondary production

http://pamela.roma2.infn.it

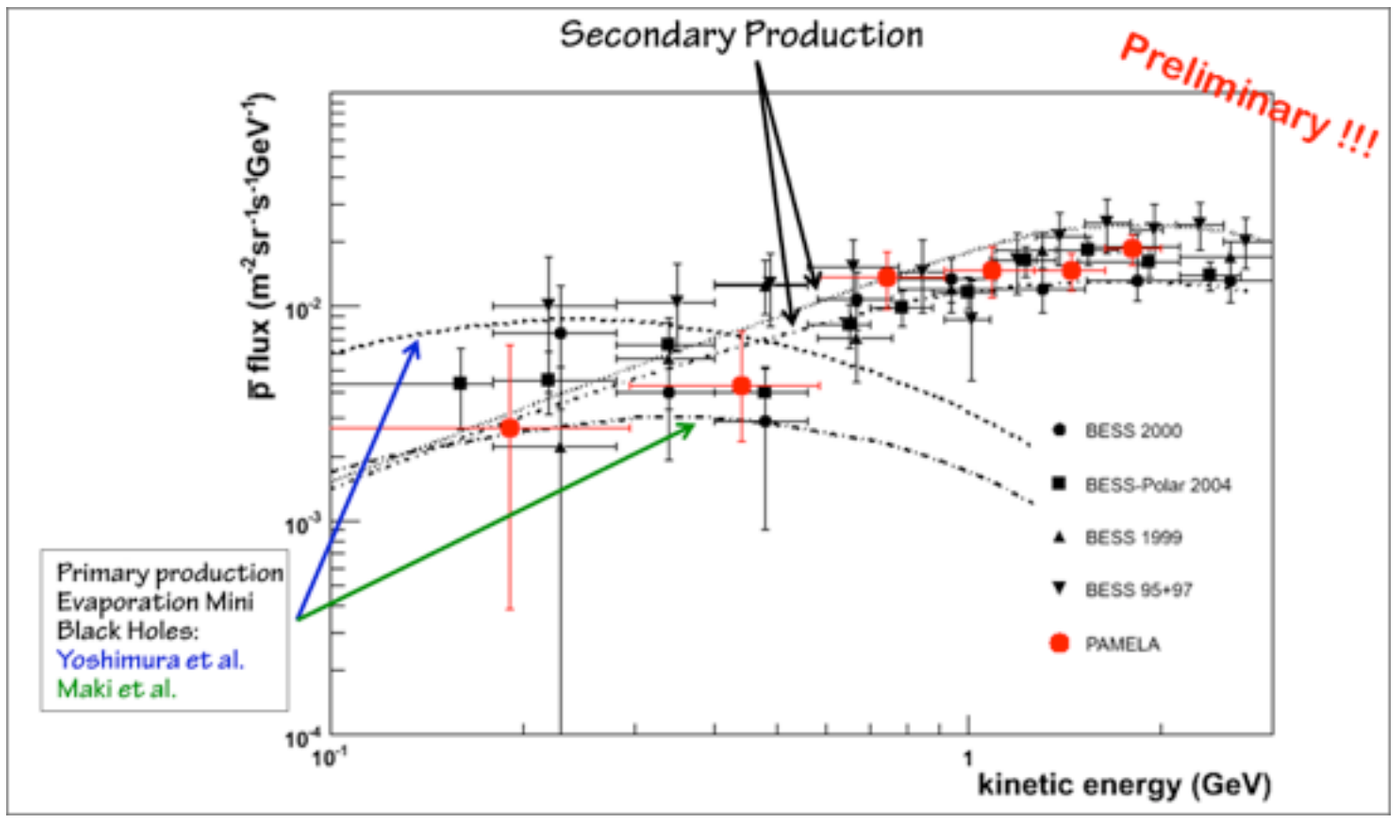

so: all appears well with antiprotons. What about positrons?

Positron excess? What positron excess? (INTEGRAL)

Galactic core signal well explained by ‘standard’ causes

http://www.physto.se/~edsjo/talks/pdf/Positron-excess-020903.pdf

Supersymmetric causes are dead....

..... long live supersymmetric causes:

“Observation of an anomalous positron abundance in the cosmic radiation”

Abstract. Recently published results from the PAMELA experiment have shown conclusive evidence for an excess of positrons at high ($\sim 10 - 100$ GeV) energies, confirming earlier indications from HEAT and AMS-01. Such a signal is generally expected from dark matter annihilations. However, the hard positron spectrum and large amplitude are difficult to achieve in most conventional WIMP models. The absence of any associated excess in anti-protons is highly constraining on models with hadronic annihilation modes. We revisit an earlier proposal, wherein the dark matter annihilates into a new light ($\lesssim$ GeV) boson ϕ, which is kinematically constrained to go to hard leptonic states, without anti-protons or π^0’s. We find this provides a very good fit to the data. The light boson naturally provides a mechanism by which large cross sections can be achieved through the Sommerfeld enhancement, as was recently proposed. Depending on the mass of the WIMP, the rise may continue above 300 GeV, the extent of PAMELA’s ability to discriminate between electrons and positrons.

Positron excess? What positron excess? (INTEGRAL)

Galactic core signal well explained by ‘standard’ causes

http://www.physto.se/~edsjo/talks/pdf/Positron-excess-020903.pdf

Supersymmetric causes are dead....

..... long live supersymmetric causes:

“Observation of an anomalous positron abundance in the cosmic radiation”

http://arxiv.org/abs/0810.4995

Abstract. Recently published results from the PAMELA experiment have shown conclusive evidence for an excess of positrons at high ($\sim 10 - 100$ GeV) energies, confirming earlier indications from HEAT and AMS-01. Such a signal is generally expected from dark matter annihilations. However, the hard positron spectrum and large amplitude are difficult to achieve in most conventional WIMP models. The absence of any associated excess in anti-protons is highly constraining on models with hadronic annihilation modes. We revisit an earlier proposal, wherein the dark matter annihilates into a new light ($\lesssim$ GeV) boson ϕ, which is kinematically constrained to go to hard leptonic states, without anti-protons or π^0’s. We find this provides a very good fit to the data. The light boson naturally provides a mechanism by which large cross sections can be achieved through the Sommerfeld enhancement, as was recently proposed. Depending on the mass of the WIMP, the rise may continue above 300 GeV, the extent of PAMELA’s ability to discriminate between electrons and positrons.

suggestive, but inconclusive
data before PAMELA

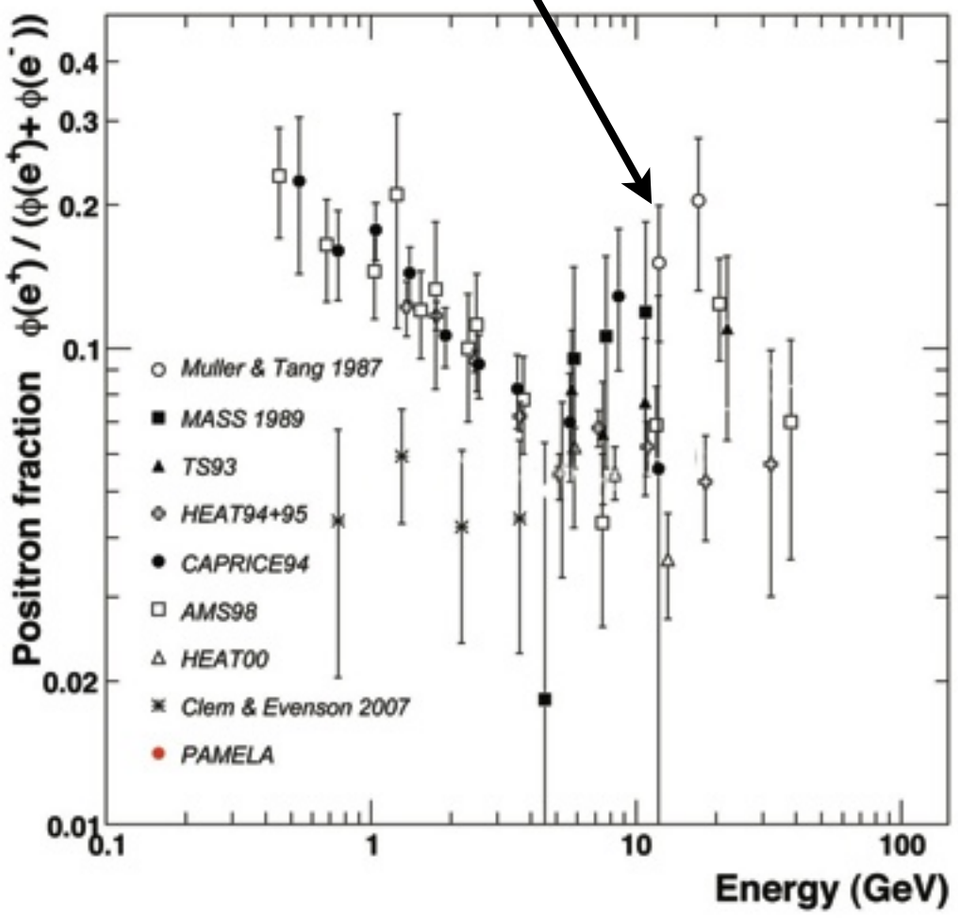

FIG. 3: **PAMELA positron fraction with other experimental data.** The positron fraction measured by the PAMELA experiment compared with other recent experimental data[24, 29, 30, 31, 32, 33, 34, 35]. One standard deviation error bars are shown. If not visible, they lie inside the data points.

suggestive, but inconclusive
data before PAMELA

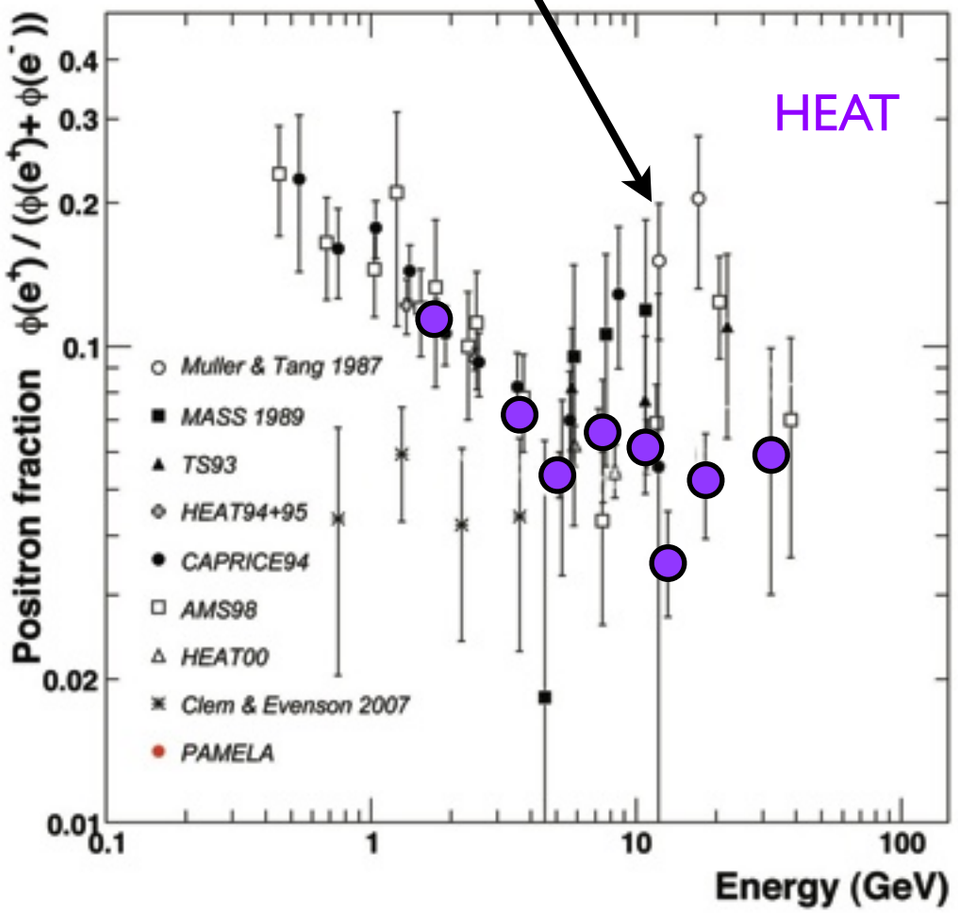

FIG. 3: **PAMELA positron fraction with other experimental data.** The positron fraction measured by the PAMELA experiment compared with other recent experimental data[24, 29, 30, 31, 32, 33, 34, 35]. One standard deviation error bars are shown. If not visible, they lie inside the data points.

suggestive, but inconclusive
data before PAMELA

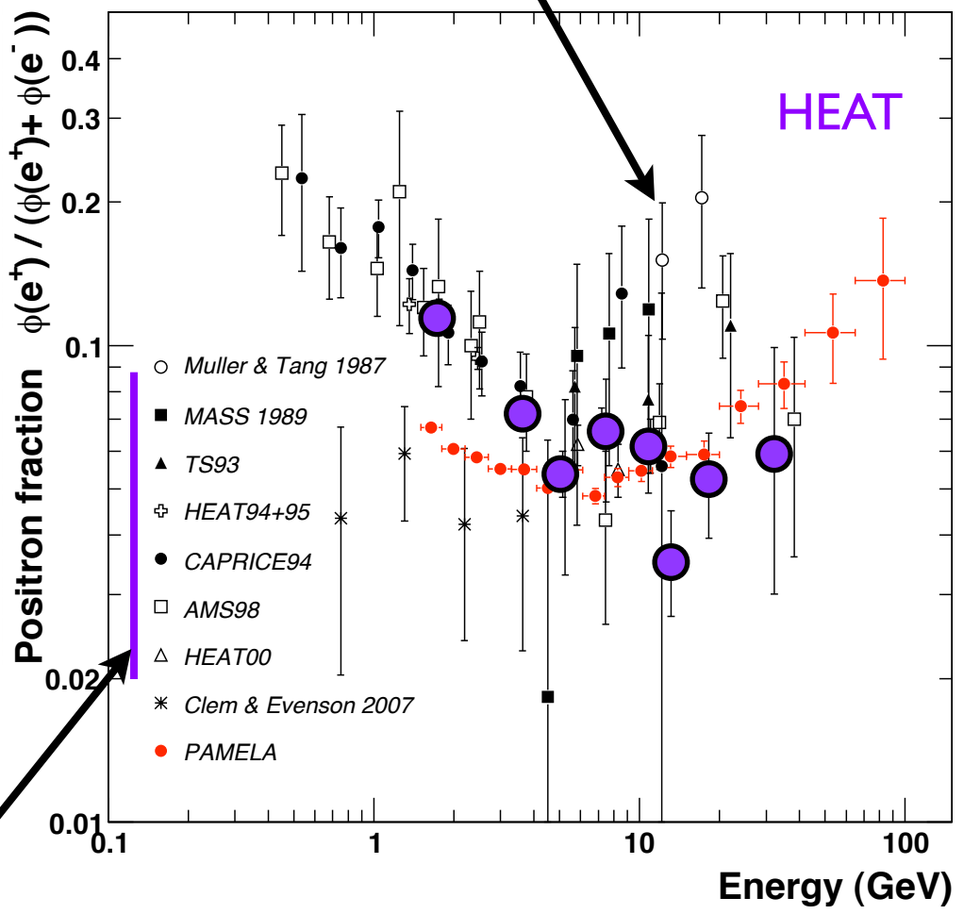

balloon experiments

FIG. 3: **PAMELA positron fraction with other experimental data.** The positron fraction measured by the PAMELA experiment compared with other recent experimental data[24, 29, 30, 31, 32, 33, 34, 35]. One standard deviation error bars are shown. If not visible, they lie inside the data points.

theoretical calculation for pure secondary production of
positrons during propagation of cosmic rays in the galaxy

Adriani et al., Nature 458, 607-609 (2009)

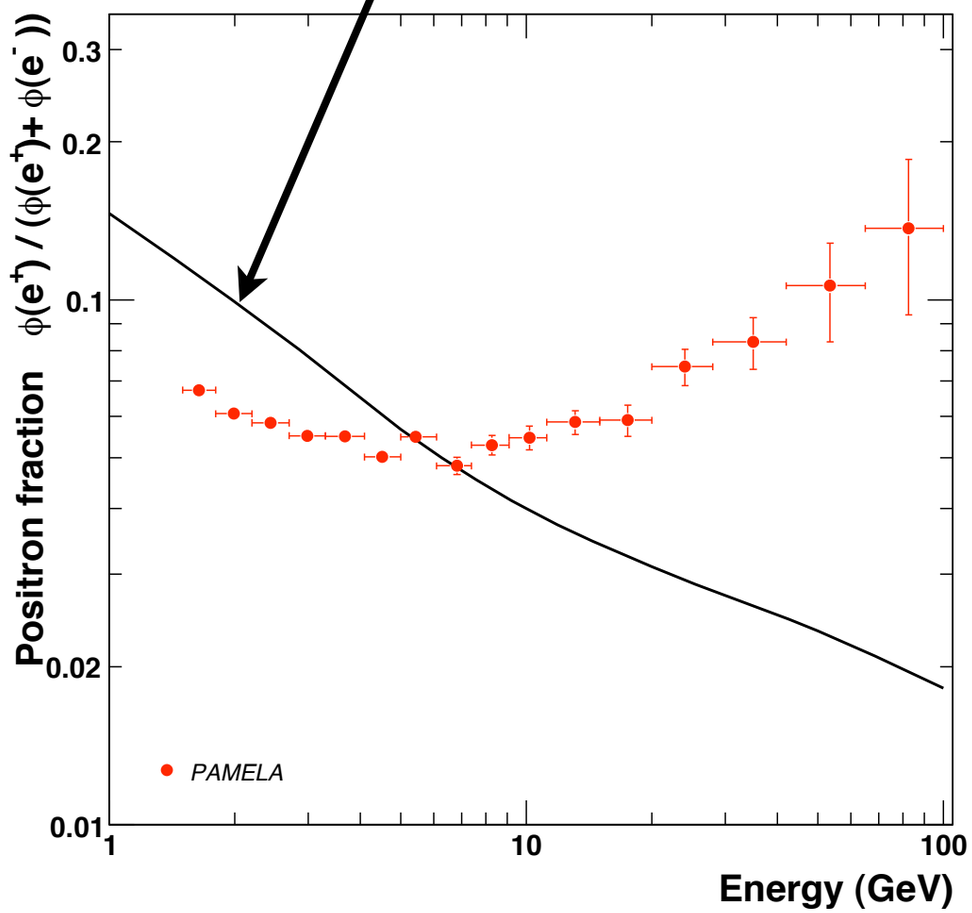

FIG. 4: **PAMELA positron fraction with theoretical models.** The PAMELA positron fraction compared with theoretical model. The solid line shows a calculation by Moskalenko & Strong[39] for pure secondary production of positrons during the propagation of cosmic-rays in the galaxy. One standard deviation error bars are shown. If not visible, they lie inside the data points.

PAMELA

http://arxiv.org/abs/0808.3725

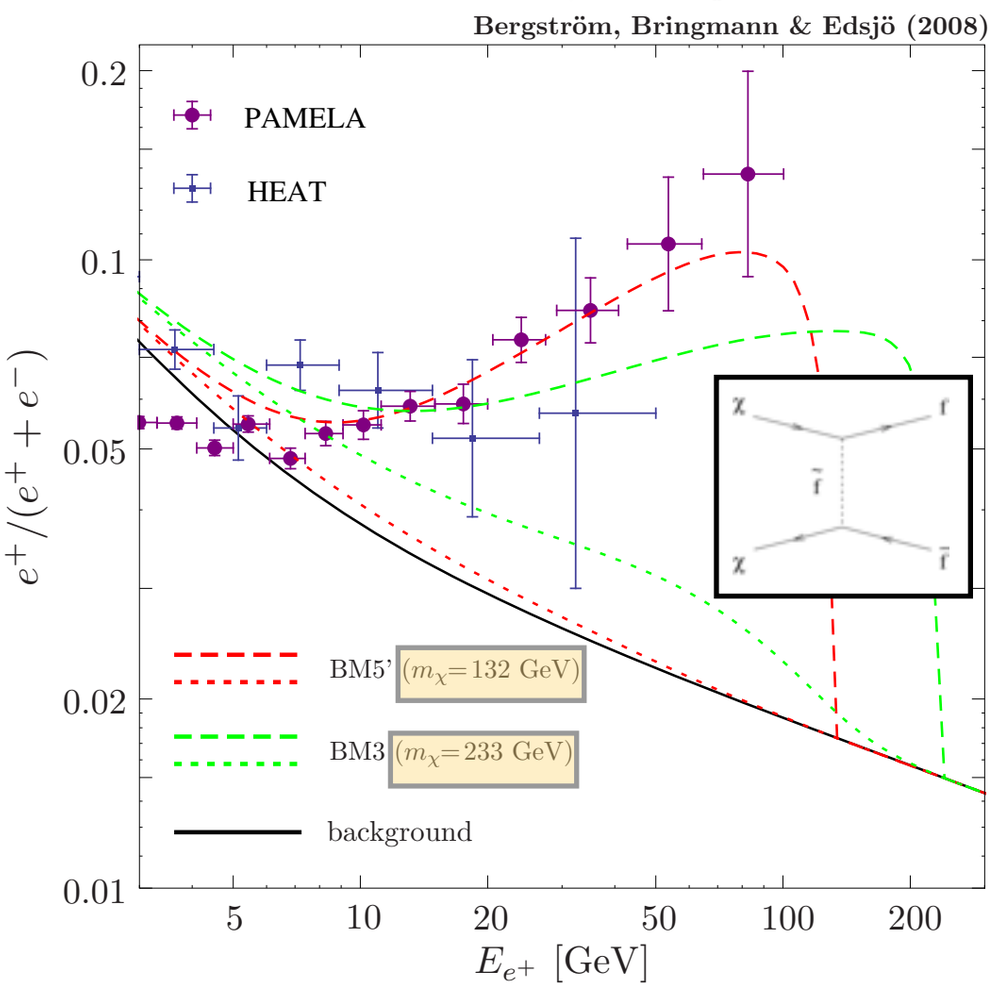

Figure 8. *The solid line is the expected flux ratio $e^+/(e^+ + e^-)$ as calculated following standard secondary production. The data points are the combined HEAT and PAMELA data. The expected flux ratio is shown without (dotted lines) and after taking into account radiative corrections (dashed lines) [11].*

http://iopscience.iop.org/1742-6596/203/1/012021/pdf/1742-6596_203_1_012021.pdf

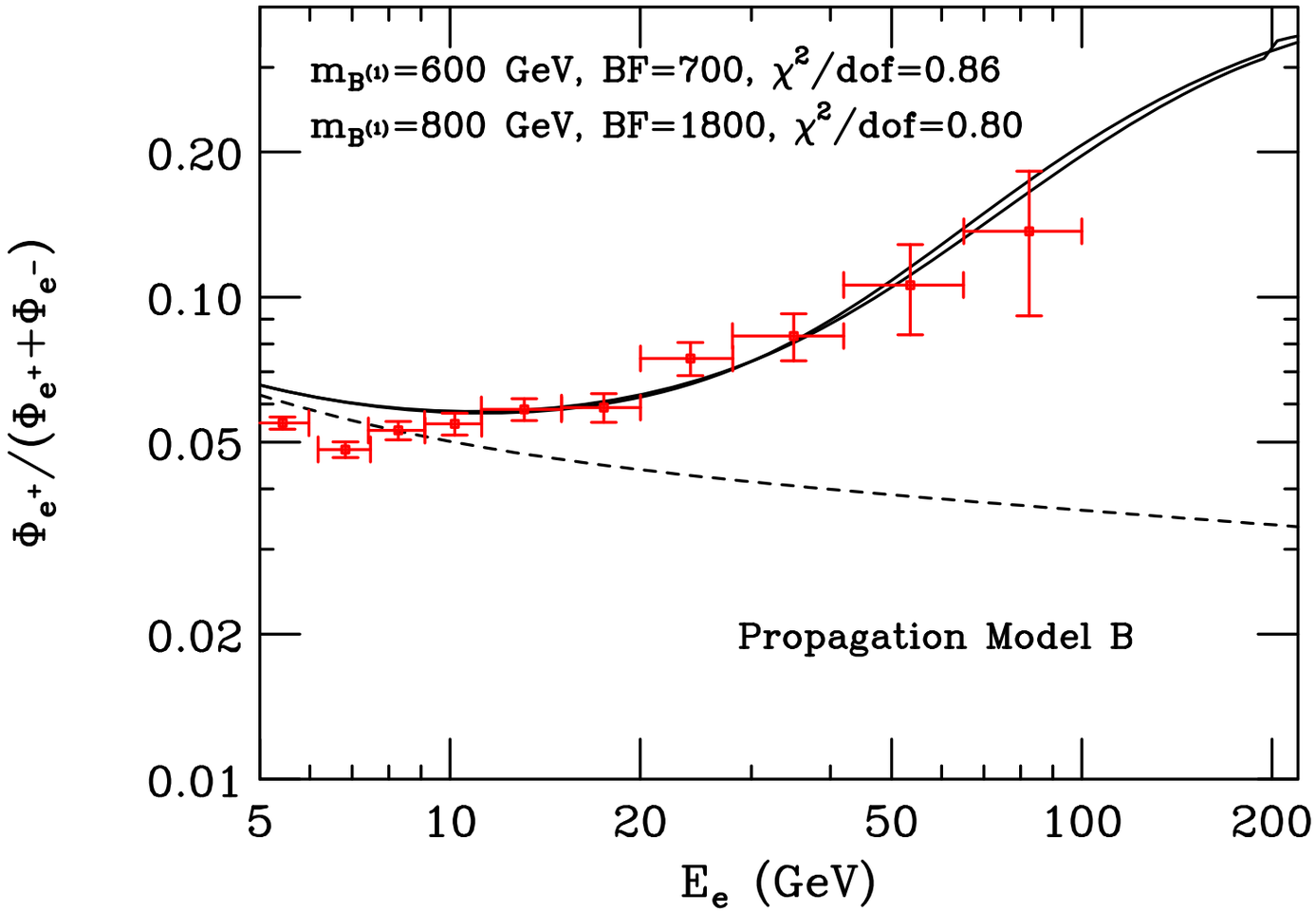

Figure 9. *The positron fraction as a function of energy including contributions from Kaluza-Klein dark matter annihilations, compared to the measurements of the PAMELA experiment. Results are shown for dark matter masses of 600 GeV and 800 GeV, and for one propagation model. The dashed line denotes the positron fraction with no contribution from dark matter (secondary positron production only) [12].*

PAMELA

http://arxiv.org/abs/0808.3725

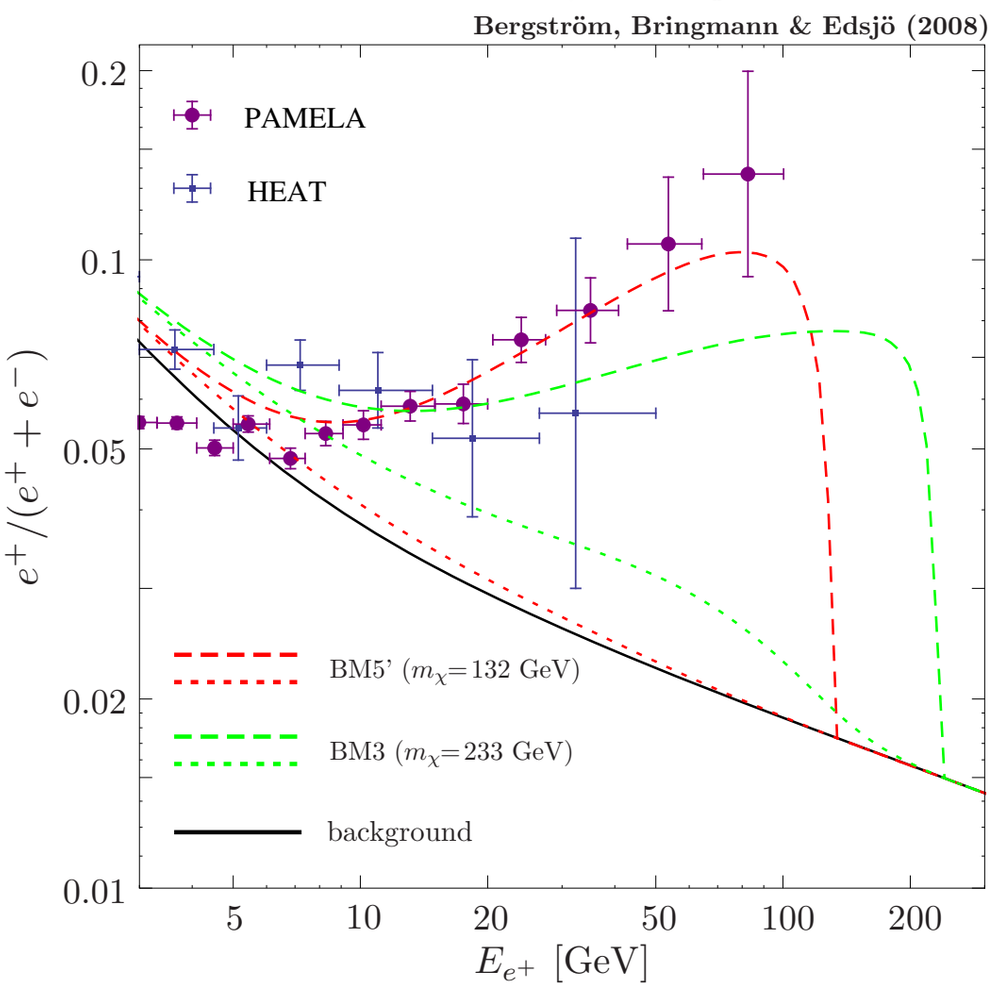

Figure 8. *The solid line is the expected flux ratio $e^+/(e^+ + e^-)$ as calculated following standard secondary production. The data points are the combined HEAT and PAMELA data. The expected flux ratio is shown without (dotted lines) and after taking into account radiative corrections (dashed lines) [11].*

http://iopscience.iop.org/1742-6596/203/1/012021/pdf/1742-6596_203_1_012021.pdf

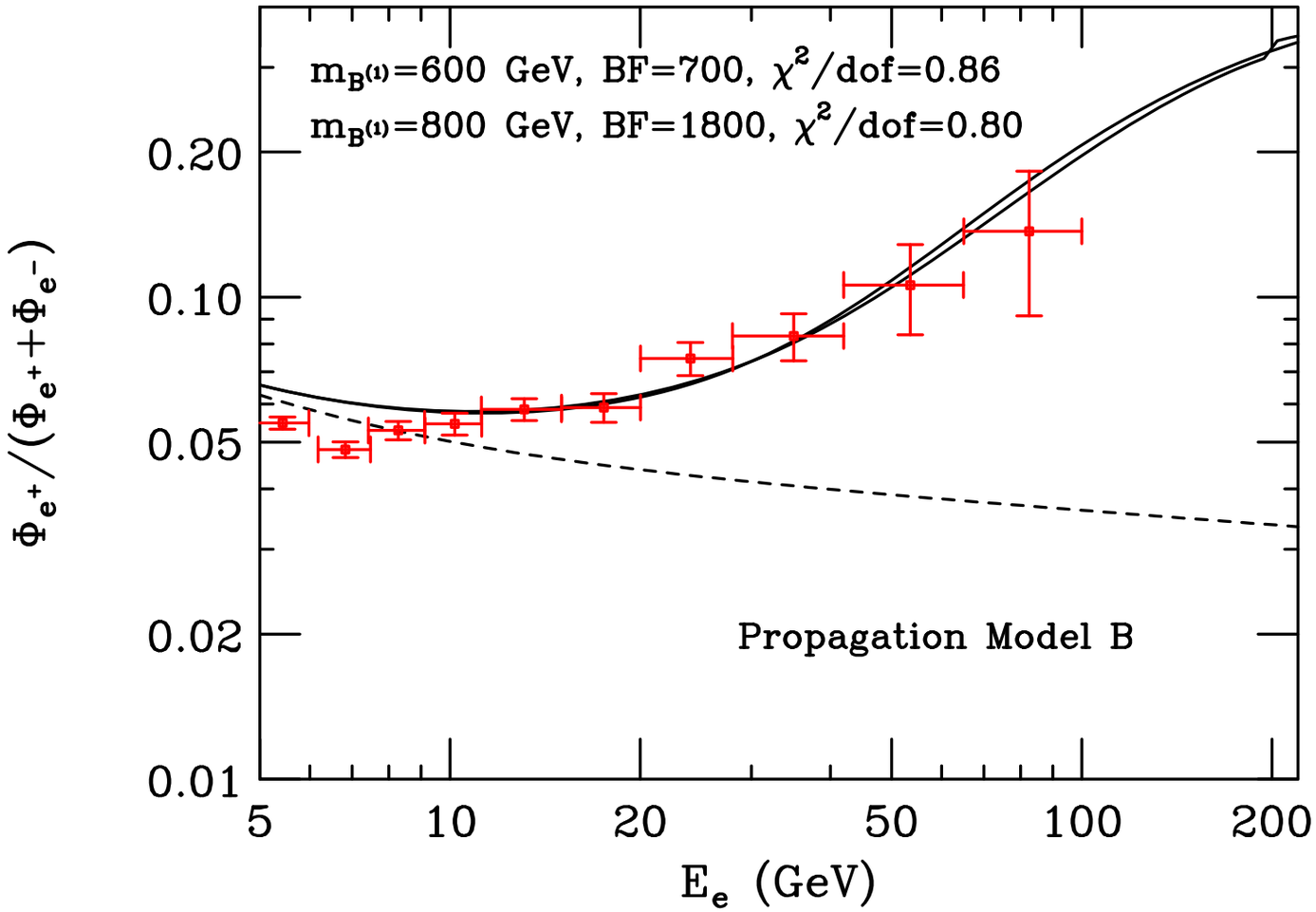

Figure 9. *The positron fraction as a function of energy including contributions from Kaluza-Klein dark matter annihilations, compared to the measurements of the PAMELA experiment. Results are shown for dark matter masses of 600 GeV and 800 GeV, and for one propagation model. The dashed line denotes the positron fraction with no contribution from dark matter (secondary positron production only) [12].*

PAMELA

A rise in the positron fraction at high energy has been postulated for the annihilation of dark matter particles in the galactic halo[5, 6, 7, 8, 9, 10, 11]. The production of positrons through pair production processes in the magnetosphere of near-by pulsars would also yield a similar positron signature[16, 17, 18, 19, 20]. We note, however, that none of the published models fit our data well and the reason for the rise remains unexplained.

next step: AMS

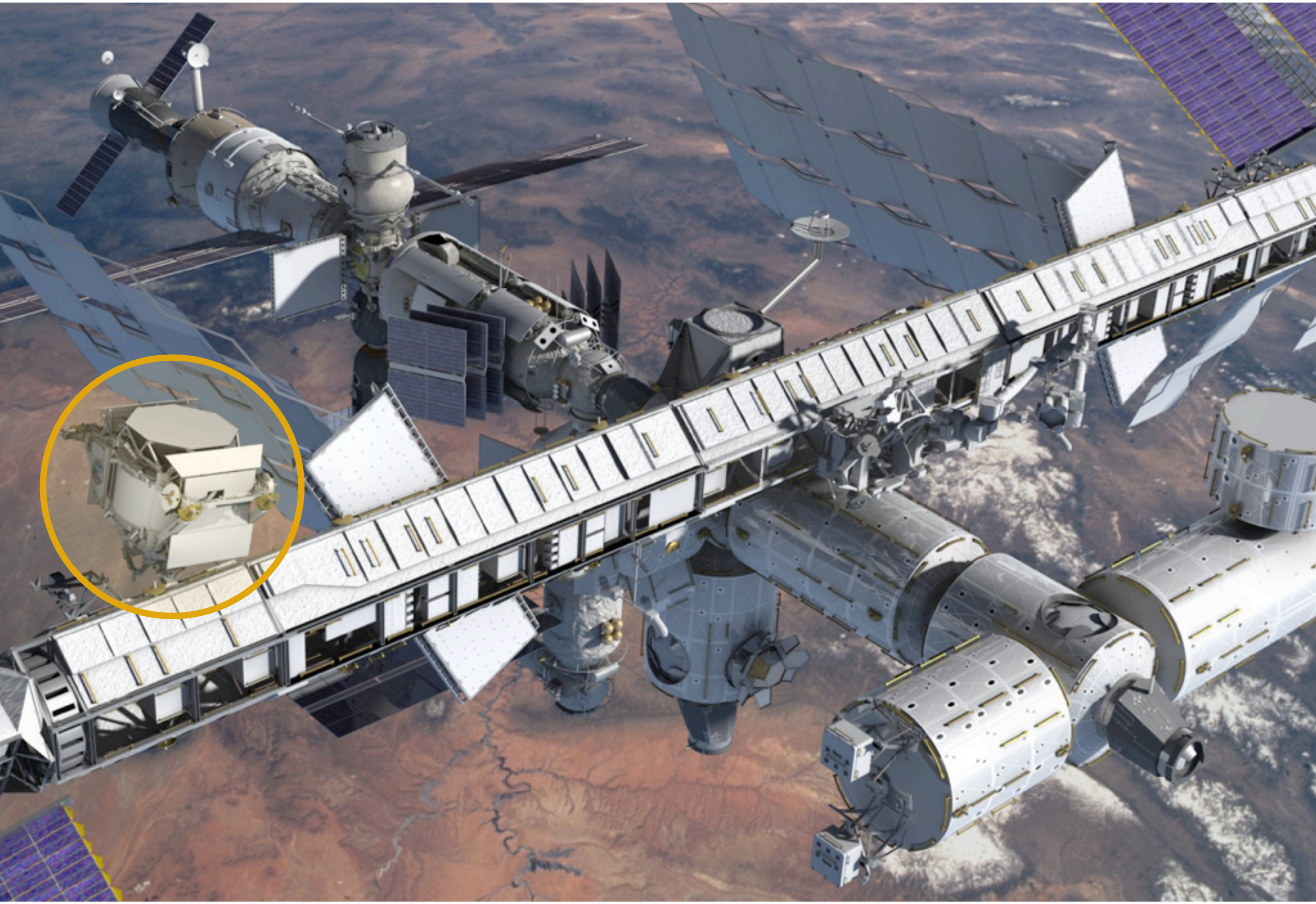

Lectures on Antimatter

Michael Doser / CERN

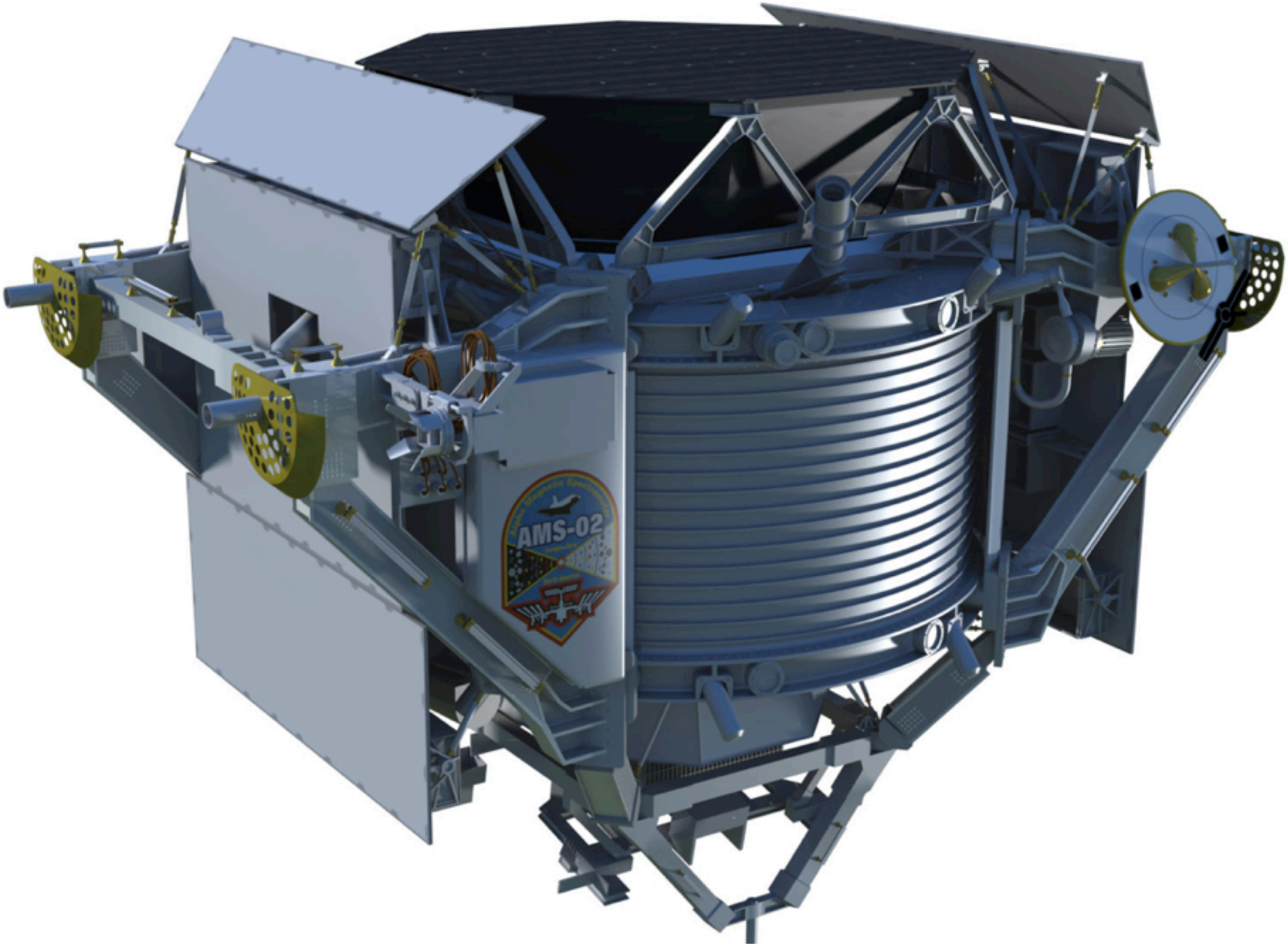
AMS-02

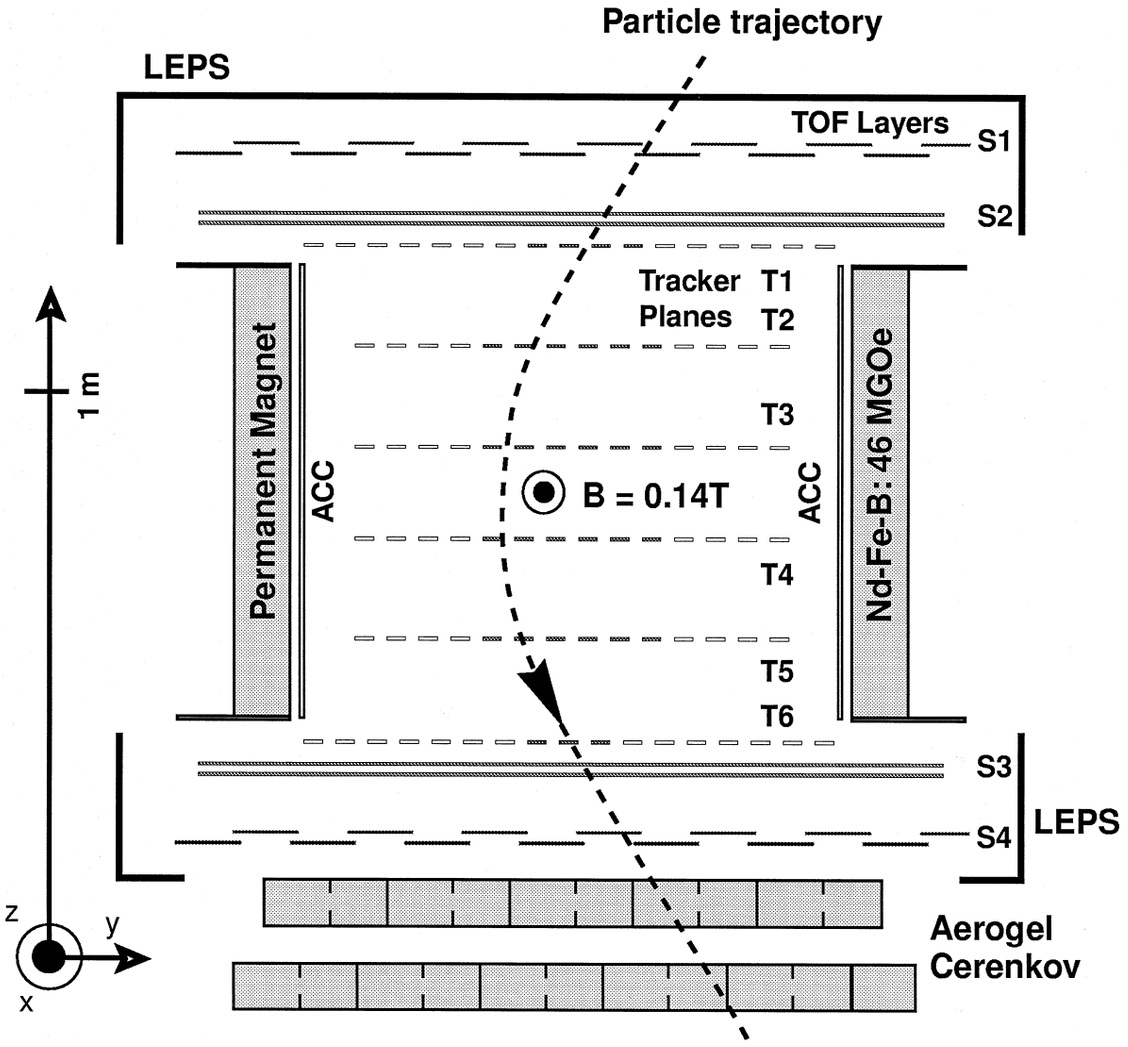

Trigger: hits in all 4 TOF planes

Track fit: determine particle 'rigidity'

Beta and direction from TOF

|Z| from energy loss in TOF, tracker

search for Z=-2 (He)

Fig. 1. Schematic view of AMS as flown on STS-91 showing the cylindrical permanent magnet, the silicon microstrip tracker planes T1 to T6, the time of flight (TOF) hodoscope layers S1 to S4, the aerogel cerenkov counter, the anticoincidence counters (ACC) and low energy particle shields (LEPS).

Main background: the huge numbers of p; e (|Z|=1) & He (Z=2) that can be multiple-scattered

Select |Z|=2 (p' of error ~ 10^{-7})

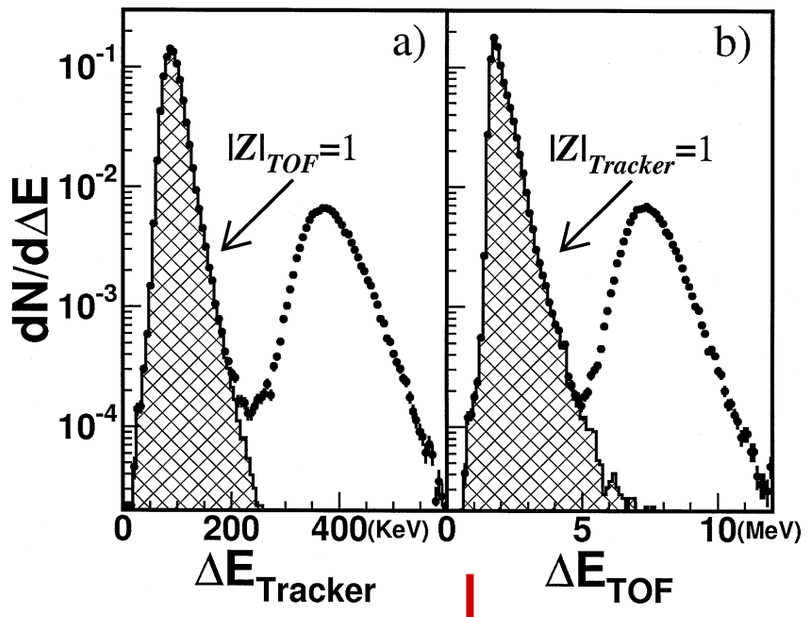

Fig. 4. Energy loss measurements (points) are made independently in the tracker (a) and TOF (b) for $|Z| \leq 2$ events. The hatched histogram shows which events were assigned to be $|Z| = 1$ by the other detector.

Remove background

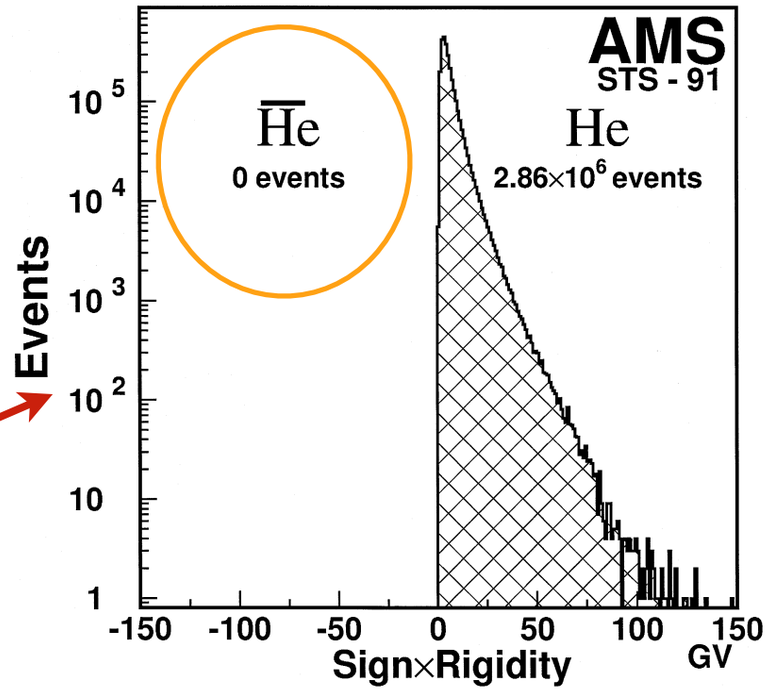

Measured rigidity times the charge sign for selected |Z| = 2 events

Determine sign

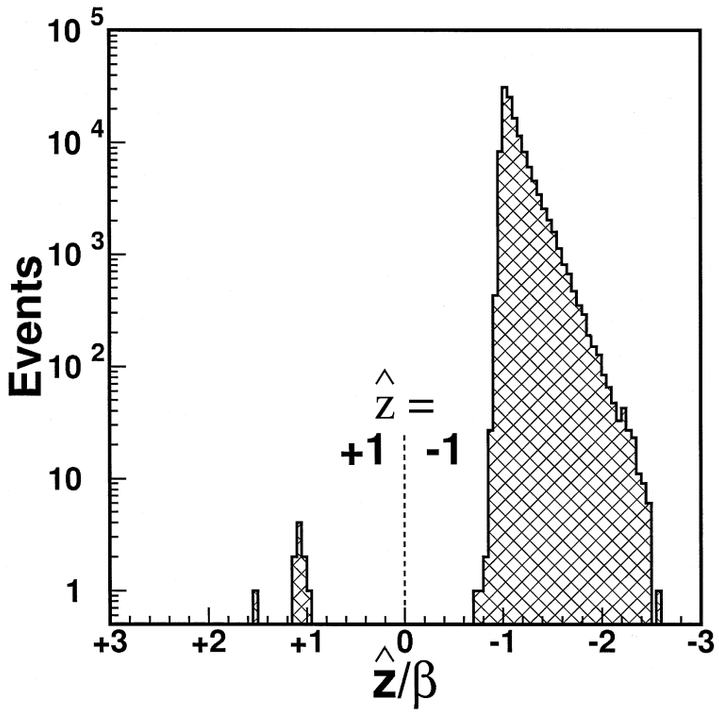

Fig. 5. A typical direction, $\hat{z}/\beta$, distribution for $|Z| = 2$ events. As seen, the $\hat{z} = +1$ (or upward) and $\hat{z} = -1$ (or downward) populations are clearly separated.

J. Alcaraz et al. / Physics Letters B 461 (1999) 387–396

Outlook

AMS: launched a few years ago on the last flight of the space shuttle, will collect data for several years, reaching 10^{-9} sensitivity to antiprotons

The real question is how sensitive, and up to which momenta, AMS is to positrons, so that the PAMELA signal can be verified and explored further. With the reduced magnetic field, its sensitivity appears limited to 50 GeV ...

Nuclear Physics B (Proc. Suppl.) 173 (2007) 51–55

Outlook

AMS: launched a few years ago on the last flight of the space shuttle, will collect data for several years, reaching 10^{-9} sensitivity to antiprotons

The real question is how sensitive, and up to which momenta, AMS is to positrons, so that the PAMELA signal can be verified and explored further. With the reduced magnetic field, its sensitivity appears limited to 50 GeV ...

Nuclear Physics B (Proc. Suppl.) 173 (2007) 51–55

UPDATE:

first data from AMS on ISS shown July 2012: positrons identified up to several 100 GeV!

PAMELA/Fermi signal confirmed

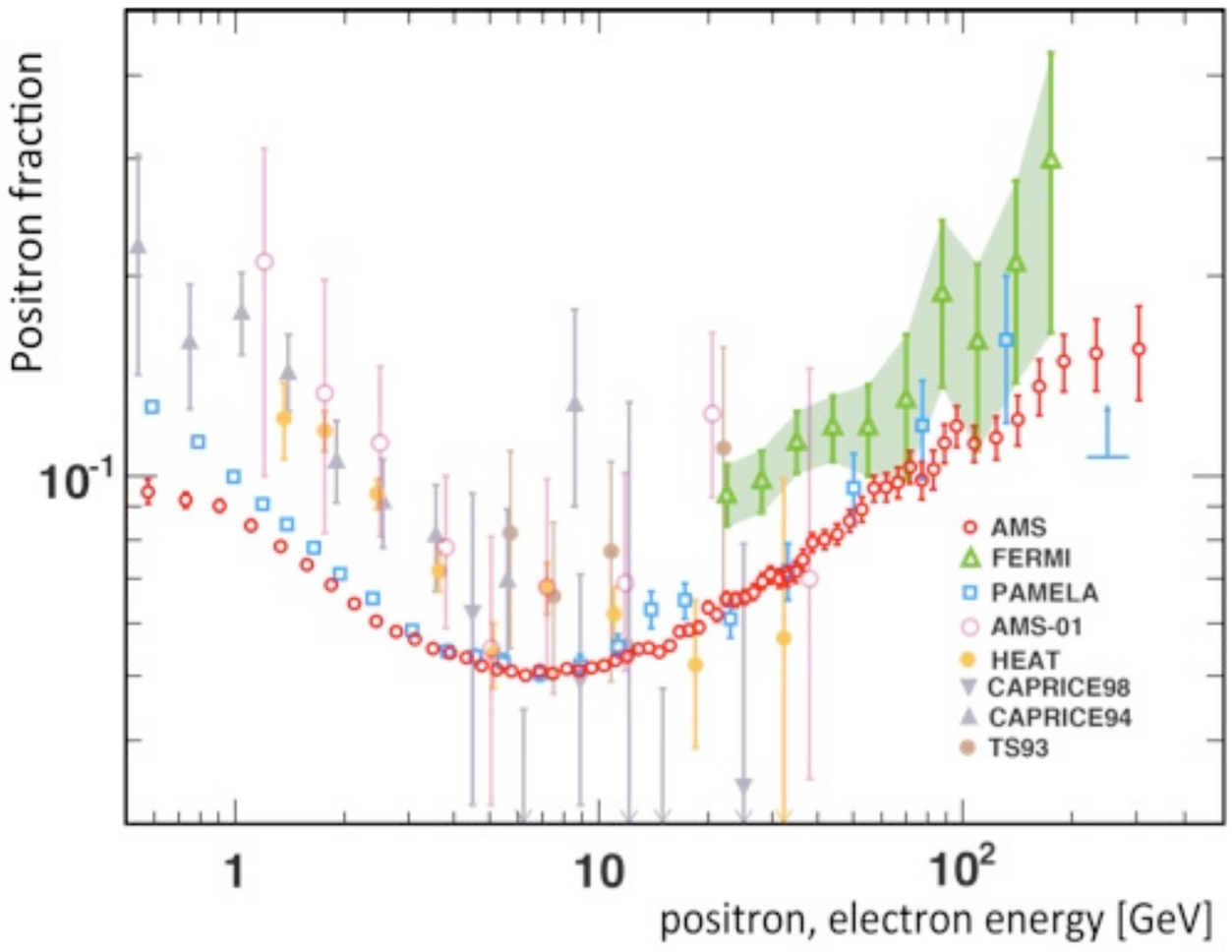

standard ("boring") astrophysical sources sufficient to explain a rise:

http://www.aanda.org/index.php?option=com_article&access=doi&doi=10.1051/0004-6361/201014225&Itemid=129

http://arxiv.org/pdf/1304.1482.pdf

is there a drop at higher energies? could then be sign of dark matter...

Spectral index: electron/positron spectra

$$\gamma_{e^\pm} = d[\log(\Phi_{e^\pm})]/d[\log(E)]$$ (over an energy-dependent E window)

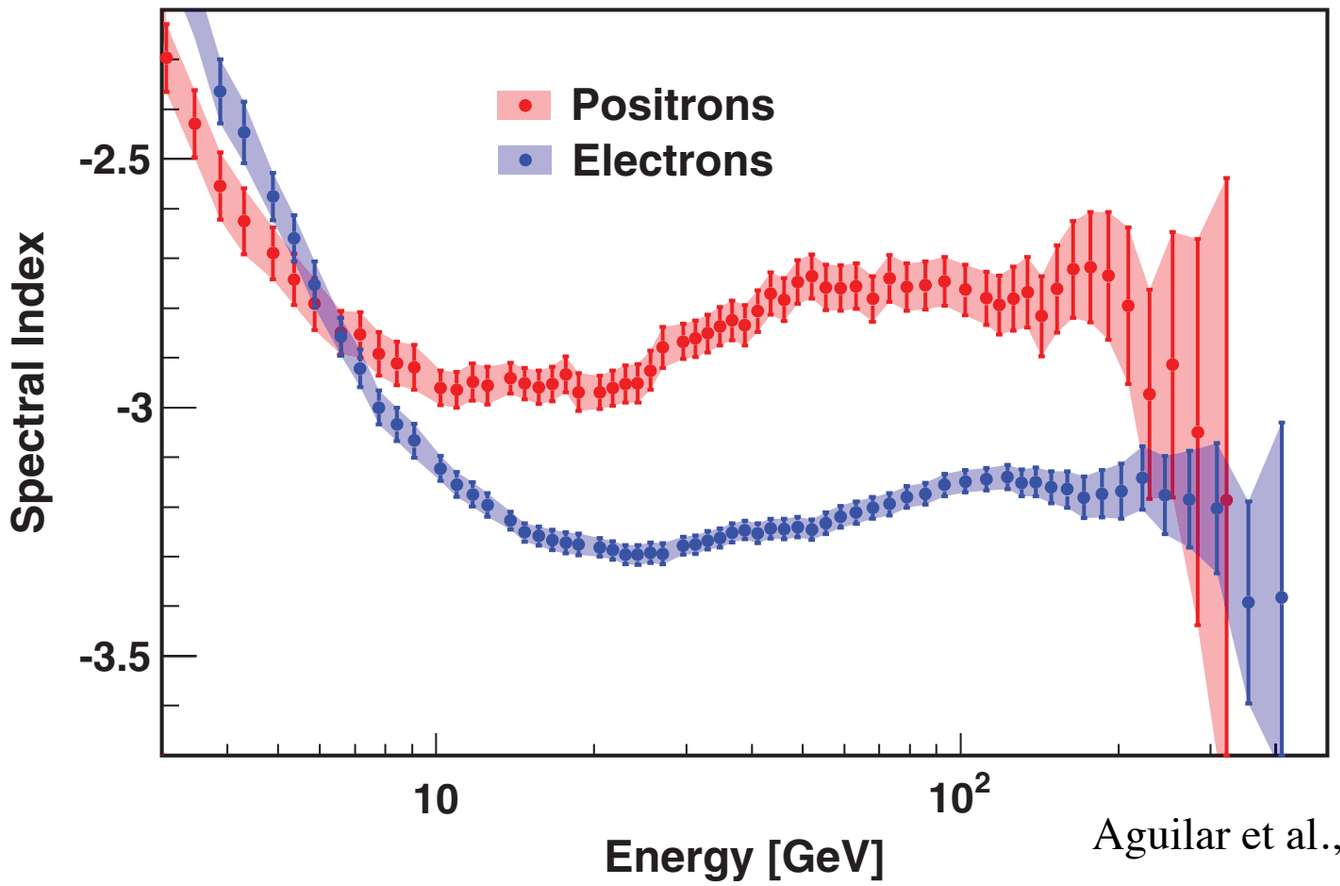

Aguilar et al.,PRL 113, 121102 (2014)

is there a drop at higher energies? could then be sign of dark matter...

stay tuned....

Overview:

1. Introduction and overview
2. Antimatter at high energies (SppS, LEP, Fermilab)
3. Meson spectroscopy (antimatter as QCD probe)

4. Astroparticle physics and cosmology
5. CP and CPT violation tests
6. Precision tests with Antihydrogen: spectroscopy

7. Precision tests with Antihydrogen:gravity
8. Applications of antimatter

Back to Earth: antimatter in the lab

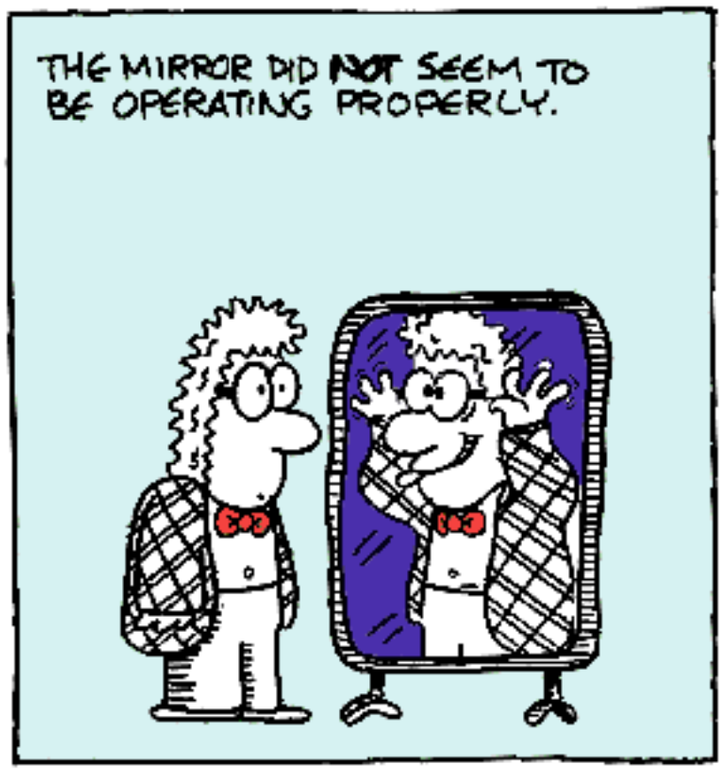

Search for some form of asymmetry between matter and antimatter : $\not{C}\not{P}$ and $\not{C}\not{P}\not{T}$

Plan A: CP violation

P violation known since 1955,

CP violation since 1964 in K^0

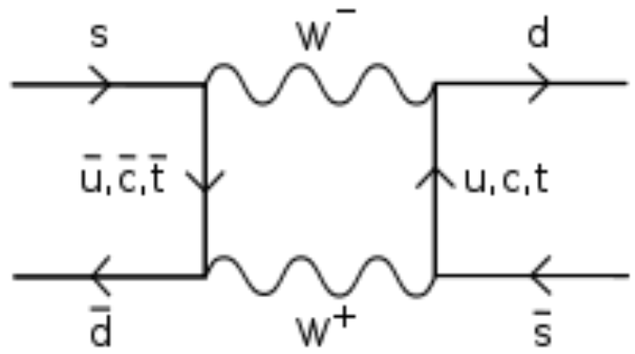

CKM matrix

CP violation in B^0 mesons (BaBar, Belle) since 2001

CP violation in D^0 mesons (LHCb) since 2011

Plan B: CPT violation

Two ways to violate CPT

- CPTV through decoherence
  - (non-unitarity; entanglement with quantum-gravity environment) - Ellis, et al.

- CPTV within quantum mechanics
  - (e.g., spontaneous Lorentz violation) Standard Model Extension (Kostelecky)

SM Lagrangian:

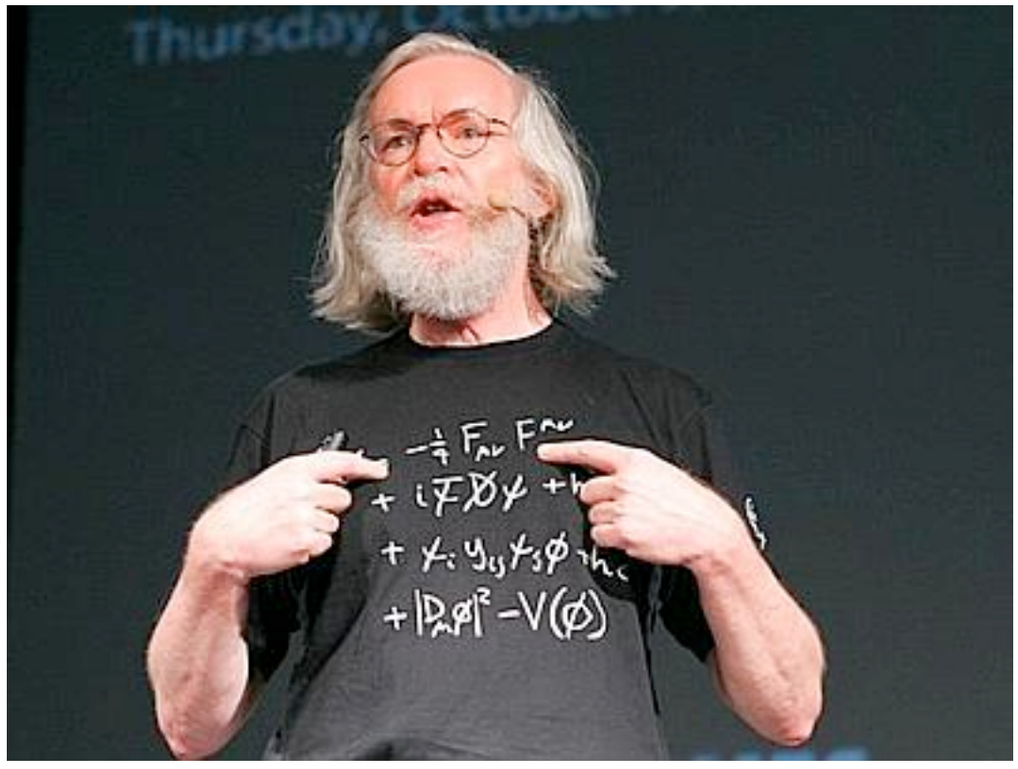

Lectures on Antimatter

Michael Doser / CERN

SME Lagrangian:

$$\mathcal{L} = \tfrac{1}{2}iee^{\mu}{}_{a}\overline{L}_{A}\gamma^{a}\overleftrightarrow{D}_{\mu}L_{A} + \tfrac{1}{2}iee^{\mu}{}_{a}\overline{R}_{A}\gamma^{a}\overleftrightarrow{D}_{\mu}R_{A} + \tfrac{1}{2}iee^{\mu}{}_{a}\overline{Q}_{A}\gamma^{a}\overleftrightarrow{D}_{\mu}Q_{A} + \tfrac{1}{2}iee^{\mu}{}_{a}\overline{U}_{A}\gamma^{a}\overleftrightarrow{D}_{\mu}U_{A} + \tfrac{1}{2}iee^{\mu}{}_{a}\overline{D}_{A}\gamma^{a}\overleftrightarrow{D}_{\mu}D_{A} - \left[(G_L)_{AB}e\overline{L}_{A}\phi R_{B} + (G_U)_{AB}e\overline{Q}_{A}\phi^{c}U_{B} + (G_D)_{AB}e\overline{Q}_{A}\phi D_{B}\right] + \text{h.c.} - e(D_{\mu}\phi)^{\dagger}D^{\mu}\phi + \mu^{2}e\phi^{\dagger}\phi$$

$$- \frac{\lambda}{3!}e(\phi^{\dagger}\phi)^{2} - \tfrac{1}{2}e\mathrm{Tr}(G_{\mu\nu}G^{\mu\nu}) - \tfrac{1}{2}e\mathrm{Tr}(W_{\mu\nu}W^{\mu\nu}) - \tfrac{1}{4}eB_{\mu\nu}B^{\mu\nu} - \tfrac{1}{2}i(c_L)_{\mu\nu AB}ee^{\mu}{}_{a}\overline{L}_{A}\gamma^{a}\overleftrightarrow{D}^{\nu}L_{B} - \tfrac{1}{2}i(c_R)_{\mu\nu AB}ee^{\mu}{}_{a}\overline{R}_{A}\gamma^{a}\overleftrightarrow{D}^{\nu}R_{B} - (a_L)_{\mu AB}ee^{\mu}{}_{a}\overline{L}_{A}\gamma^{a}L_{B} - (a_R)_{\mu AB}ee^{\mu}{}_{a}\overline{R}_{A}\gamma^{a}R_{B}$$

$$-\tfrac{1}{2}i(c_Q)_{\mu\nu AB}ee^{\mu}{}_{a}\overline{Q}_{A}\gamma^{a}\overleftrightarrow{D}^{\nu}Q_{B} - \tfrac{1}{2}i(c_U)_{\mu\nu AB}ee^{\mu}{}_{a}\overline{U}_{A}\gamma^{a}\overleftrightarrow{D}^{\nu}U_{B} - \tfrac{1}{2}i(c_D)_{\mu\nu AB}ee^{\mu}{}_{a}\overline{D}_{A}\gamma^{a}\overleftrightarrow{D}^{\nu}D_{B} - (a_Q)_{\mu AB}ee^{\mu}{}_{a}\overline{Q}_{A}\gamma^{a}Q_{B} - (a_U)_{\mu AB}ee^{\mu}{}_{a}\overline{U}_{A}\gamma^{a}U_{B} - (a_D)_{\mu AB}ee^{\mu}{}_{a}\overline{D}_{A}\gamma^{a}D_{B} - \tfrac{1}{2}\left[(H_L)_{\mu\nu AB}ee^{\mu}{}_{a}e^{\nu}{}_{b}\overline{L}_{A}\phi\sigma^{ab}R_{B}\right.$$

$$\left. + (H_U)_{\mu\nu AB}ee^{\mu}{}_{a}e^{\nu}{}_{b}\overline{Q}_{A}\phi^{c}\sigma^{ab}U_{B} + (H_D)_{\mu\nu AB}ee^{\mu}{}_{a}e^{\nu}{}_{b}\overline{Q}_{A}\phi\sigma^{ab}D_{B}\right] + \text{h.c.} - \tfrac{1}{2}(k_{\phi W})^{\mu\nu}e\phi^{\dagger}W_{\mu\nu}\phi - \tfrac{1}{2}(k_{\phi B})^{\mu\nu}e\phi^{\dagger}\phi B_{\mu\nu} + i(k_{\phi})^{\mu}e\phi^{\dagger}D_{\mu}\phi + \text{h.c.}$$

$$+\tfrac{1}{2}(k_{\phi\phi})^{\mu\nu}e(D_{\mu}\phi)^{\dagger}D_{\nu}\phi + \text{h.c.} - \tfrac{1}{4}(k_B)_{\kappa\lambda\mu\nu}eB^{\kappa\lambda}B^{\mu\nu} - \tfrac{1}{2}(k_G)_{\kappa\lambda\mu\nu}e\mathrm{Tr}(G^{\kappa\lambda}G^{\mu\nu}) - \tfrac{1}{2}(k_W)_{\kappa\lambda\mu\nu}e\mathrm{Tr}(W^{\kappa\lambda}W^{\mu\nu}) + (k_3)_{\kappa}\epsilon^{\kappa\lambda\mu\nu}e\mathrm{Tr}(G_{\lambda}G_{\mu\nu} + \tfrac{2}{3}ig_3G_{\lambda}G_{\mu}G_{\nu}) + (k_2)_{\kappa}\epsilon^{\kappa\lambda\mu\nu}e\mathrm{Tr}(W_{\lambda}W_{\mu\nu}$$

$$+ \tfrac{2}{3}igW_{\lambda}W_{\mu}W_{\nu}) + (k_1)_{\kappa}\epsilon^{\kappa\lambda\mu\nu}eB_{\lambda}B_{\mu\nu} + (k_0)_{\kappa}eB^{\kappa} + \frac{1}{16\pi G_N}\left[e(1-u)R - 2e\Lambda + es^{\mu\nu}R_{\mu\nu} + et^{\kappa\lambda\mu\nu}R_{\kappa\lambda\mu\nu}\right]$$

Kostelecký, PRD **69**, 105009 (2004)

Type II: "Model" for CPTV: standard model extention SME

CPT violation and the standard model

Don Colladay and V. Alan Kostelecký
Department of Physics, Indiana University, Bloomington, Indiana 47405
(Received 22 January 1997)

CPT & Lorentz violation

Modified Dirac eq. in SME

$$(i\gamma^\mu D_\mu - m_e - a_\mu^e\gamma^\mu - b_\mu^e\gamma_5\gamma^\mu - \tfrac{1}{2}H_{\mu\nu}^e\sigma^{\mu\nu} + ic_{\mu\nu}^e\gamma^\mu D^\nu + id_{\mu\nu}^e\gamma_5\gamma^\mu D^\nu)\psi = 0\,.$$

Lorentz violation

- Spontaneous Lorentz symmetry breaking by (exotic) string vacua
- Note: there is a preferred frame, sidereal variation due to earth rotation may be detectable

Verifications of CPT symmetry

Tests of particle/antiparticle symmetry (PDG)

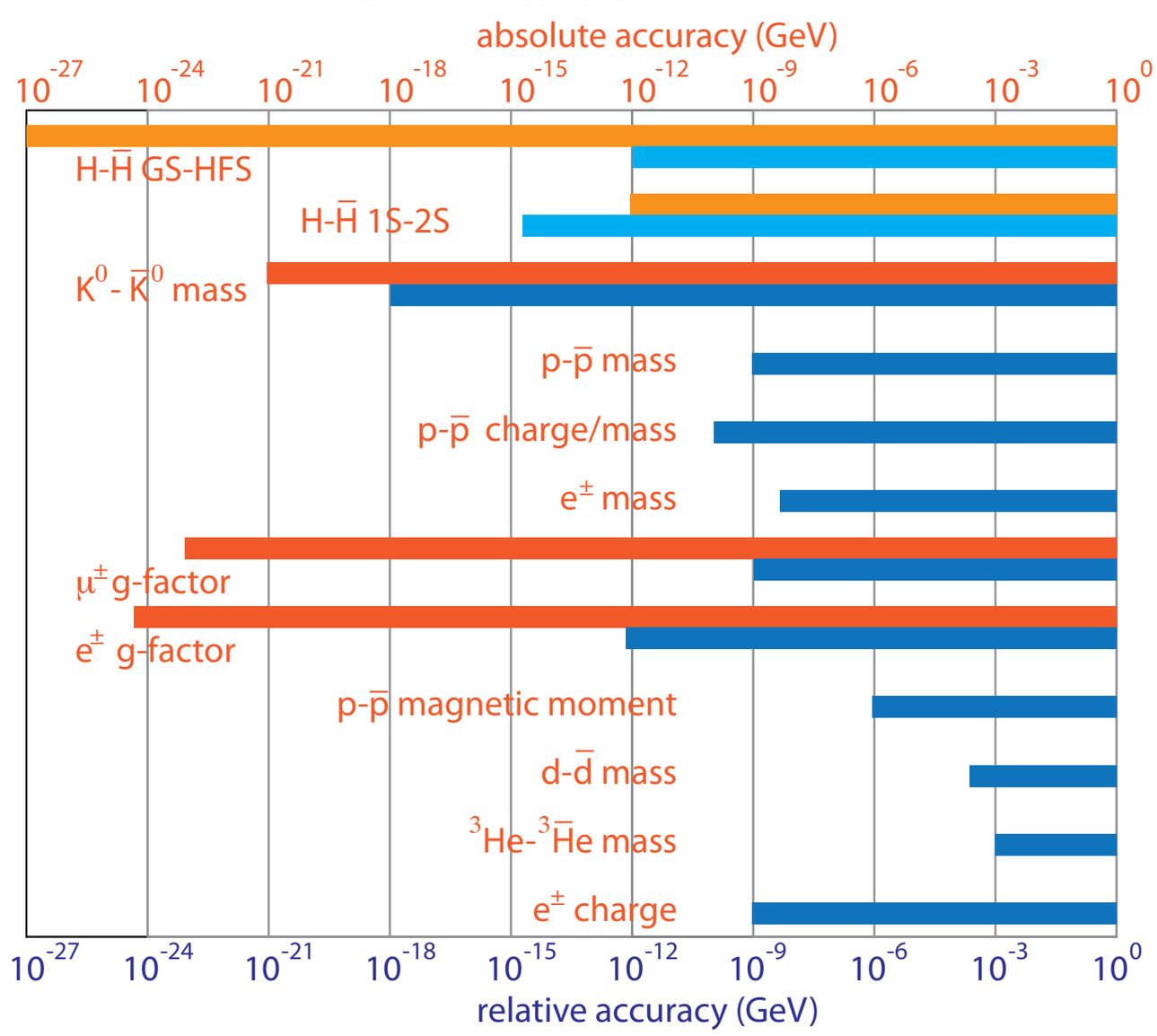

Inconsistent definition of figure of merit: comparison difficult

Pattern of CPT violation unknown (P: weak interaction; CP: mesons)

Absolute energy scale: standard model extension (Kostelecky)

AD: Antimatter Factory

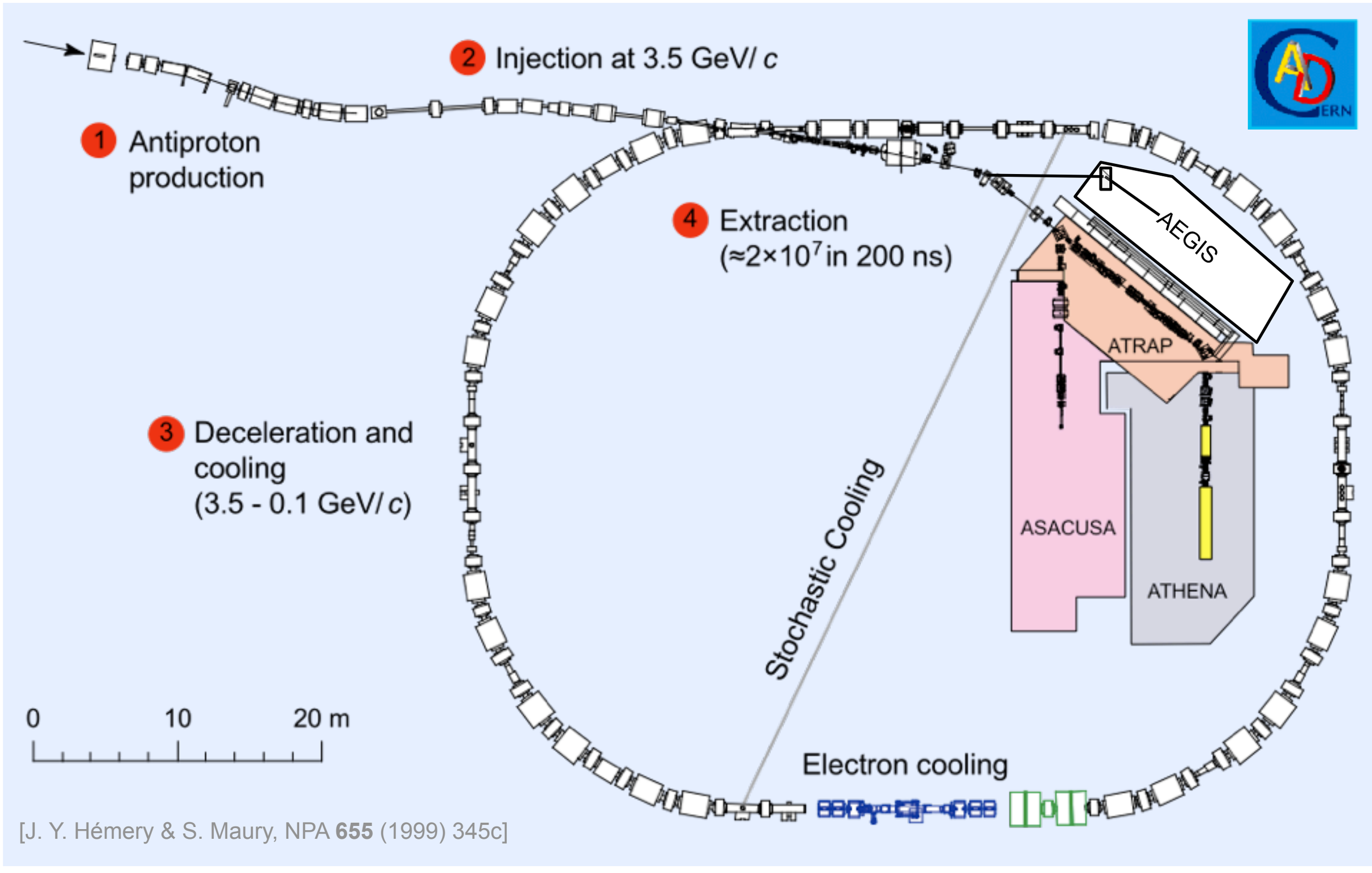

[J. Y. Hémery & S. Maury, NPA **655** (1999) 345c]

1) q/m measurement of the (anti)proton

In a magnetic field, charged particles follow cyclotron orbits:

$$\omega_c = Bq/m$$

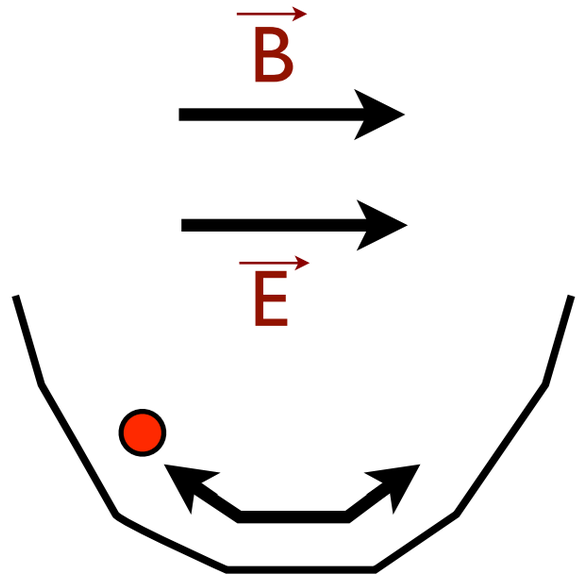

Add an electrical potential well:

$$\omega_z^2 = Vq/md^2$$

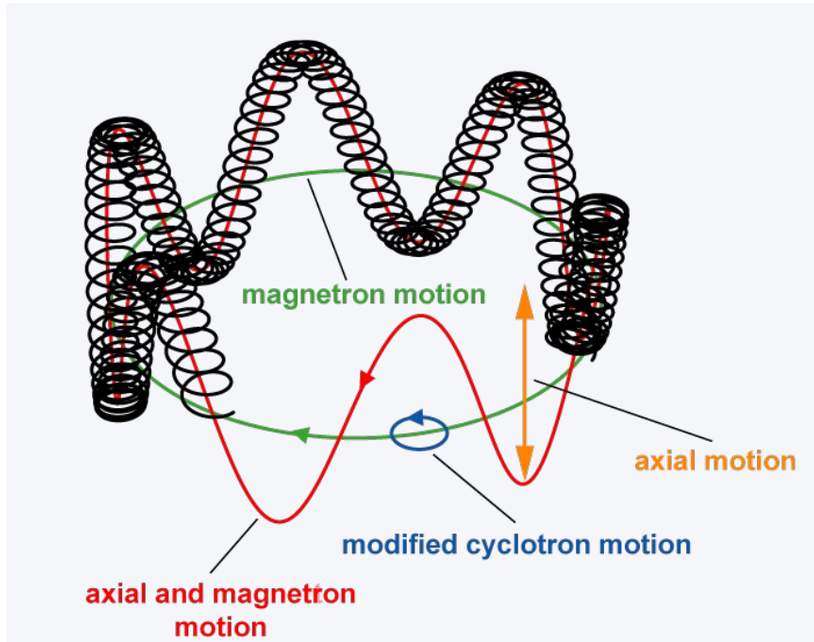

More generally: motion in Penning trap:

← strong homogeneous axial magnetic field to confine particles radially and a quadrupole electric field to confine the particles axially

modified cyclotron motion

$$\omega_+ = \frac{\omega_c}{2} + \sqrt{\left(\frac{\omega_c}{2}\right)^2 - \frac{\omega_z^2}{2}}$$

O(100 MHz)

magnetron motion

$$\omega_- = \frac{\omega_c}{2} - \sqrt{\left(\frac{\omega_c}{2}\right)^2 - \frac{\omega_z^2}{2}}$$

O(1 MHz)

axial motion

$$\omega_z = \sqrt{\frac{q}{m_p} 2c_2 U_0}$$

O(10 kHz)

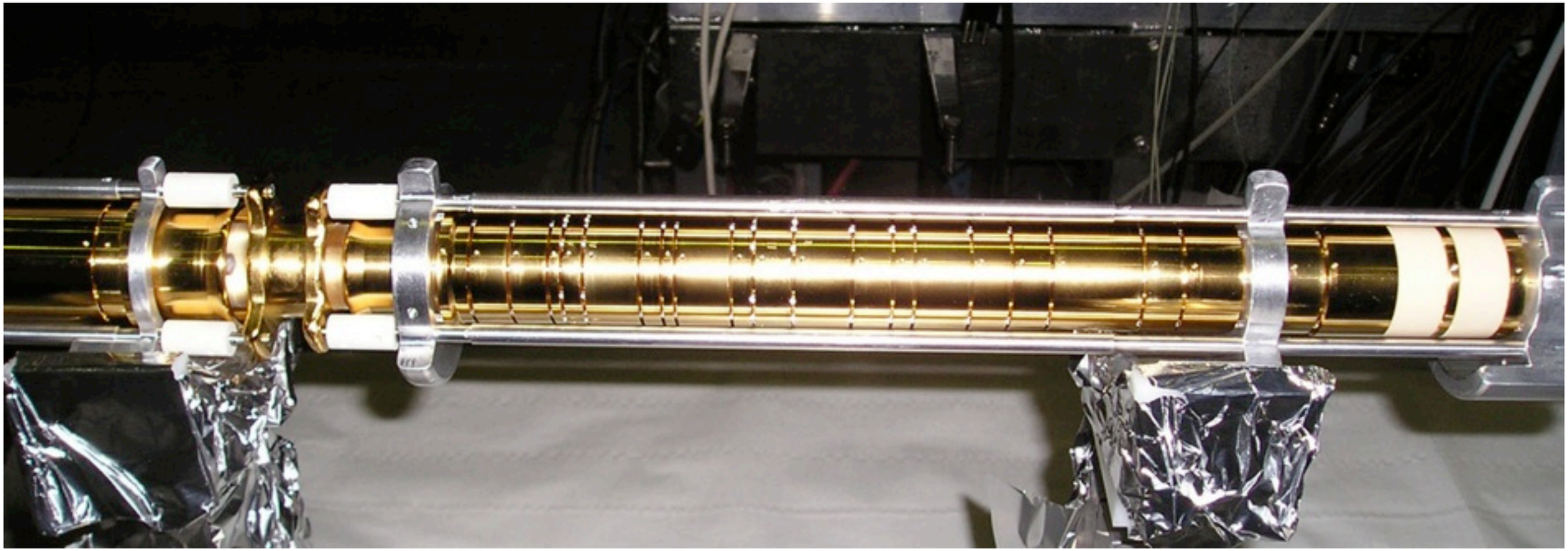

Antiproton and proton in Penning trap:

- first scheme: alternate proton and antiproton (systematics!)

- advanced measurement: compare antiproton with H^- held simultaneously in Penning trap

  requires advanced particle manipulation schemes (“parking”, high-sensitivity and high-selectivity tuned circuit)

Cyclotron frequency of the antiproton

$$\nu_c = \frac{1}{2\pi}\frac{Q_{\bar{p}}}{M_{\bar{p}}}B$$

- ν_c gives Q/M
- Problem: accuracy of B?
- Compare particles in same magnetic field
  - Antiproton, proton
  - Antiproton, H^-
- Final accuracy
  - 10^{-10}

$$\frac{Q_{\bar{p}}}{M_{\bar{p}}} \Big/ \frac{Q_p}{M_p} = -0.999'999'999'91(9)$$

G. Gabrielse et al.,
PRL 82 (1999) 3198

$(q/m)_{\bar{p}} / (q/m)_p - 1 = 1(69) \times 10^{-12}$

S. Ulmer et al.,
Nature 524, 196 (2015)

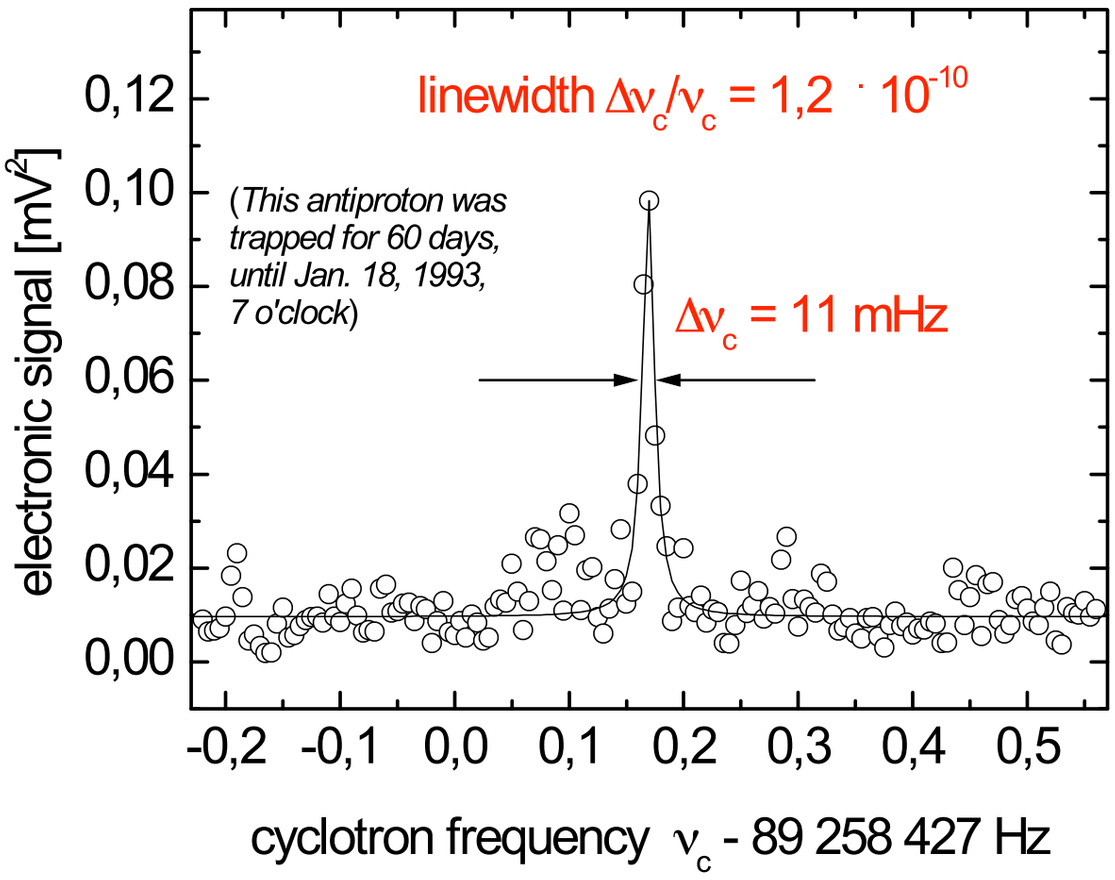

G. Gabrielse, D. Phillips, W. Quint, 1993

2) measurement of the magnetic moment of the (anti)proton via antiprotonic helium

- stopping of negatively charged particles in matter
  - slowing down by ionization (normal energy loss)
  - end when kinetic energy < ionization energy
  - capture in high-lying orbits with n~√(M*/me)

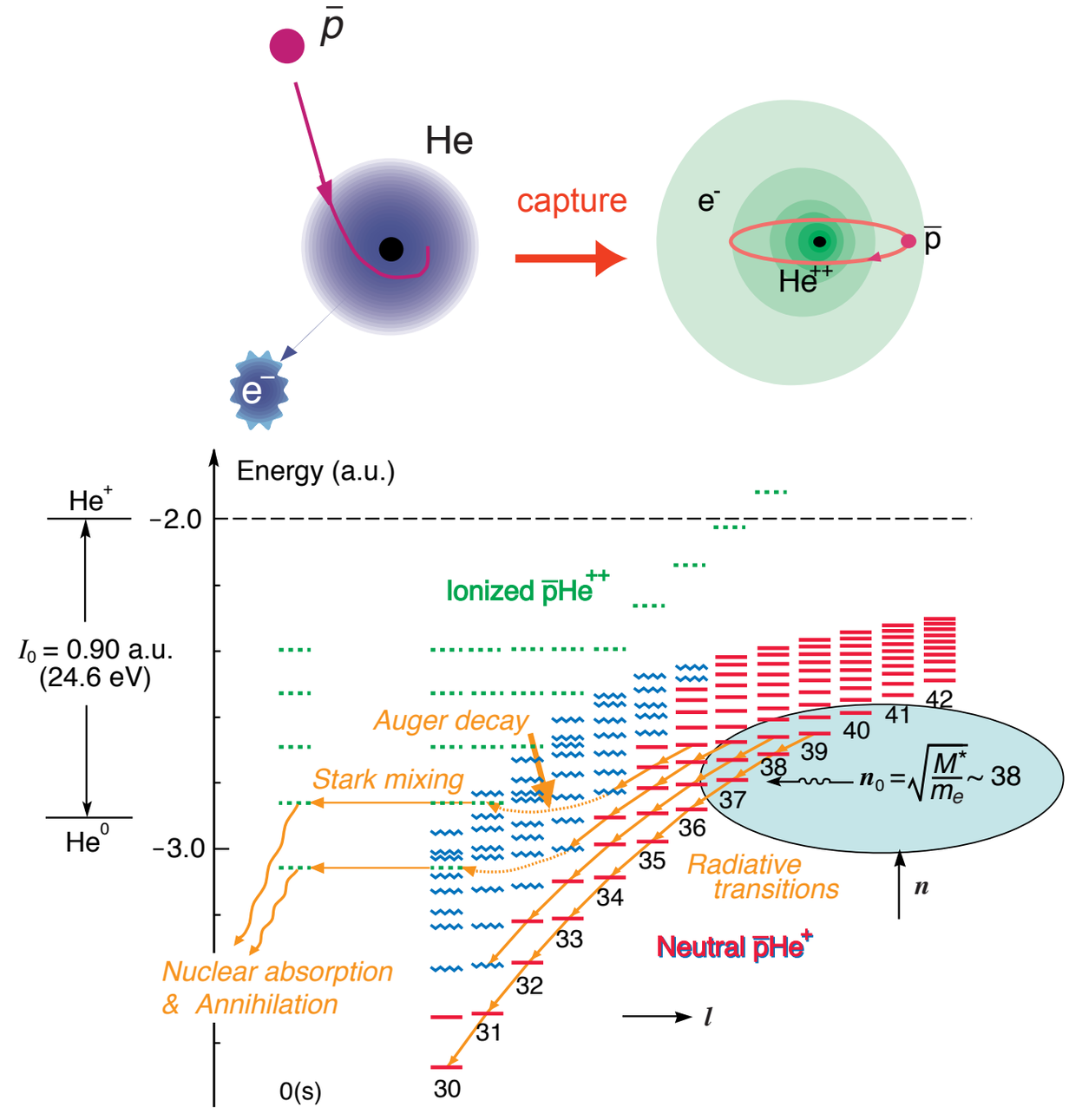

example: antiprotonic helium

determination of $\mu_{\bar{p}}$

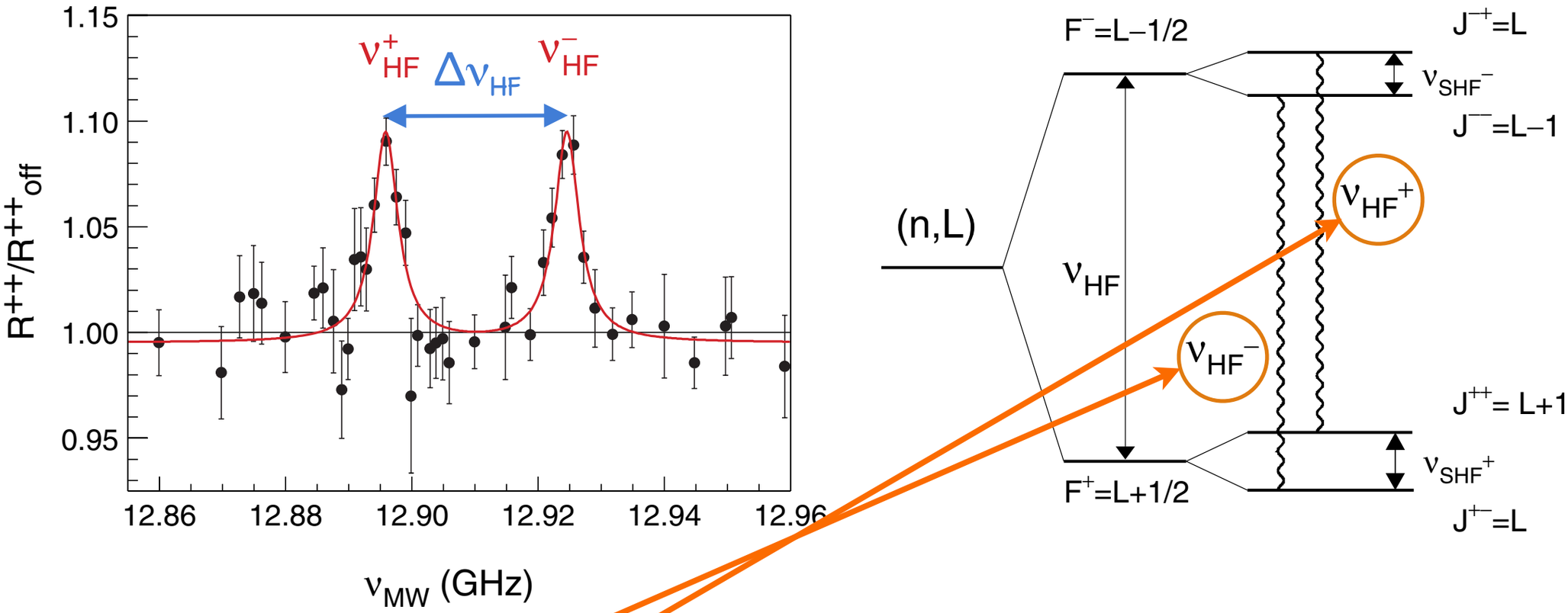

- ν_{SHF}^+ , ν_{SHF}^- most sensitive, but impossible to measure (power requirement)
- $\Delta\nu_{HF} = \nu_{HF}^- - \nu_{HF}^+ = \nu_{SHF}^+ - \nu_{SHF}^-$: sensitive to $\mu_{\bar{p}}$
- sensitivity factors from theory (D. Bakalov and E.W., PRA 76 (2007) 012512)
  - $S(F,J) = \partial E_{nFLJ} / \partial \mu_{\bar{p}} \,|_{\mu_{\bar{p}} = -\mu_p}$
  - $S(\nu_{HF}^+) = S(F^- J^{--}) - S(F^+ J^{+-})$

Magnetic moment of the antiproton

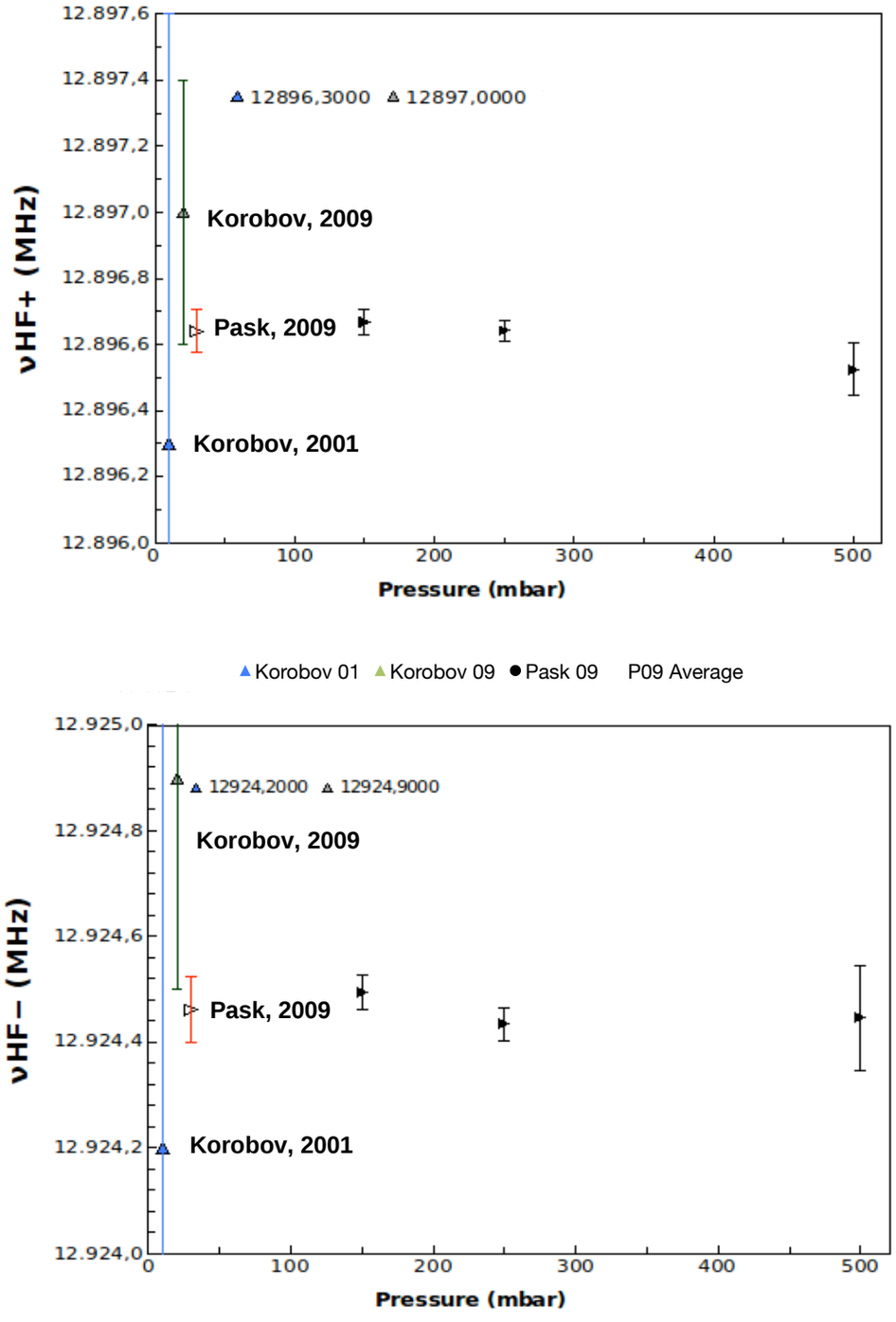

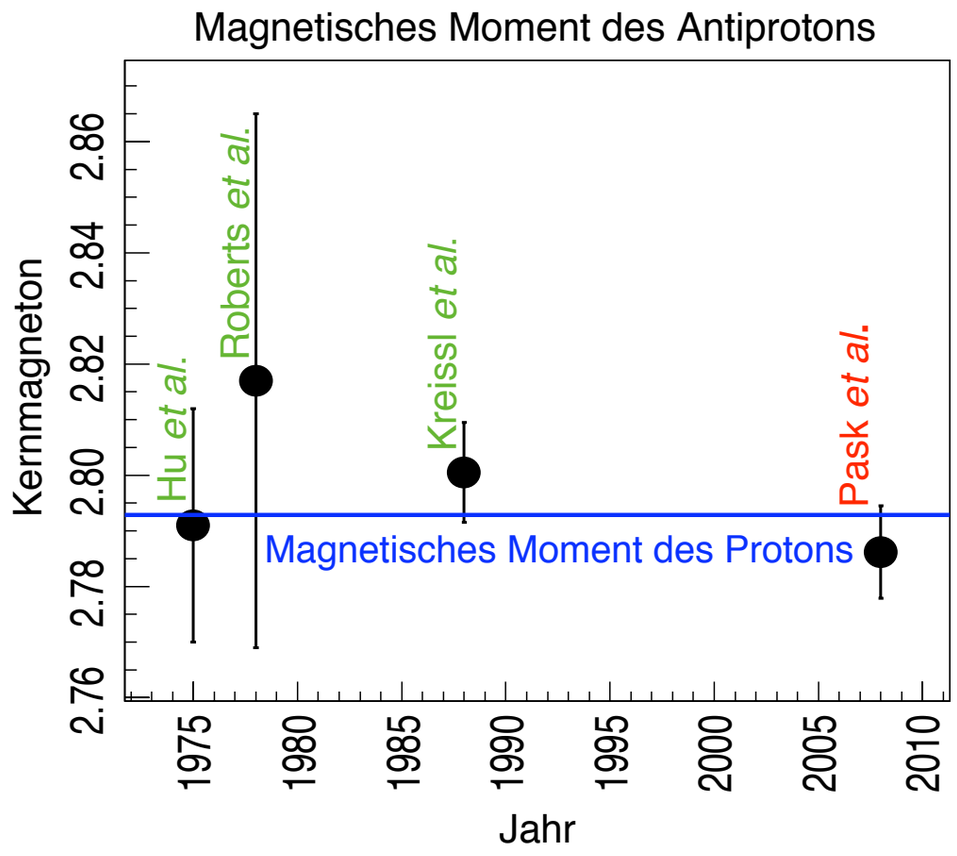

Comparison theory-experiment

$$\mu_s^{\bar{p}} = -2.7862(83)\mu_N$$

$$\frac{\mu_s^p - |\mu_s^{\bar{p}}|}{\mu_s^p} = (2.4 \pm 2.9) \times 10^{-3}$$

T. Pask et al. / Physics Letters B 678 (2009) 55–59

Magnetic moment of the antiproton

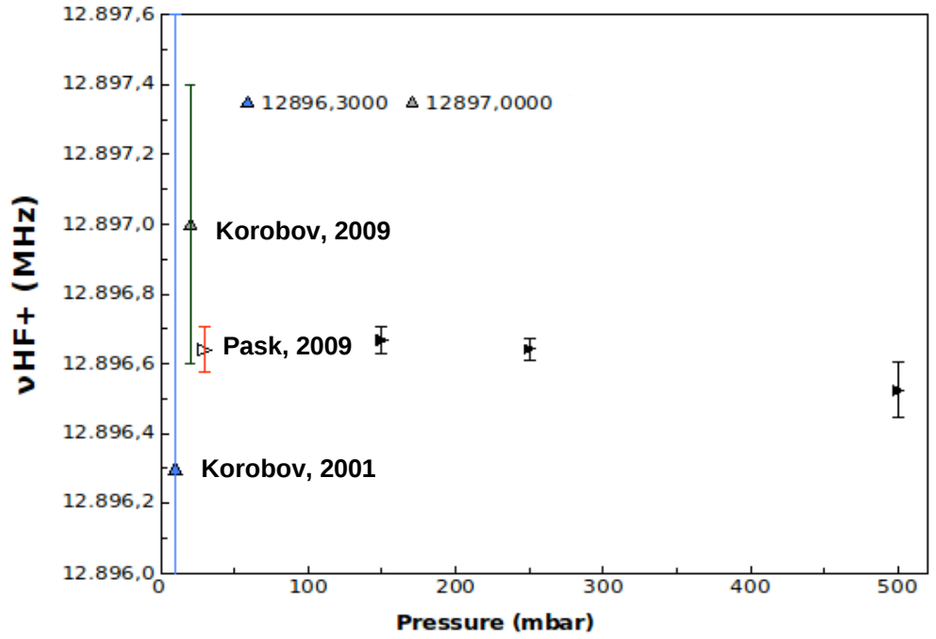

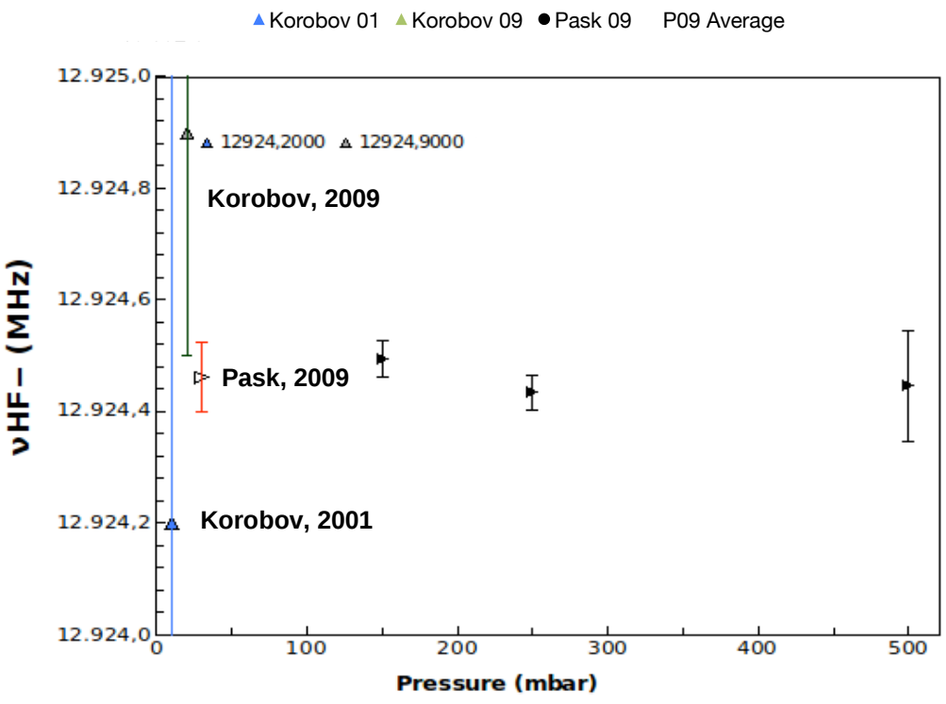

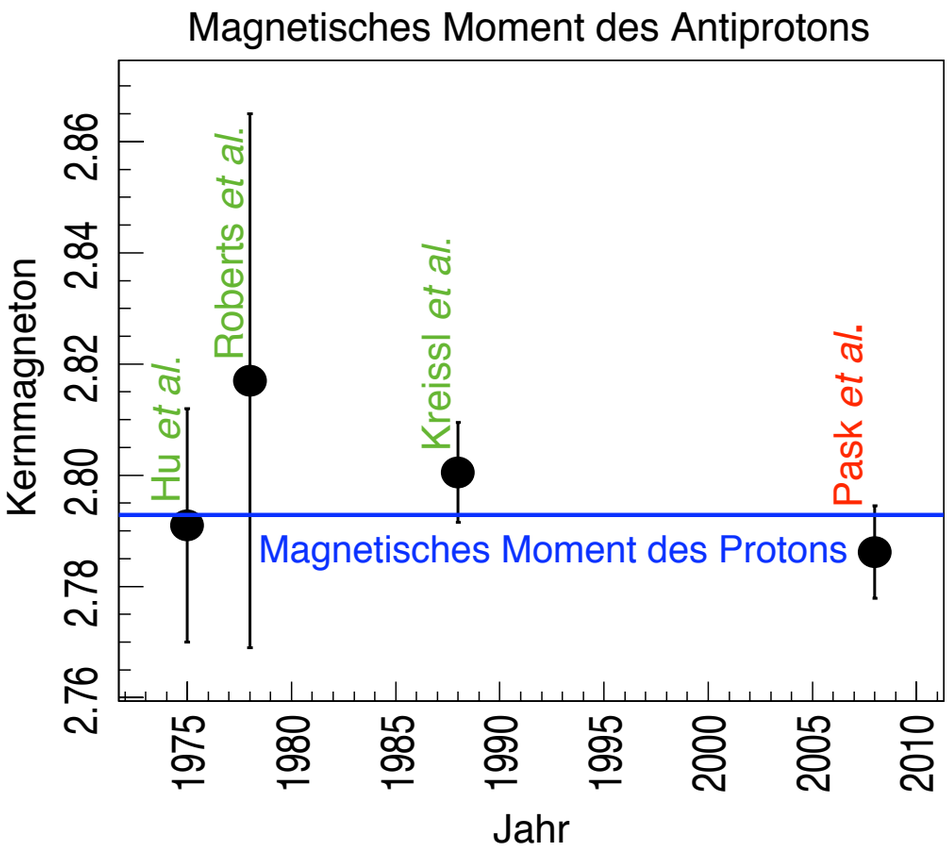

Comparison theory-experiment

$$\mu_s^{\bar{p}} = -2.7862(83)\mu_N$$

$$\frac{\mu_s^p - |\mu_s^{\bar{p}}|}{\mu_s^p} = (2.4 \pm 2.9) \times 10^{-3}$$

since 2013, known to 10^{-6}

J.DiSciacca et al., PRL 110, 130801 (2013)

T. Pask et al. / Physics Letters B 678 (2009) 55–59

Overview:

1. Introduction and overview
2. Antimatter at high energies (SppS, LEP, Fermilab)
3. Meson spectroscopy (antimatter as QCD probe)

4. Astroparticle physics and cosmology
5. CP and CPT violation tests
6. Precision tests with Antihydrogen: spectroscopy

7. Precision tests with Antihydrogen:gravity
8. Applications of antimatter

Goal of comparative spectroscopy: test CPT symmetry

Hydrogen and Antihydrogen

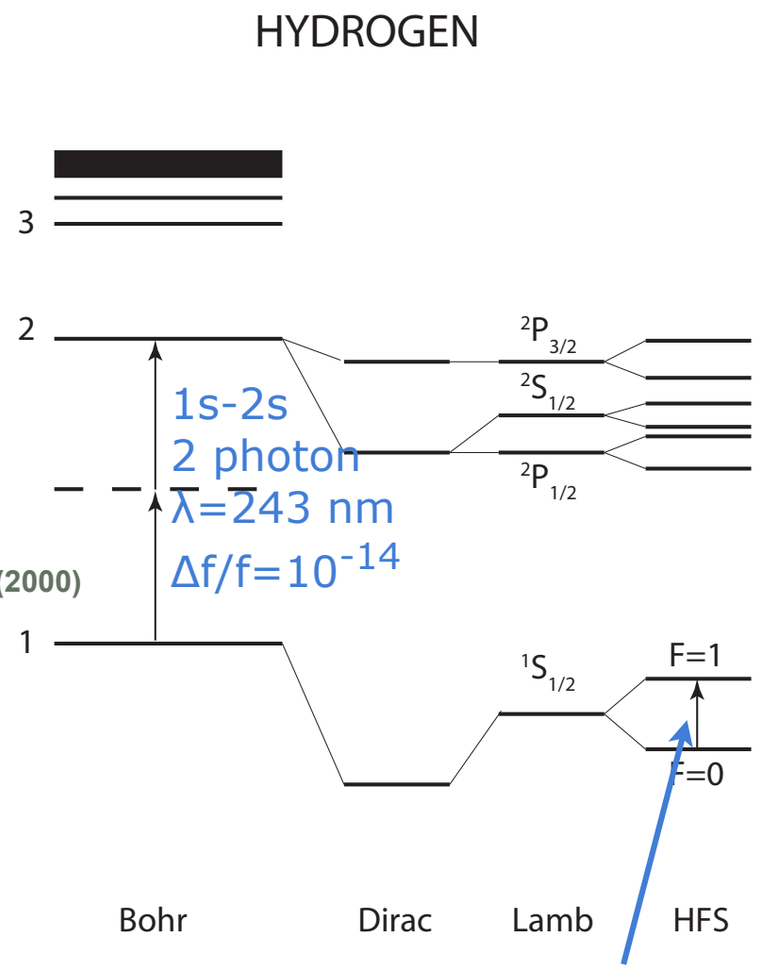

T. Hänsch et al.,
Phys. Rev. Lett. 84, 5496–5499 (2000)

N. F. Ramsey,
Physica Scripta T59, 323 (1995)

Ground state
hyperfine splitting
f = 1.4 GHz
Δf/f=10^{-12}

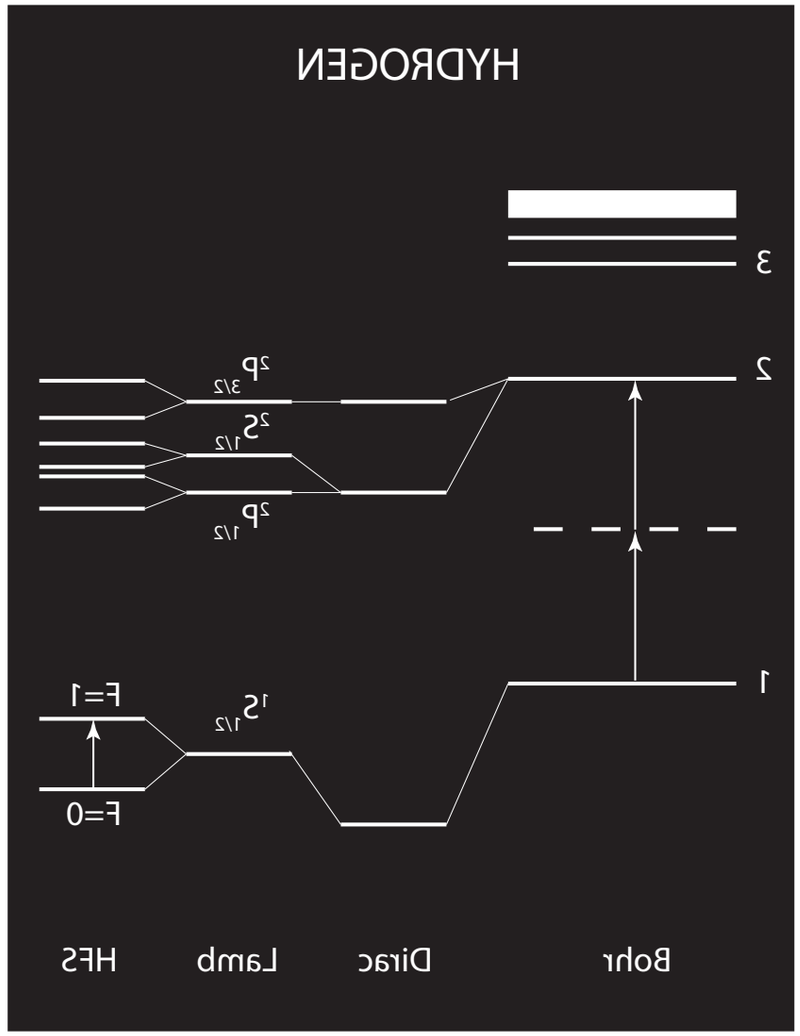

The reality

Making Antihydrogen

Plan A:
Trapping Antihydrogen

Cooling Antihydrogen
Boundary conditions (magnetic field, limited solid angle, *low* numbers of particles)

Plan B:
Atomic beam

Antihydrogen production

(one of two methods)

Nested-well technique: Penning trap for $\bar{p}$, e^+ : B=1T (plasma stability)

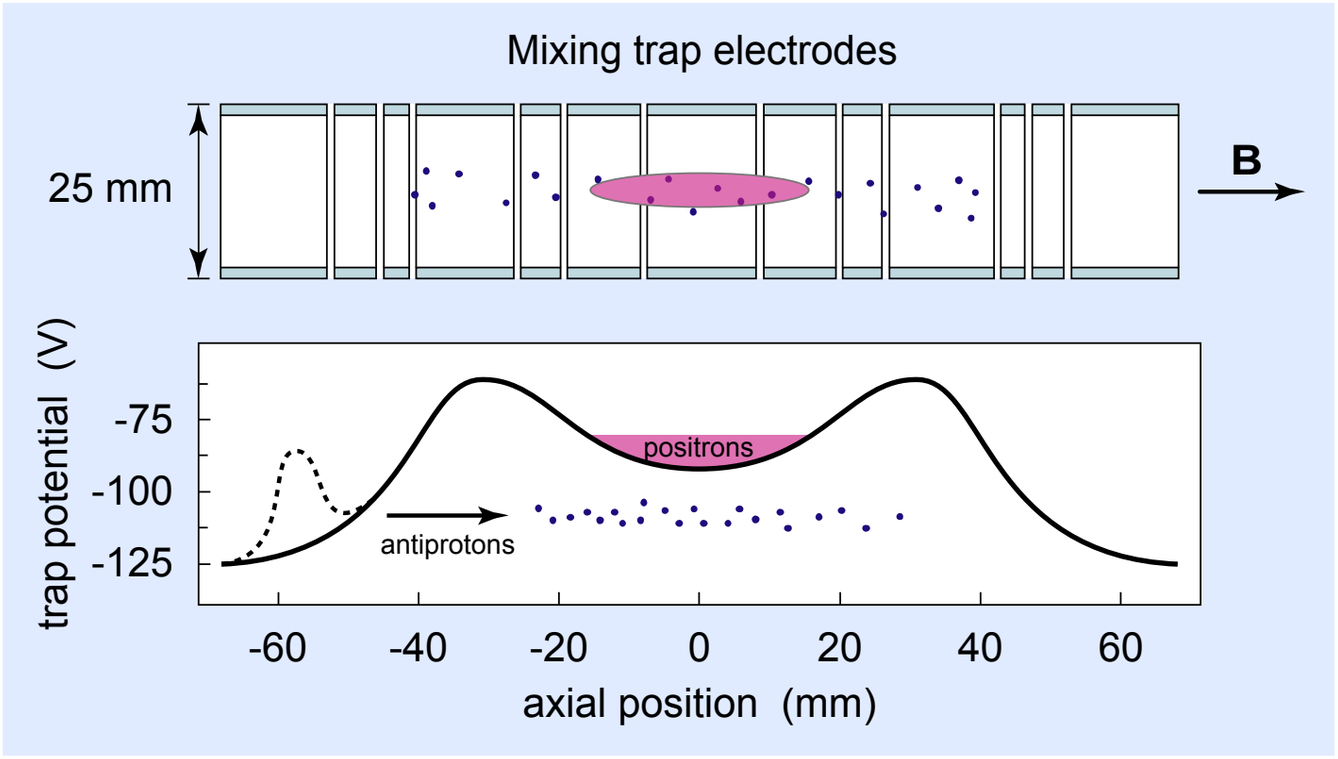

ATHENA

e^+ $N \approx 5\times10^7$ $n \approx 2\times10^8$ cm^{-3}

$\bar{p}$ $N \approx 10^4$

ATRAP

e^+ $N \approx 2\times10^6$

$\bar{p}$ $N \approx 10^5$

[G. Gabrielse *et al.*, Phys. Lett. A **129** (1988) 38]

- Positrons cool by emission of synchrotron radiation
- Antiprotons launched into pre-cooled positrons
- $\bar{H}$ production sets in spontaneously at high rates
- Disadvantage:

plasma temperature, re-ionization, high-n states

[G. Gabrielse *et al.*, Phys. Rev. Lett. **93** (2004) 073401;
N. Madsen *et al.* (ATHENA), Phys. Rev. Lett. **94** (2005) 033403]

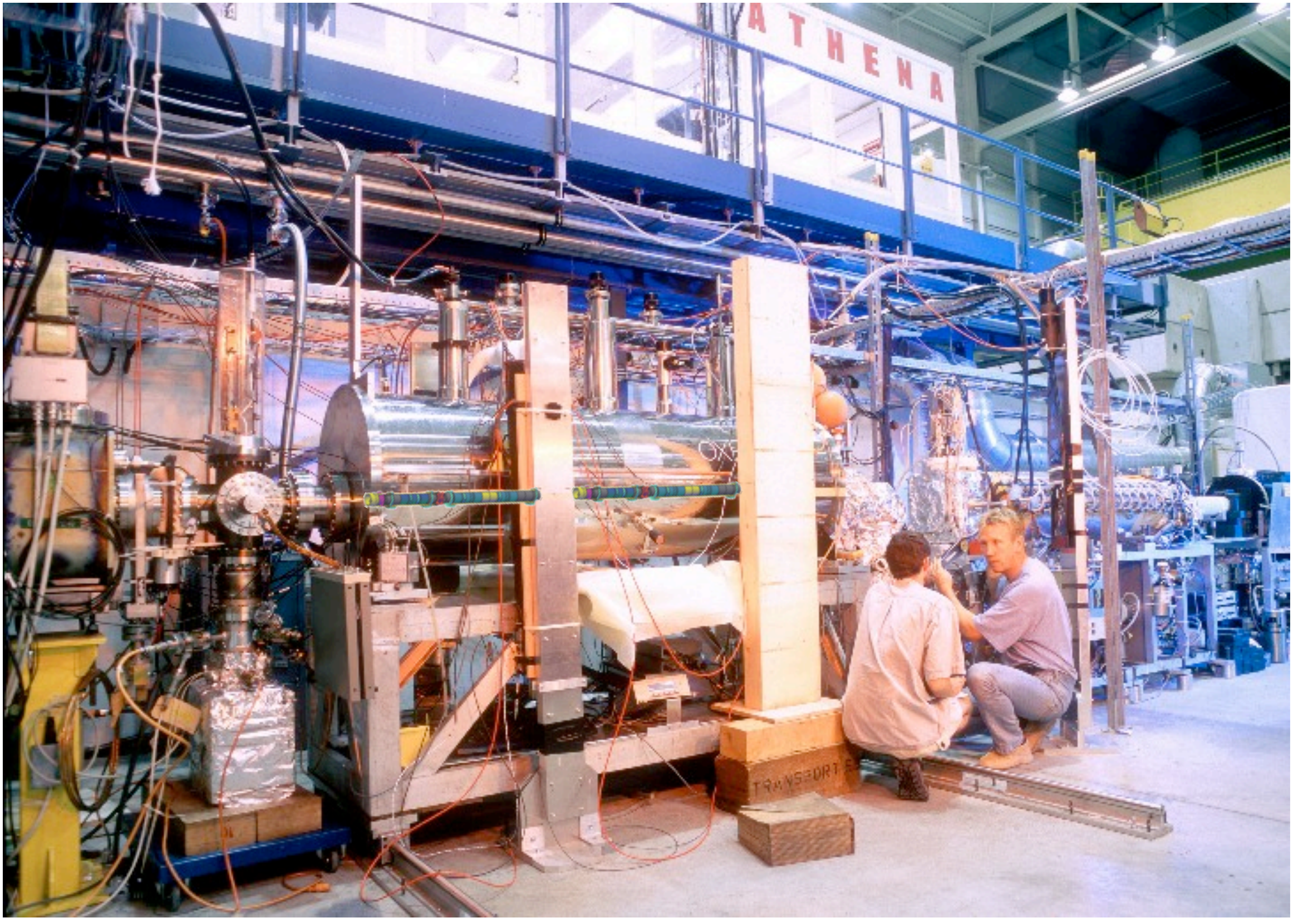
ATHENA

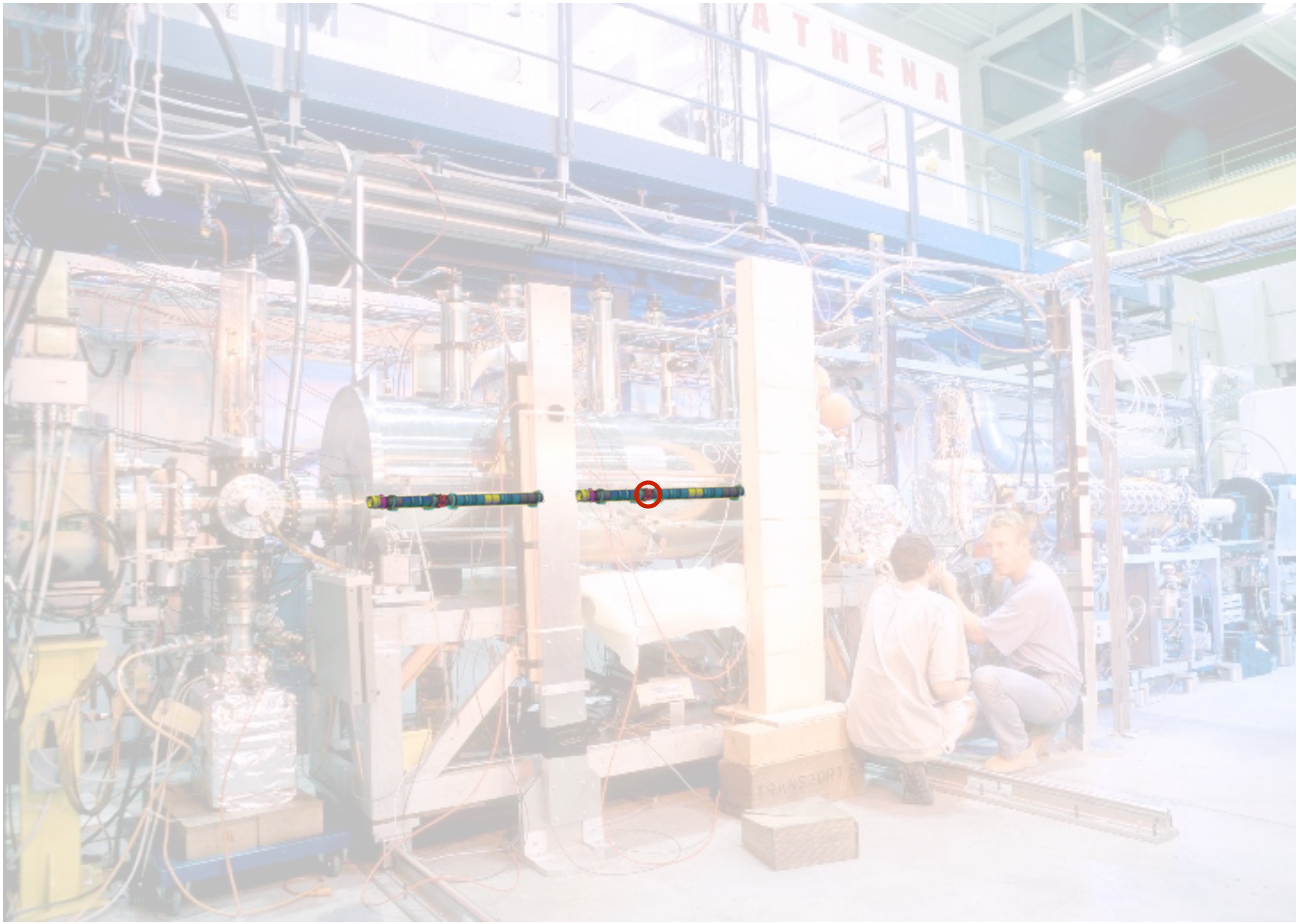
ATHENA

First Cold Antihydrogen 2002 @ AD

advance online publication

Production and detection of cold antihydrogen atoms

M. Amoretti*, C. Amsler†, G. Bonomi‡§, A. Bouchta‡, P. Bowe‖, C. Carraro*, C. L. Cesar¶, M. Charlton#, M. J. T. Collier#, M. Doser‡, V. Filippini☆, K. S. Fine‡, A. Fontana☆**, M. C. Fujiwara††, R. Funakoshi††, P. Genova☆**, J. S. Hangst‖, R. S. Hayano††, M. H. Holzscheiter‡, L. V. Jørgensen#, V. Lagomarsino*‡‡, R. Landua‡, D. Lindelöf†, E. Lodi Rizzini§☆, M. Macrì*, N. Madsen†, G. Manuzio*‡‡, M. Marchesotti☆, P. Montagna☆**, H. Pruys†, C. Regenfus†, P. Riedler‡, J. Rochet†#, A. Rotondi☆**, G. Rouleau‡#, G. Testera*, A. Variola*, T. L. Watson# & D. P. van der Werf#

ATHENA
Nature 419
(2002) 456

Nested Penning traps
Capture energy: few keV

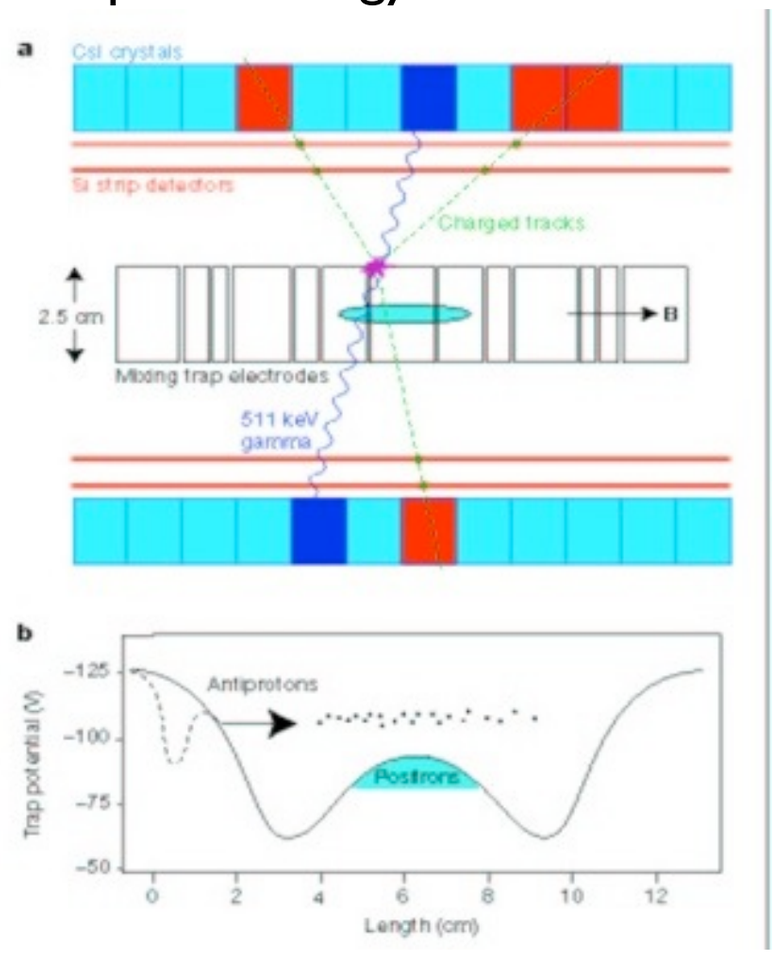

VOLUME 89, NUMBER 21 PHYSICAL REVIEW LETTERS 18 NOVEMBER 2002

Background-Free Observation of Cold Antihydrogen with Field-Ionization Analysis of Its States

G. Gabrielse,[1,*] N. S. Bowden,[1] P. Oxley,[1] A. Speck,[1] C. H. Storry,[1] J. N. Tan,[1] M. Wessels,[1] D. Grzonka,[2] W. Oelert,[2] G. Schepers,[2] T. Sefzick,[2] J. Walz,[3] H. Pittner,[4] T. W. Hänsch,[4,5] and E. A. Hessels[6]

(ATRAP Collaboration)

[1]*Department of Physics, Harvard University, Cambridge, Massachusetts 02138*
[2]*IKP, Forschungszentrum Jülich GmbH, 52425 Jülich, Germany*
[3]*CERN, 1211 Geneva 23, Switzerland*
[4]*Max-Planck-Institut für Quantenoptik, Hans-Kopfermann-Strasse 1, 85748 Garching, Germany*
[5]*Ludwig-Maximilians-Universität München, Schellingstrasse 4/III, 80799 München, Germany*
[6]*York University, Department of Physics and Astronomy, Toronto, Ontario, Canada M3J 1P3*
(Received 11 October 2002; published 31 October 2002)

ATRAP PRL 89 (2002) 213401

First "Cold" Antihydrogen 2002 @ AD

advance online publication

Production and detection of cold antihydrogen atoms

M. Amoretti*, C. Amsler†, G. Bonomi‡§, A. Bouchta‡, P. Bowe‖, C. Carraro*, C. L. Cesar¶, M. Charlton#, M. J. T. Collier#, M. Doser‡, V. Filippini☆, K. S. Fine‡, A. Fontana☆**, M. C. Fujiwara††, R. Funakoshi††, P. Genova☆**, J. S. Hangst‖, R. S. Hayano††, M. H. Holzscheiter‡, L. V. Jørgensen#, V. Lagomarsino*‡‡, R. Landua‡, D. Lindelöf†, E. Lodi Rizzini§☆, M. Macrì*, N. Madsen†, G. Manuzio*‡‡, M. Marchesotti☆, P. Montagna☆**, H. Pruys†, C. Regenfus†, P. Riedler‡, J. Rochet†#, A. Rotondi☆**, G. Rouleau‡#, G. Testera*, A. Variola*, T. L. Watson# & D. P. van der Werf#

ATHENA
Nature 419
(2002) 456

Nested Penning traps
Capture energy: few keV

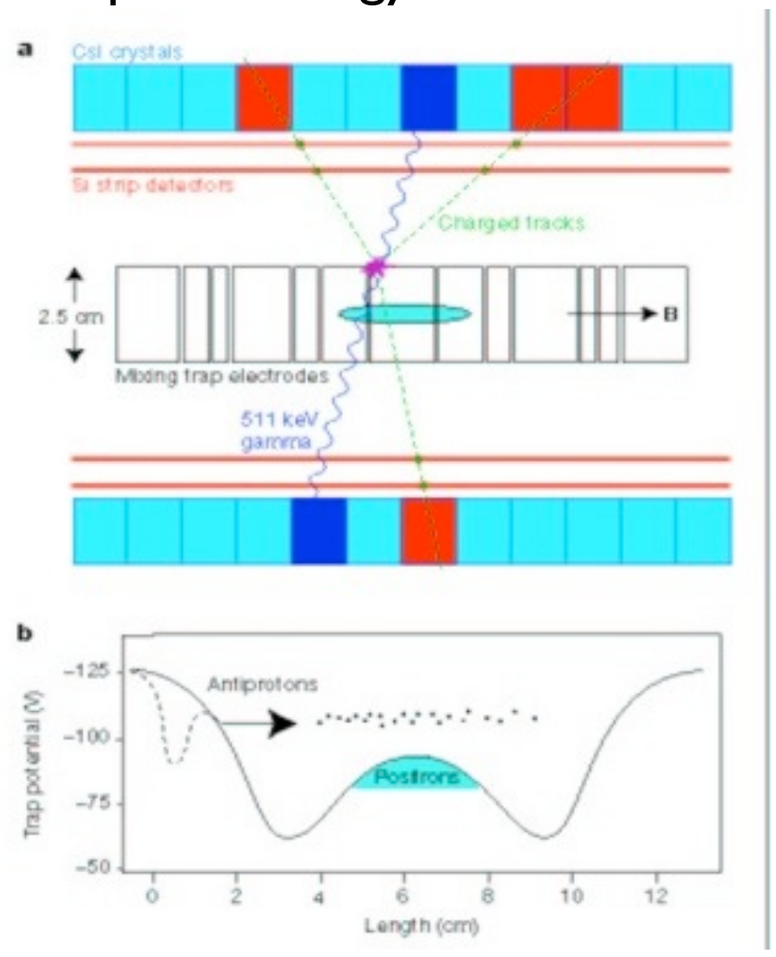

VOLUME 89, NUMBER 21 PHYSICAL REVIEW LETTERS 18 NOVEMBER 2002

Background-Free Observation of Cold Antihydrogen with Field-Ionization Analysis of Its States

G. Gabrielse,[1,*] N. S. Bowden,[1] P. Oxley,[1] A. Speck,[1] C. H. Storry,[1] J. N. Tan,[1] M. Wessels,[1] D. Grzonka,[2] W. Oelert,[2] G. Schepers,[2] T. Sefzick,[2] J. Walz,[3] H. Pittner,[4] T. W. Hänsch,[4,5] and E. A. Hessels[6]

(ATRAP Collaboration)

[1]*Department of Physics, Harvard University, Cambridge, Massachusetts 02138*
[2]*IKP, Forschungszentrum Jülich GmbH, 52425 Jülich, Germany*
[3]*CERN, 1211 Geneva 23, Switzerland*
[4]*Max-Planck-Institut für Quantenoptik, Hans-Kopfermann-Strasse 1, 85748 Garching, Germany*
[5]*Ludwig-Maximilians-Universität München, Schellingstrasse 4/III, 80799 München, Germany*
[6]*York University, Department of Physics and Astronomy, Toronto, Ontario, Canada M3J 1P3*
(Received 11 October 2002; published 31 October 2002)

ATRAP PRL 89 (2002) 213401

Trapping of $\bar{H}$?

Trapping of $\bar{H}$?

Antihydrogen Production within a Penning-Ioffe Trap

G.Gabrielse et al., Phys. Rev. Lett. 100, 113001 (2008)

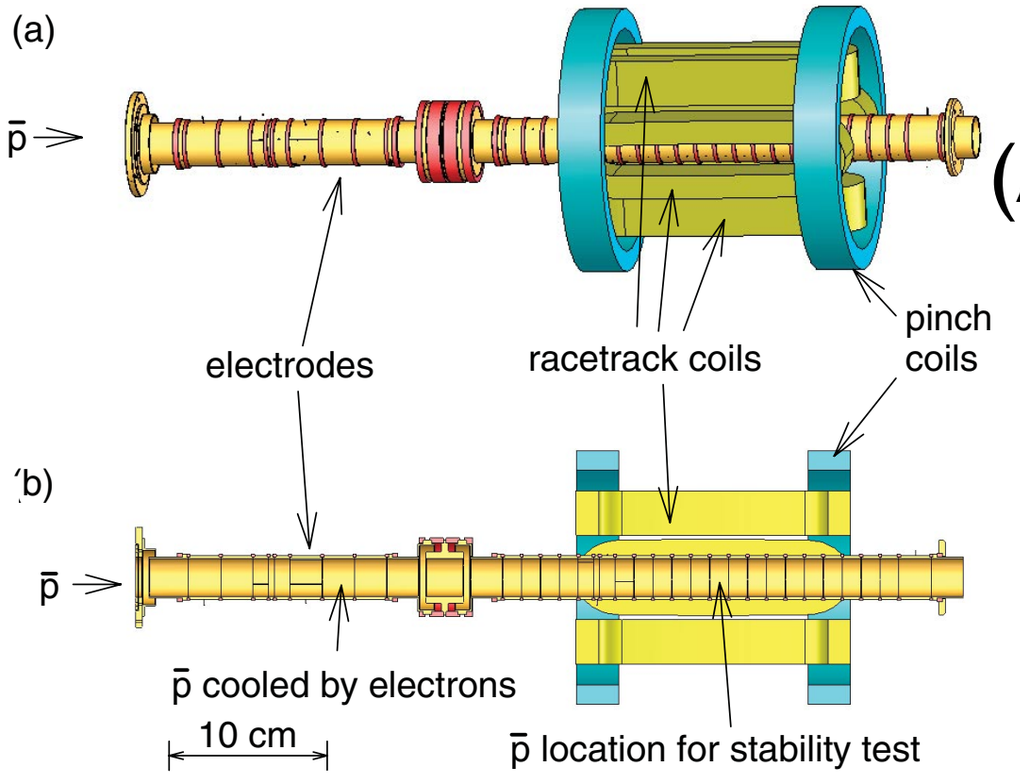

(ATRAP)

Zeeman splitting

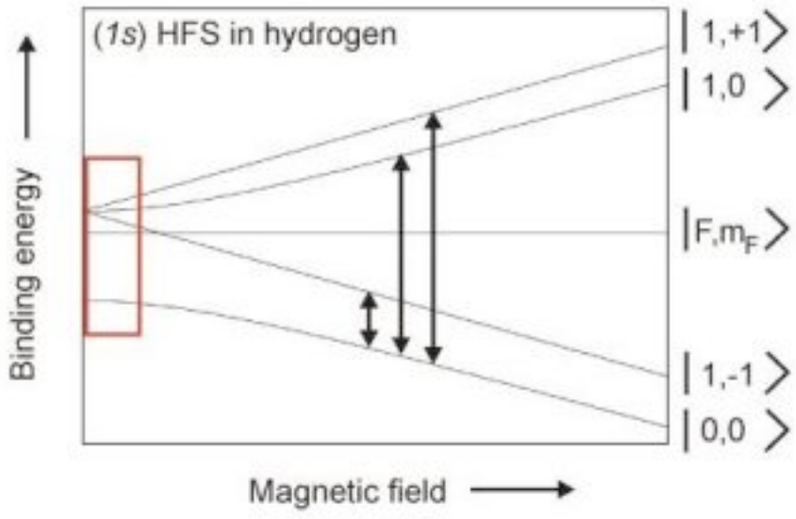

(ALPHA)

trap depth ~500 mK

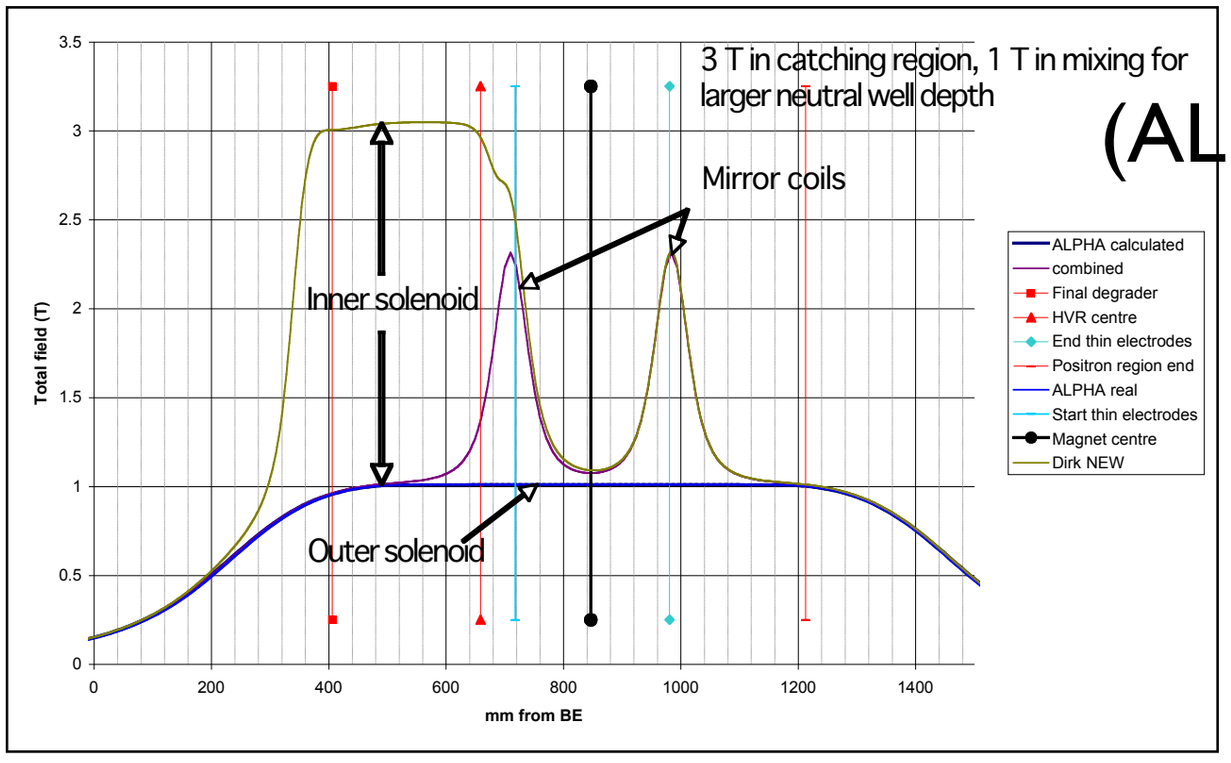

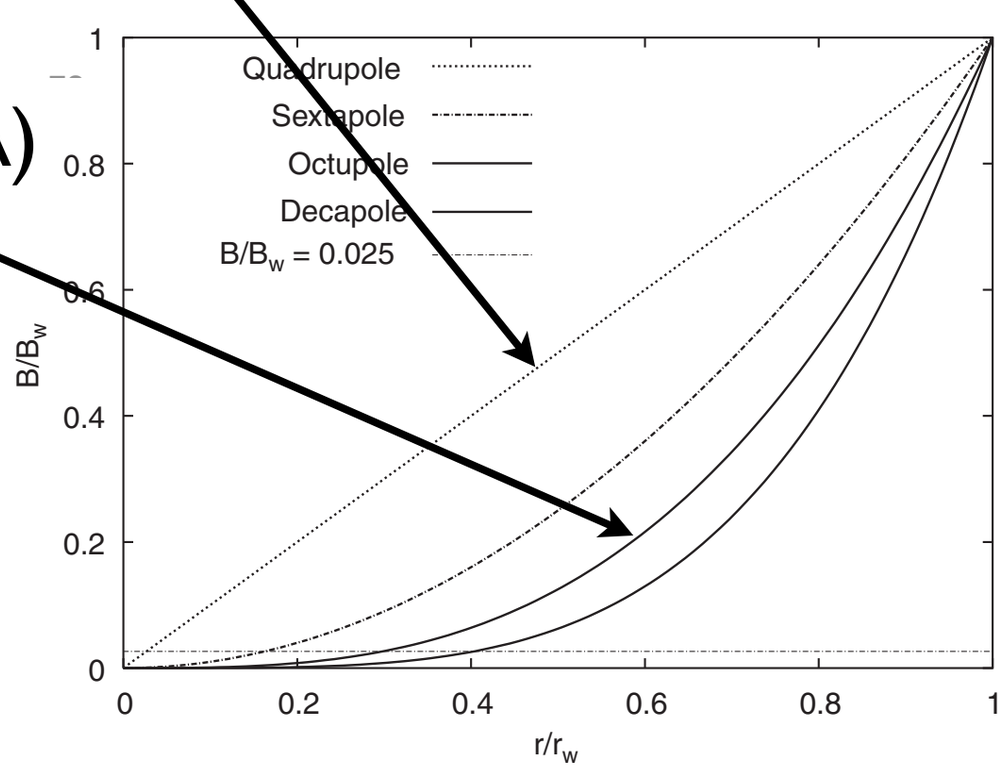

Reaching the few K regime

evaporative cooling of antiprotons (ALPHA)

PRL **105,** 013003 (2010)

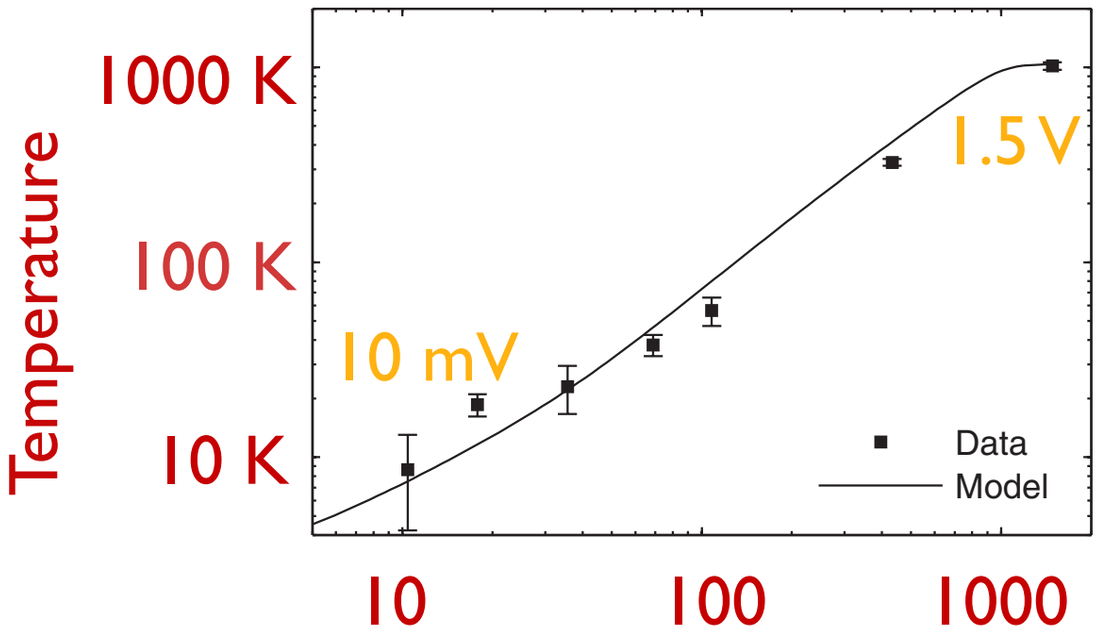

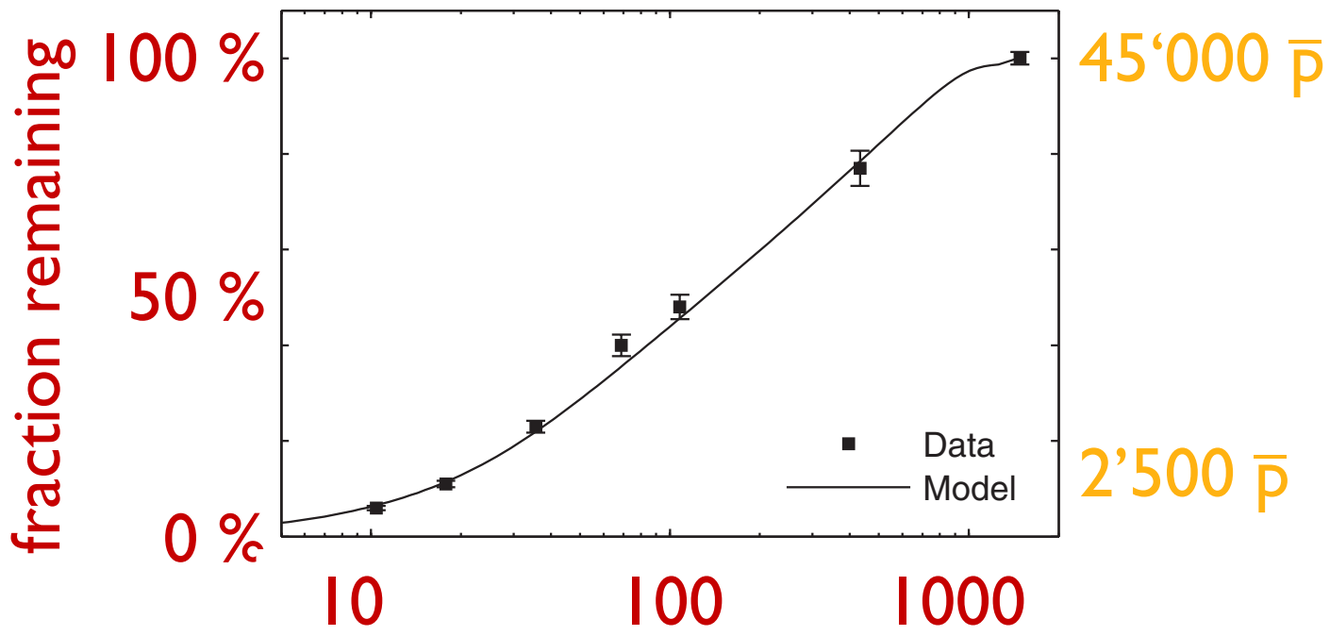

essential to avoid reheating:

- great care needed on noise reduction;
- can not use electron cooling to pre-cool
- bring e^+ to cold $\bar{p}$, not vice-versa, or use autoresonant excitation of $\bar{p}$

Successful trapping!

(ALPHA)

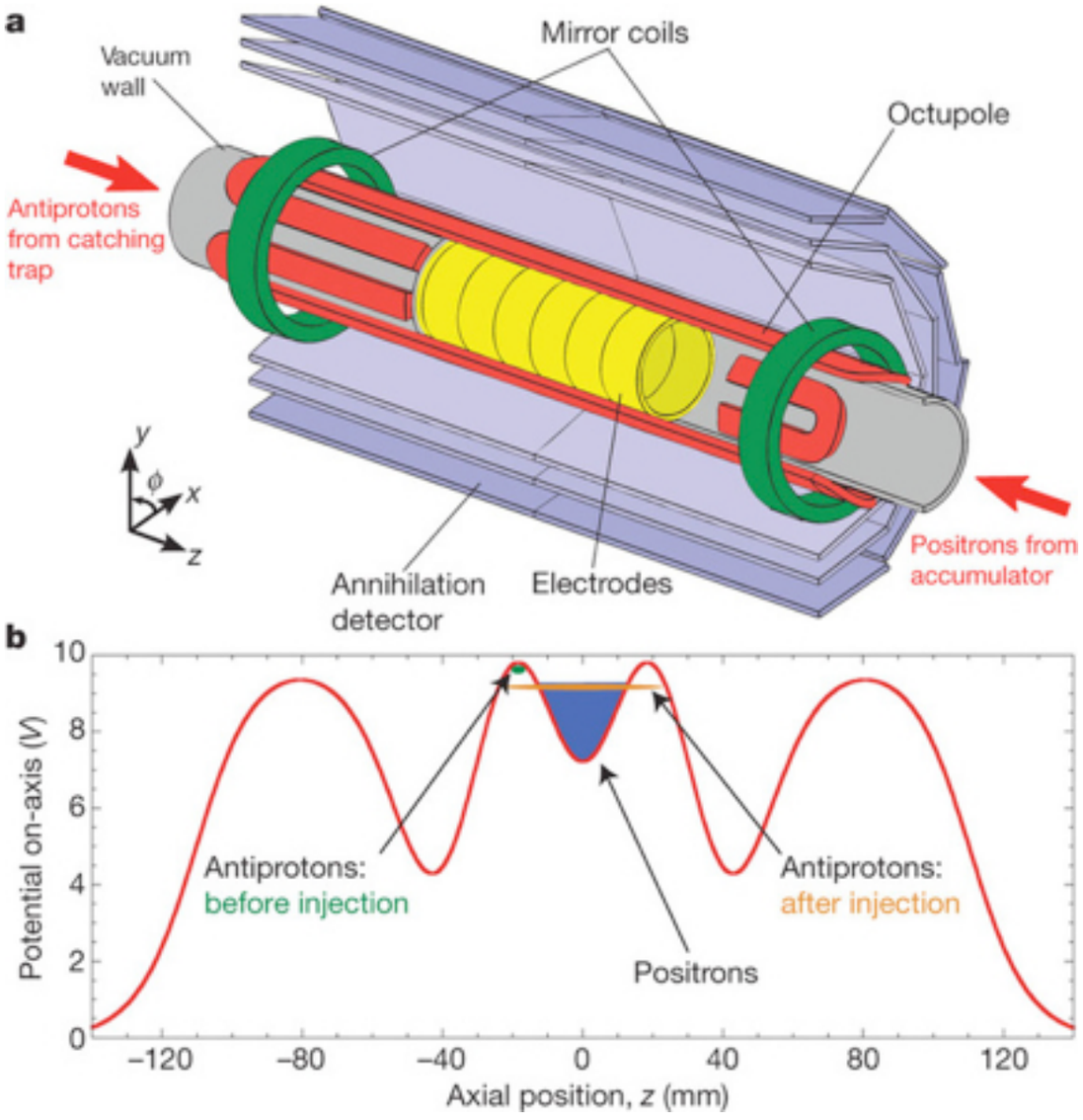

antihydrogen or antiprotons?

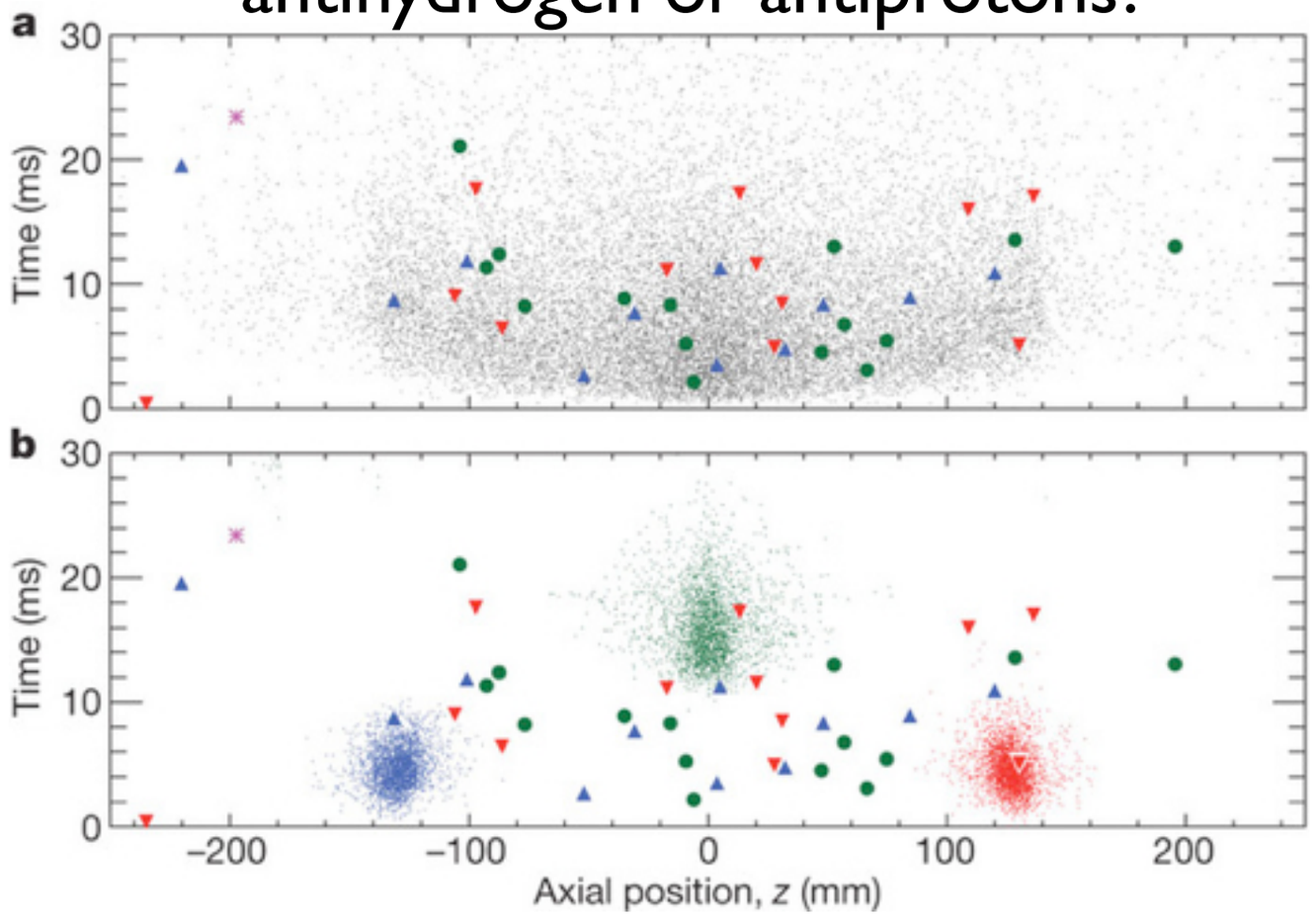

quick opening of magnetic trap (20 ms)
+ sensitive detector for antihydrogen

microwave spectroscopy in traps

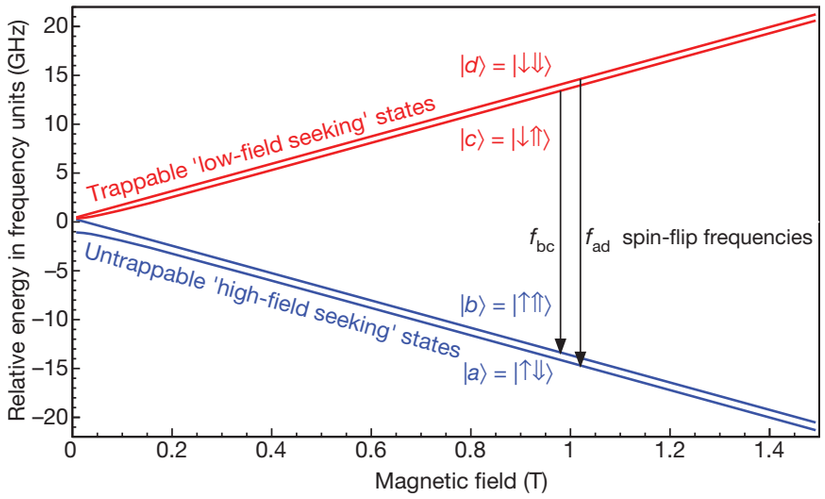

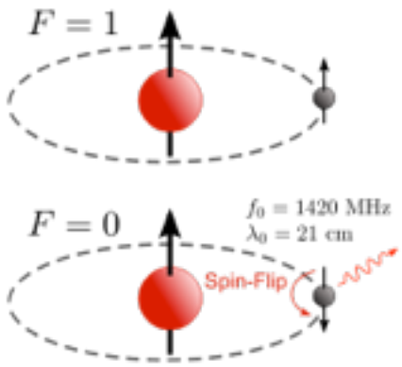

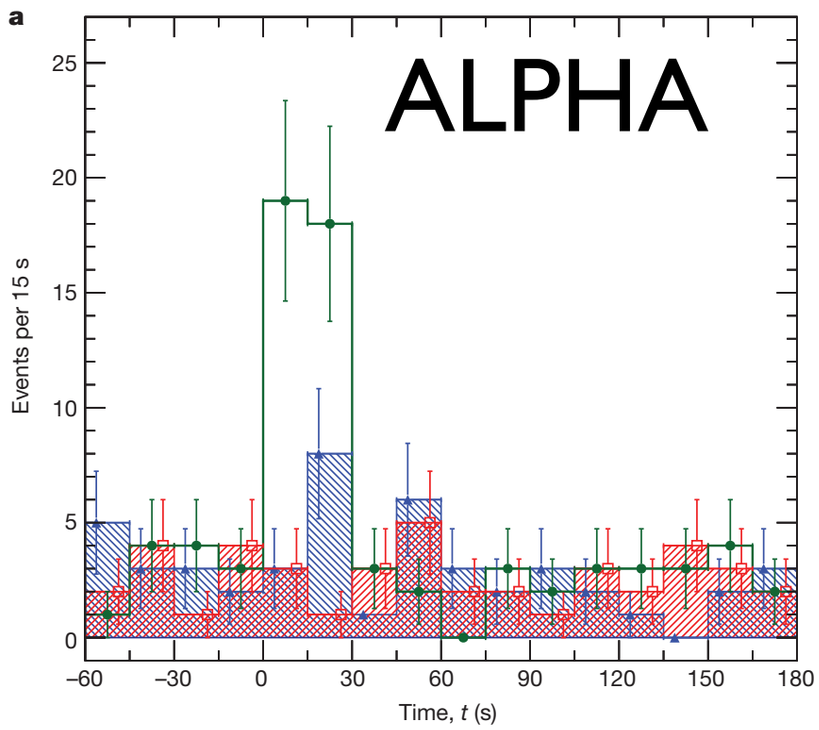

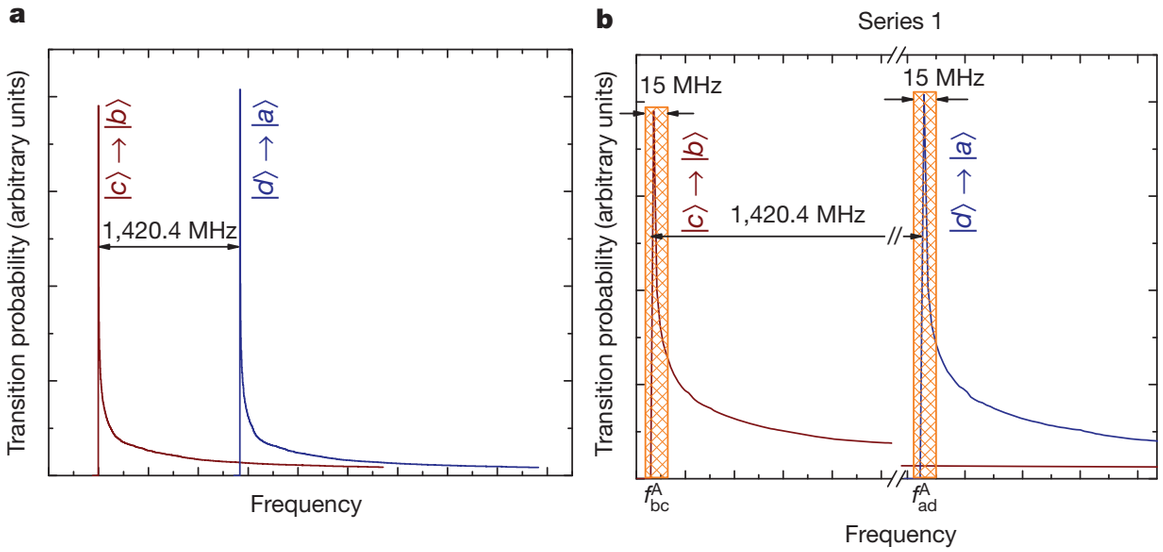

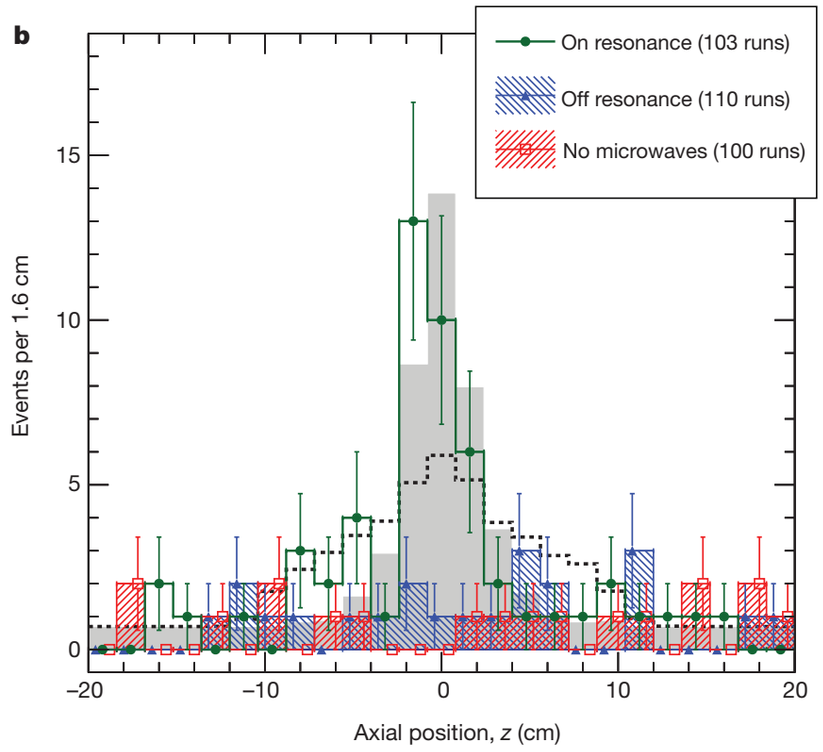

C Amole et al., Nature 483, 439 (2012)

Plan B: antihydrogen beam
(entering unknown territory...)

- Magnetic bottle
- e^- trapping achieved
- Neutral atoms were also trapped!

Formation by 3-body recombination
Formed Hbar spin-selected
Polarized beam?
Cold atoms could be trapped?

Cusp trap

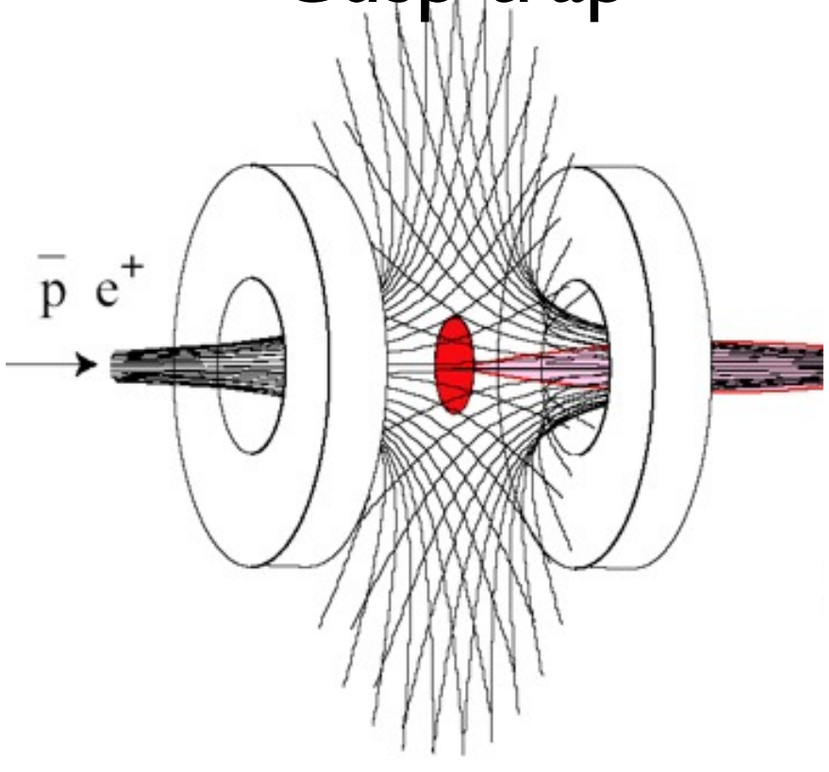

$\bar{H}$ beam

Paul trap

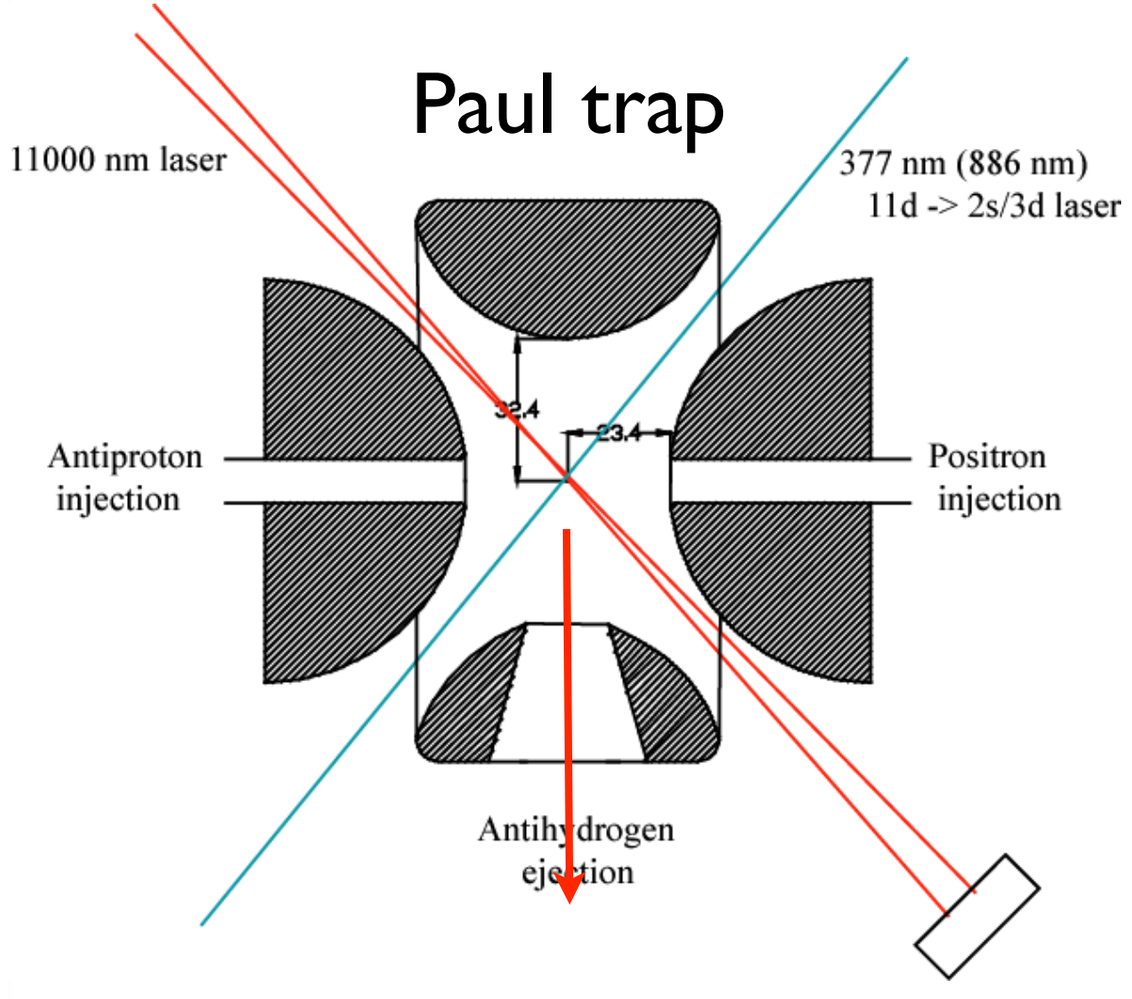

Mohri A and Yamazaki Y 2003 Europhys. Lett. 63 207

Plan B: antihydrogen beam
(entering unknown territory...)

- Magnetic bottle
- e^- trapping achieved
- Neutral atoms were also trapped!

Formation by 3-body recombination
Formed Hbar spin-selected
Polarized beam?
Cold atoms could be trapped?

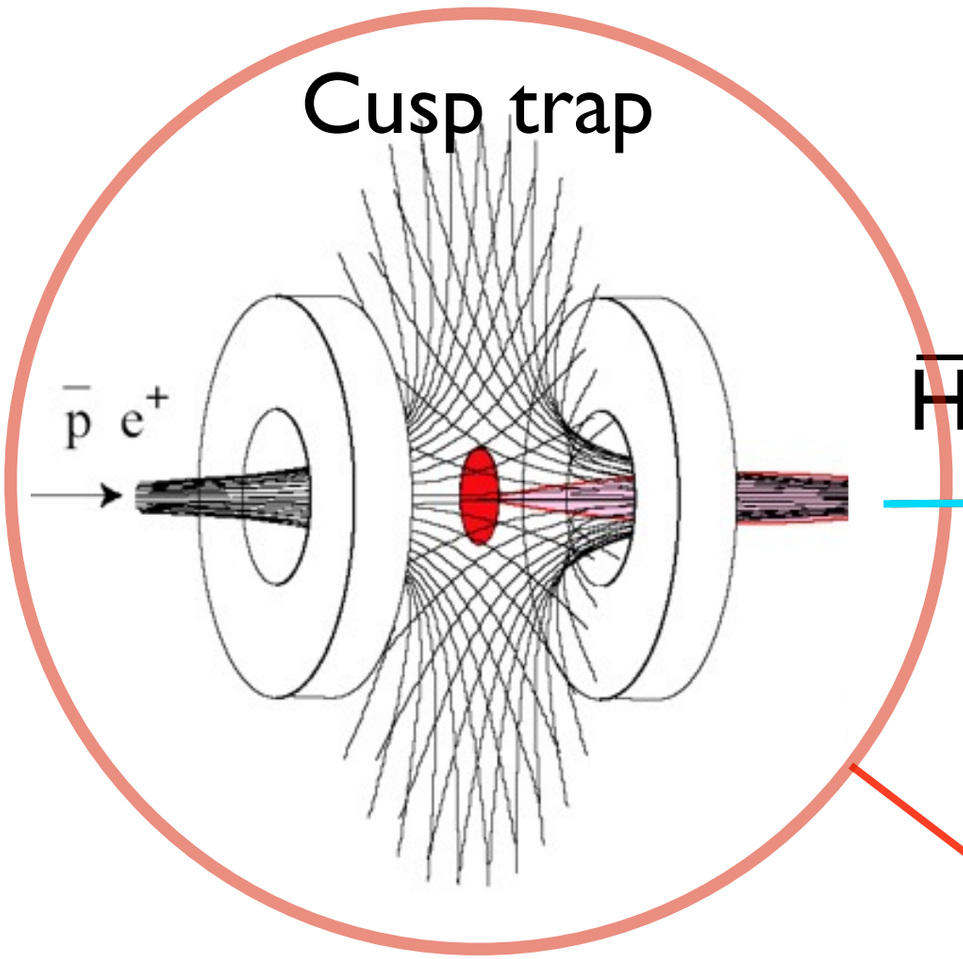

$\bar{H}$ beam

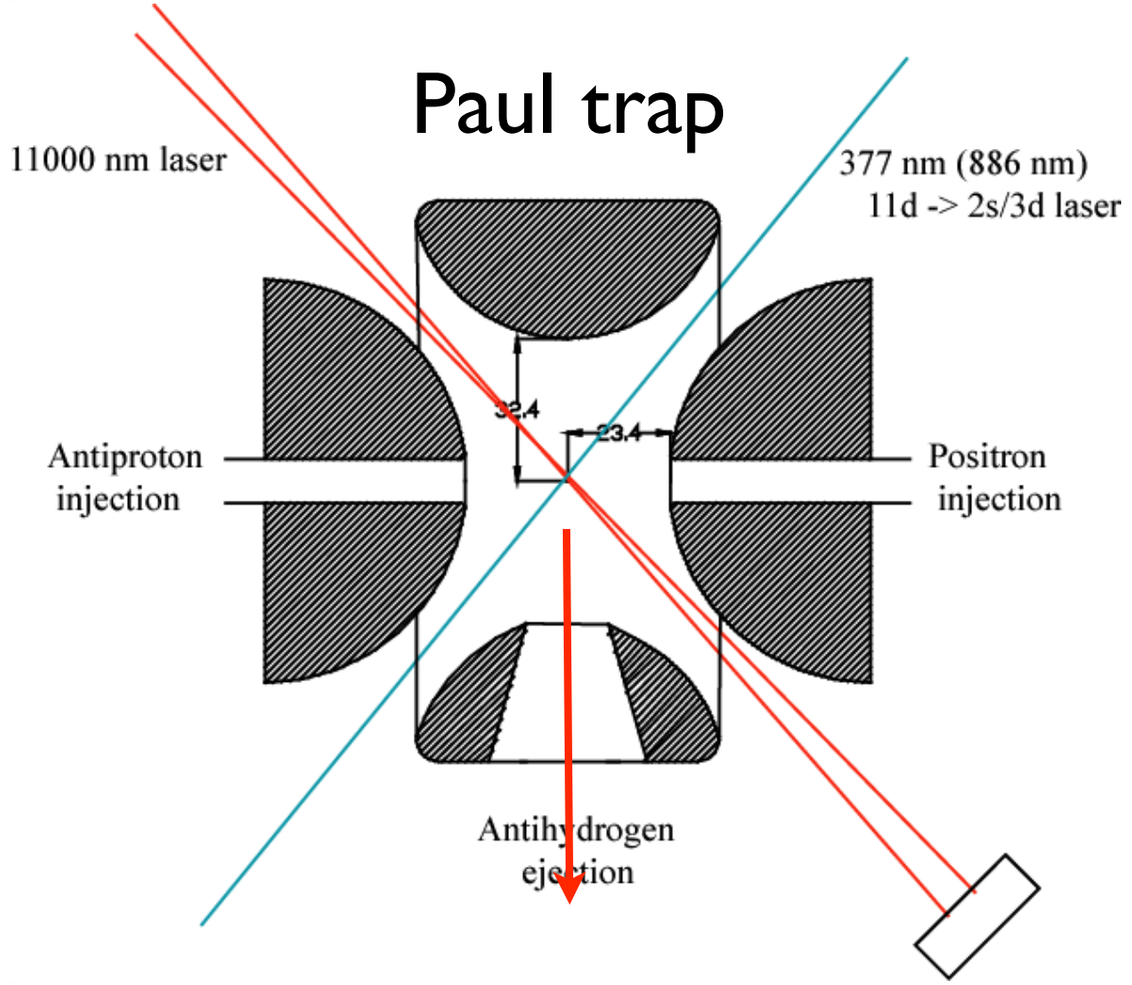

Mohri A and Yamazaki Y 2003 Europhys. Lett. 63 207

http://www.nature.com/ncomms/2014/140121/ncomms4089/full/ncomms4089.html

the end

(well.... actually, there's one more thing: the ***real*** trap for Antihydrogen is a MOT...)